Low Energy Building with Novel Cooling Unit Using PCM

Dissertation

zur Erlangung des akademischen Grades

Doktoringenieur (Dr.-Ing.)

vorgelegt der Fakultät für Maschinenbau

der Technischen Universität Ilmenau

von Frau M.Sc.-Ing. Samar Jaber

geboren am 24. Mai 1982

in Amman/Jordanien

vorgelegt am: 07.10.2011

wissenschaftliche Aussprache am: 13.02.2012

Gutachter: 1. Prof. Dr.-Ing. habil. Ajib, Salman

2. Univ.-Prof. Dr.-Ing. habil.Prof. h.c.P Kurtz

3. Univ.-Prof. Dipl.-Ing. Dr.techn. W. Streicher

urn:nbn:de:gbv:ilm1-2012000183

Low Energy Building with Novel Cooling Unit Using PCM

Dissertation

for the attainment of the academic degree of

Doktoringenieur (Dr.-Ing.)

Submitted to the Faculty of Mechanical Engineering
of the Technical University of Ilmenau

by M.Sc.-Ing. Samar Jaber
born on the 24th of May 1982
in Amman/Jordan

submitted on the 07.10.2011
convocation on the 13.02.2012

Examinars:
1. Prof. Dr.-Ing. habil. Ajib, Salman
2. Univ.-Prof. Dr.-Ing. habil.Prof. h.c.P Kurtz
3. Univ.-Prof. Dipl.-Ing. Dr.techn. W. Streicher

urn:nbn:de:gbv:ilm1-2012000183

To my country

To my love

To all the people who have in a way or another,
contributed to the successful completion of this thesis.

Acknowledgements

First of all, I have to thank God for helping me in writing this thesis.

I would like to thank my husband for his unconditional love, encouragement and support, especially through these hard years. My special thanks go to my family for all they have done for me during the writing of this thesis.

I would like to give special thanks to Univ.-Prof. Dr. rer. nat. habil. André Thess, head of the Thermodynamics and Fluid Mechanics Department, for his kind assistance provided to carry out this investigation. I express my special thanks and appreciation to my advisor, PD Dr. Ing. habil. Salman Ajib, for his continuous guidance, support and encouragement during his supervision of this research work. American University of Madaba (AUM) is also thanked for funding my PhD study.

Special thanks to Univ.Prof. Dipl.-Ing.Dr.techn. Wolfgang Streicher, Insbrück University and Univ.-Prof. Dr.-Ing. habil. Prof. h. c. Peter Kurtz, Technical University of Ilmenau for their interest in reviewing this thesis.

Thanks to Eng. Eman Abdelhafed, Ms. Fairouz Jafar and Ms. Alia Jafar for their kind assistance to fulfill this work.

Finally, it is a pleasure to have the opportunity to express my gratitude to my colleagues in Technical University of Ilmenau and to all the people who have in a way or another, contributed to the successful completion of this research.

With all of them I share the joy of fulfilling this work.

Abstract

This thesis aims to reduce the energy consumption as well as greenhouse gases to the environment without negatively affecting the thermal comfort. In the present work, thermal, energetic and economic impacts of employing passive solar systems combined with energy conservation systems have been investigated. These energy systems have been integrated with a typical residential building located in three different climate zones in Europe and Middle East regions.

Hour-by-hour energy computer simulations have been carried out using TRNSYS and INSEL programs to analyze the performance of integrated energy systems. Furthermore, IESU software module has been developed to simulate a novel cooling unit using Phase Change Material (PCM). This unit is named as Indirect Evaporative and Storage Unit (IESU). Thereafter, complete economic equations for the Life Cycle Cost (LCC) criterion have been formulated. Furthermore this criterion has been optimized for different variables as a function of thermal parameters and economic figures from local markets.

An optimum design of both residential buildings and energy systems has great impact on energy consumption. In fact, results showed that the energy consumption is reduced by 85.62%, 86.33% and 74.05% in Berlin, Amman and Aqaba, respectively. Moreover, the LCC criterion is reduced by 41.85% in Berlin, 19.21% in Amman and 15.22% in Aqaba.

The macro economic analysis shows that once this research is applied in one million typical residential buildings in the selected climate zones, the annual avoided CO_2 emissions are estimated to be about 5.7 million Tons in Berlin. In Aqaba, around 2.96 million Tons CO_2 emissions will be saved annually and in Amman about 2.98 million Tons will be reduced. The payback period from the achieved saving is 18 years, 11 years and 8.6 years in Amman, Aqaba and Berlin, respectively.

Kurzfassung

Die vorliegende Arbeit dient der Minimierung des Energieverbrauchs von Wohngebäuden, ohne die thermische Behaglichkeit negativ zu beeinflußen und trägt damit zur Verringerung von CO_2-Emissionen bei. Es wurden thermische, energetische und wirtschaftliche Gesichtspunkte betrachtet. Der Einsatz von Passivsolarsystemen und Energieeinsparungssysteme wurde für typische Wohnhäuser mit einer Whonfläche vom 154 m^2 in Europa und dem Nahen Osten in drei verschiedenen Klimazonen untersucht.

Um die Performance der Energiesysteme zu analysieren, wurden Simulationsrechnungen mit den kommerziellen Programmpaketen TRNSYS und INSEL durchgeführt. Darüberhinaus wurde eine Verdampfungs- und Speichereinheit, die ein Phasenwechselesmaterial enthält simuliert. Zu diesem Zweck wurde ein Software Module in Visual Basic entwickelt und eingesetzt. Dieses Software Module heißt IESU software. Eine Gleichung zur Beschreibung der Lebenszykluskosten (LCC) wurde in Abhängigkeit thermischer Parameter und ökonomischer Faktoren der lokalen Märkte aufgestellt und eine Optimierungsrechnung durchgeführt.

Das optimale Design von Wohnhäusern und Energiesystemen hat großen Einfluss auf den Energieverbrauch. Die Ergebnisse zeigen, dass der Energieverbrauch um 85,62% in Berlin, um 86,33% in Amman und um 74,05% in Aqaba gesenkt werden kann. Darüberhinaus konnte das LCC Criterion in Berlin um 41,85%, in Amman um 19,21% und in Aqaba um 15,22% gesenkt werden.

Die makkroökonomische Analyse zeigt, dass eine Anwendung der präsentierten Methoden bei Million typischen Wohngebäuden die jährlich CO_2-Einsparungen in Höhe von 5,7 Mio.t in Berlin, 2,98 Mio.t in Amman und 2,96 Mio.t in Aqaba zur Folge hätte. Die Amortisierungszeit beträgt 18 Jahre in Berlin, 11 Jahre in Amman und 8,6 Jahre in Aqaba.

Publication

The present thesis is based on several previously published articles. They are:

Journal Papers

- Evaporative Cooling as an Efficient System in Mediterranean Region, 2011, Applied Thermal Engineering, 31(14-15):2590-2596.
- Optimum, Technical and Energetic Residential Building Design in Mediterranean region, 2011, Energy and Buildings, 43(8):1829-1834.
- Optimum Design of Trombe Wall System in Mediterranean Region, 2011, Solar Energy, 85(9):1891-1898.
- Thermal and Economic Windows Design for Different Climate Zones, 2011, Energy and Buildings, In Press.
- Novel Cooling Unit Using PCM for Residential Application, submitted to International Journal of Refrigeration.
- Optimum Design of Heat Recovery System in Mediterranean Region, 2012, Sustainable Cities and Society, In Press, Corrected Proof, Available online 25 January 2012.

Conference Papers

- Thermal and Economical Design of Low Energy House in Jordan, 2010, International Engineering Conference on Hot Arid Regions (IECHAR), Al-Ahsa - Kingdom of Saudi Arabia.
- Technical and Economical Comparison of Windows in Europe and Middle East, 2011, Global Conference on Renewable Energy Efficiency for Dessert Regions (GCREEDER), Amman - Jordan.
- Evaporative Cooling as an Efficient System in Mediterranean Region, 2011, Global Conference on Renewable Energy Efficiency for Dessert Regions (GCREEDER), Amman - Jordan.
- Thermal and Economical Investigation of Evaporative Air-Conditioning in Europe and Middle East, 2011, 4^{th} International Conference Solar Air-Conditioning, Larnaka - Cyprus.

Contents

List of Figures

List of Tables

Nomenclature

A : area (m^2)

a : Trombe wall area ratio (%)

C : cost (€)

$\dot{C}$: capacity rate (kJ/s.K)

C_p : specific heat (kJ/kg.K)

D_h : hydraulic diameter (m).

f : fraction (%)

g : acceleration gravity (m/s^2)

h : heat transfer coefficient (W/m^2K), height (m)

i : inflation rate (%)

k : thermal conductivity (W/m.K)

L : length (m).

$\dot{m}$: mass flow rate (kg/s)

m : mass (kg)

N : life time (year)

Nu : Nusselt number

P : perimeter (m), power (W)

P_c : conventional energy price (€/kWh)

Pr : Prandtl number

Q : energy (kWh)

$\dot{Q}$: heat (kJ/s)

R : thermal resistance (m^2K/W)

R^2 : coefficient of determination

r : interest rate (%)

Re : Reynolds number

T : Temperature (°C)

t : thickness (m)

U : overall heat transfer coefficient (W/m^2K)

$\bar{V}$: average velocity (m/s)

$\dot{V}$: volume flow rate (l/s)

w : percentage of windows' area from total façade area (%)

W : width

w : humidity ratio (kg_w/kg_a)

x : design variable

z : investment (€)

Δp : pressure drop (pa)

$\Delta\ T_{lm}$: log mean temperature difference (K)

Δt : length of time step (hour)

Greek Symbols

α_p : fictive convective heat transfer coefficient (W/m^2K)

ε : effectiveness (%)

η : efficiency (%)

λ : latent heat of fusion (kJ/kg)

υ : air velocity (m/s).

ρ : Density (kg/m^3)

Acronyms

ACH : Air Change per Hour

AREE : Aqaba Residence Energy Efficiency

ASHRAE : American Society of Heating, Refrigerating and Air conditioning Engineers

CBJ : Central Bank of Jordan

CLF : Cooling Load Factor

COP : Coefficient of Performance

DEAC : Direct Evaporative Air-Conditioning

DOS : Department Of Statistic

ERS : Energy Recovery System

HX : heat exchanger

IAQ : Indoor Air Quality

IEAC : Indirect Evaporative Air-Conditioning

IESU : Indirect Evaporative and Storage Unit

INSEL : INtegrated Simulation Environment Language

GDP : Gross Domestic Product.

GHG : Green House Gasses.

GRG : Generalized Reduced Gradient

KIRS : Kuwait Institute for Scientific Research.

LCC : Life Cycle Cost

NREL : National Renewable Energy Laboratory

NTU : Number of Transfer Units

PbP : Payback Period

PCM : Phase Change Material

PWF : Present Worth Factor

RSS : Royal Scientific Society

SC : Shading Coefficient

SHGC : Solar Heat Gain Coefficient

TOE : Ton Oil Equivalent

TRNSYS : TRaNsient SYstem Simulation

WBDE : Wet-Bulb Depression Efficiency

Subscripts

a : air

amb : ambient

aux : auxiliary

b : basic

c : ceiling, cooling

cond : conduction

conv : convection

d : diesel

e : exhaust, electricity, IEAC heat exchanger

E : East

f : film

f,m : fan and motor

h : heating

i : inner, inlet, time step

i.c : initial cost

ins : insulation

m : maintenance, mean, melting

max : maximum

min : minimum

N : North

o : outer, outlet

p : PCM heat exchanger

pi : primary inlet

po : primary outlet

r : room

r.e : running energy

S : South

s : supply, saving

si : secondary inlet

so : secondary outlet

salv : salvage

tr : transmission

T.W : Trombe Wall

W : West

w : wall

wb : wet-bulb

Chapter 1

Introduction

The present study involved thermal and economic impact of employing passive and energy conservation systems for residential buildings as first step. Thereafter, technical and economical optimization of a novel cooling system integrated with Phase Change Material (PCM) has been investigated.

1.1 Background

These days, the energy supply and demand coupled with pollutants emission is one of the greatest threats. The share of electric energy consumption will increase from 16% in 2002 to 20% in 2030. The coal-fired power plants generate 45% of the developing world energy requirement and will increase to 47% in 2030. The world Gross Domestic Product (GDP) is expected to be 3.2% from 2002 to 2030. The 1% increase of the GDP corresponds to 0.6% increase of the primary energy consumption [10]. This will emit a lot of Green House Gases (GHG) particularly CO_2.

Energy consumption is directly related to population size. The present population is 6.2 billion and expected to grow 1% yearly. Thus, the population size will be 8.1 billion in 2030. Migration of population from the rural areas to urban centers will happen and tends to further increase the energy demand [11].

The cost of heating and cooling our houses is becoming a larger component of the average household budget, since most modern houses are not designed with energy conservation in mind. Most houses are too cold in winter and become too hot in summer.

After 1973 energy crises, interest in designing buildings with significantly less energy has rapidly increased. Such buildings often employ bio-climatic designs in which the principles of "design with climate" are integrated with modern building technology and materials, incorporating energy efficiency and renewable energy technologies [12].

For the long-term future, ensuring the security of energy supplies is a highly important issue. The main aim is to draw attention to the possibilities and measures for the appropriate development of energy resources towards the establishment of a "self-dependence energy policy". Furthermore, with the increase in oil prices renewable energy sources as well as energy conservation systems will soon become economically feasible if research and development efforts concentrate on cost reduction of these systems, i.e., development of cheaper materials, simpler and more efficient systems in conjunction with storage technologies.

1.2 Problem Identification

It is now universally conceded that fossil fuel resources in the world are finite and it is only a matter of time before reserves will essentially be depleted. Jordan is an energy-importing country, about 98.8% of its needs being supplied from abroad as crude oil, gas and refined products. The imported fuel in Jordan totaled to 5.082 million Tons Oil Equivalent (TOE) in 2010. The energy consumption in residential sector consists about 21%, as shown in Figure (1.1).

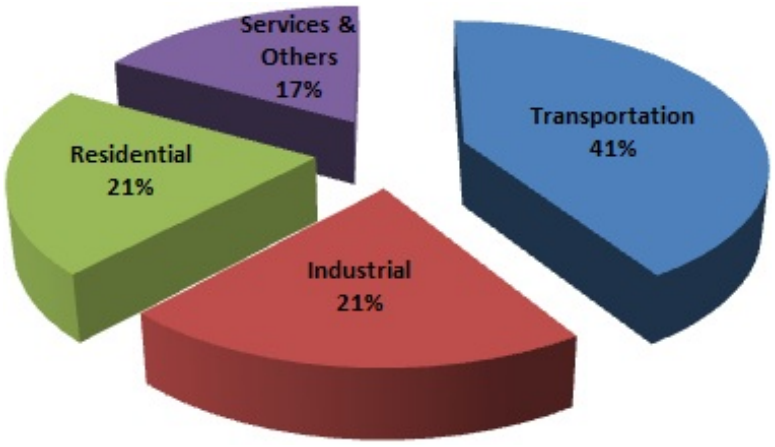

Figure 1.1: Energy Consumption By Sector in Jordan [1]

On the other hand, solar energy is the origin of most renewable energies on earth. The annual daily average solar irradiance in Jordan (average insulation intensity on a horizontal surface) ranges between 5 - 7 kWh/m^2. This corresponds to a total annual of 1600 - 2300 kWh/m^2. The average sunshine duration is more than 300 days per year [13], nevertheless the use of solar energy sources in Jordan is very low.
In addition, building technology in Jordan pays little attention to the climatic and thermal design, which gives buildings suffering from design related problems, where the indoor climate of these buildings does not provide the required comfort levels for

their occupants. Most designers do not consider climate as one of the main criteria in their design of buildings. Consequently, many of these buildings don't provide the occupants with a comfortable environment, which satisfies their aspiration. In order to achieve the aspired comfortable environment, high energy consumption is needed which put too much pressure on the Jordanian economy.
In fact, air cooling and heating equipment contribute a lot of GHG [14]. Using traditional air-conditioning during Summer period in Jordan is becoming very popular especially last two years due to climate change. These systems consume huge amount of electrical energy that is largely dependent upon fossil fuel which leads to increase the amount of CO_2 emissions. The air-conditioning can be used in all climates but it is expensive as well as its highly running cost. Thus, this type of air-conditioning is neither sustainable nor environment-friendly.
Moreover, Jordan has a rapid population growth, 2.2% per annum [15]. From one side, the human demand for better and comfortable condition is getting high. From another side, urbanization is happening; migration of population from the rural areas to urban centers. Furthermore, the global environmental problem is a serious one.
All above problems are complex as there are many parameters and considerations to be deeply looked into. These problems have become globally political, economic and technological problems. Hand in hand solutions for these problems are a must to attain a common goal.

1.3 State of Art

In 1981 the Royal Scientific Society (RSS)/Jordan and the Kuwait Institute for Scientific Research (KISR) performed a joint project to study the possibilities of solar heating and cooling in buildings. To meet the objectives of this project, a house was designed and built at RSS location in Amman. It was concluded that the heating demand was reduced by about 50% when passive and active design criteria were considered. Tests showed that the space heating isn't economically feasible [13].
Aqaba Residence Energy Efficiency (AREE) building was the first sustainable residential building in Aqaba-Jordan. The construction began in early 2007 and was completed in 2008. The building accommodates 420 m^2 of residential space. The design and construction method saves 30% of the cooling load when compared to a conventional residential building. Furthermore, sustainable solar cooling concept "adsorption cooling" was applied. This is the first application of a solar cooling installation in Jordan and it is a promising concept. The solar cooling system led to total savings on electricity costs of 72%. The expected Payback Period (PbP) of solar cooling system is less than nine years [16].

Number of passive residential buildings around the world in late 2008 is estimated from 15,000 to 20,000 buildings [17; 18]. In August 2010, there were approximately 25,000 certified buildings in Europe, while in the United States there were only 13 buildings [19]. The first passive house residence was built in Darmstadt, Germany in 1990, and occupied by the clients by the following year.

Schnieders addressed the question "Which measures are required in order to achieve a typical solution for a heat load of 10 W/m^2?". The results show that for Germany, typical passive house windows with an overall U-value of 0.85 W/m^2K must be used and U-values for the walls have to be about 0.13 W/m^2K. For Vienna more insulation is needed to achieve a heat load of 10 W/m^2. For Norway, insulation levels are chosen similar to Germany. Since minimum temperatures during the night may be as low as -25°C in Oslo, a very good insulation and further optimized windows are required. Helsinki (Finland) climate combines two difficulties; very low temperatures and radiation levels close to zero in December and January. In order to build passive houses in Helsinki, extremely good insulation, small, highly insulated windows and a compact building shell are required [20].

Mathematical model for estimating building cooling load was developed by Ansari *et al.* [21]. The effect of significant building parameters like orientation, window glass shade type, number of glass panes, wall insulation, roof type and floor type can be easily investigated by his model. Bokel [22] calculates the yearly energy demand for heating, cooling and electric lighting as a function of window position, window size and window shape for an office environment in the Netherlands.

A systematic approach for optimization of insulation material thickness was developed and applied in Palestine by Hassan [23]. In Hong Kong, thermal insulation is seldom applied to the fabric of high rise residential buildings as noted by Bojic *et al.* [24]. The detailed building heat transfer simulation program HTB2 was employed to calculate the yearly cooling loads and the maximum cooling demand in an insulated high rise residential building. Ucar [25] obtained the optimum insulation thickness for various cities from four climate zones of Turkey, namely, Antalya, Istanbul, Elazig and Erzurum. On the other hand, Yu [26] investigated the optimum thicknesses of five insulation materials including expanded polystyrene, extruded polystyrene, foamed polyurethane, perlite and foamed polyvinyl chloride are calculated with a typical residential wall.

Many theoretical and experimental studies have shown that indoor comfort is improved as well as reduction in annual heating energy due to a well designed Trombe walls [27; 28; 29; 30]. Chel *et al.* [31] estimated the passive heating potential of Trombe wall for a honey storage building by using TRNSYS building simulation software. It was concluded that energy conservation up to 3,312 kWh/year can be achieved. PbP was assumed to be about 7 months [31]. Fernández-González [32] presents a summary of the

thermal performance of five different passive solar test-cells (Direct Gain, Trombe wall, Waterwall, Sunspace, and Roofpond) during 2002 - 2003 heating season in Muncie, Indiana. Fernández-González [32] concluded that Trombe wall produces an extremely stable indoor environment with low variation in the operating temperature. Furthermore, Trombe walls have been integrated into the envelope of a recently completed Zion Visitor Center at Zion National Park, Utah and the Solar Energy Research Facility and the National Renewable Energy Laboratory (NREL) Visitor Center in Golden, Colorado. The wall is 44% of the total South facing wall area. In the Visitor Center, 20% of the annual heating was supplied by Trombe wall [33].

The impact of Energy Recovery System (ERS) on annual cooling and heating energy consumption is investigated in a different research [34; 35; 36; 37]. Fehrm *et al.* [36] showed that heat recovery system lowered the primary energy consumption by 19.4% and CO_2 emissions by 18.4%. Moreover, Membrane-based Energy Recovery Ventilator could save about 58% of the annual energy required for conditioning fresh air in hot and humid regions [38]. Furthermore, the impact of ERS on annual cooling and heating energy consumption is investigated by modeling a 10-storey office buildings in four US cities representing four different climatic conditions by using TRNSYS simulation program [39]. Results showed that depending on the climate and system effectiveness, the operation of ERS with capability of moisture recovery reduces the annual heating energy consumption by 40% during heating season. Furthermore, when ERS operated under the proposed optimum control, up to 20% annual cooling energy was saved depending on location and ERS effectiveness.

Direct Evaporative Air Conditioning (DEAC) has been discussed in open literature [40; 41]. The disadvantages of such system are the noise, difficult in controlling the interior temperature, and the quality of conditioned air due to adding moisture to the air. To improve the comfort level of conditioned air, the indirect Evaporative Air Conditioning (IEAC) is introduced [41; 42; 43; 44]. Maheshwari *et al.* [45] investigated IEAC in coastal and interior locations in Kuwait. The seasonal energy savings of IEAC were 12,418 and 6,320 kWh for the interior and coastal areas, respectively. This paper didn't take the water consumption into consideration. Moreover, all energetic advantages had been evaluated by an economic point of view, in terms of net present worth and discounted PbP of the investment, by Lazzarin and Noro [46]. They concluded that evaporative cooling techniques are energy saving for a wide range of climates.

Thermal energy storage in general, and PCMs in particular, have been a main topic in research for the last 20 years [47; 48; 49; 50; 51; 52; 53; 54; 55]. The current research for PCM application in buildings has been focused on three fields. The first one is the reduction of temperature swings of light-weight buildings by increasing their thermal mass [48; 56; 57; 58]. The second one is the cooling of buildings through intermediate

storage of cold from the night ventilation [59; 60; 61; 62; 63; 64; 65; 66; 67; 68; 69; 70; 71; 72; 73; 74]. The third one of application is for heat storage in space heating systems [75]. The free cooling technique by using PCMs in buildings can provide better indoor thermal comfort, and help reduce the need of air-conditioning use and sizes [70; 71; 73; 74]. However, this concept is only feasible in climate conditions with relatively large temperature differences between day and night in Summer [65; 66].

1.4 Scope of Investigation

Low energy building combines state of the art and energy efficient construction in order to minimize energy consumption of conventional energy. As building design needs to consider other requirements and constrains (architectural functions, indoor environmental conditions, and economic effectiveness), a pragmatic goal of this research is to provide the occupants with thermal comfort at least cost.

As first step ideal energy conservation building envelop can be achieved by optimization of thermo-physical properties to increase decay and delay affects and to meet the requirements of human thermal comfort. Thus, the passive use of solar energy is optimized by the orientation and layout of the building. Then, the optimum type and size of windows in all façades will be investigated, the thermal insulation thickness of external walls and ceiling will be studied in three scenarios in order to find the technical and economic optimum thickness. Movable shades are used to prevent solar warming in Summer period, but allow for solar heat to enter during Winter to minimize the heating load.

Trombe walls are among the important passive solar systems. Thermal, environment and economic impact of Trombe wall system for residential building will be investigated in this work. The annual energy demand will be estimated while both thermal insulation thicknesses added to the walls and ceiling as well as the Trombe wall area ratio are varied.

The applicability of Energy Recovery System (ERS) will be extensively studied. Meanwhile, through a residential building, the amounts of heating and cooling loads will be analyzed and compared for different ERS heat transfer areas. Moreover, economic impact of employing ERS will be investigated. This work hasn't discussed before especially for Middle East.

Technological innovation is needed for future sustainable energy systems [76]. Furthermore, the whole issue of storage in a technico-economic context isn't found in the reviewed papers [77]. Thus, in this research new unit will be designed and optimized to maintain thermal comfort inside the building. IEAC will be integrated with PCM heat exchanger to give a novel unit called Indirect Evaporative and Storage Unit (IESU).

This unit will cool the building through cheap source as well as store cold in PCM. Code will be written to simulate the hourly performance of IESU. To author knowledge, there are no studies about IESU in the open literature. IESU will be very promising unit with respect to energy saving.
An optimum size of passive solar systems, ERS and IESU in residential buildings will be determined by using Life Cycle Cost (LCC) criterion. PbP will be calculated beside LCC criterion. This optimization will be estimated using economic figures from local markets. This will lead to develop an approach for designing the most economic residential building.
Finally, a comparison of thermal and economic impact of employing passive solar systems, ERS and IESU in residential buildings in three different climate zones in Middle East and Europe will be illustrated.
This research, if applied, will improve building situation and saving money due to reduction in energy consumption from non-renewable energy sources. Also, it is expected to reduce CO_2 emission, which leads to reduce the pollution, due to reduction of fuel consumption for heating and cooling purposes. Furthermore, such building is designed to continue functioning even during blackouts and improved human comfort by reducing temperature fluctuations. In addition, criteria for the design and construction of building in Mediterranean and Europe climate will be developed to enhance the thermal performance of future residential buildings.

1.5 Phase Change Material

PCM's are a substance in which the heat at the solid-liquid phase transition point is used in applications for storing large amounts of thermal energy at a certain temperature [78]. The first best-known PCM is water. It has been used for cold storage for more than 2000 years. Nowadays, cold storage with ice is state of the art and even cooling with natural ice and snow is used again.
The phase change solid-liquid by melting and solidification can store large amounts of heat or cold within a very narrow temperature range, if a suitable material is selected. Melting is characterized by a small volume change, usually less than 10%. If a container can fit the phase with larger volume change the pressure isn't changed significantly [78]. Table (1.1) shows a comparison between the sensible (rock bed and water tank) and latent (organic and non-organic PCM) heat storage. The advantage of the latent heat over the sensible heat is clear from the comparison of the volume and mass of the storage unit required for storing a certain amount of heat. It is also clear from Table (1.1) that inorganic compounds, such as hydrated salts, have a volumetric thermal storage density higher than organic compounds due to their higher latent heat and density.

Table 1.1: Comparison Between Different Methods of Heat Storage [8]

Property	Rock	Water	Organic PCM	Inorganic PCM
Density (kg/m^3)	2,240	1,000	800	1,600
Specific heat (kJ/kg)	1.0	4.2	2.0	2.0
Latent heat (kJ/kg)	-	-	190	230
Latent heat (kJ/m^3)	-	-	152	368
Storage mass for 10^6J (kg)	67,000	16,000	5,300	4,350
Storage volume for 10^6J (m^3)	30	16	6.6	2.7
Relative storage mass	15	4	1.25	1.0
Relative storage volume	11	6	2.5	1.0

1.5.1 Properties

PCM's to be used for thermal energy storage must have a large latent heat and high thermal conductivity. They should have a melting temperature lying in the practical range of operation, melt congruently with minimum subcooling and be chemically stable, low in cost, nontoxic and non-corrosive [79].
PCM's have been studied during the last 40 years are: hydrated salts, paraffin waxes, fatty acids and eutectics of organic and non-organic compounds. The melting temperature and enthalpy of these materials are shown in Figure (1.2). A close look at this Figure indicates that energy density is roughly proportional to the melting temperature.

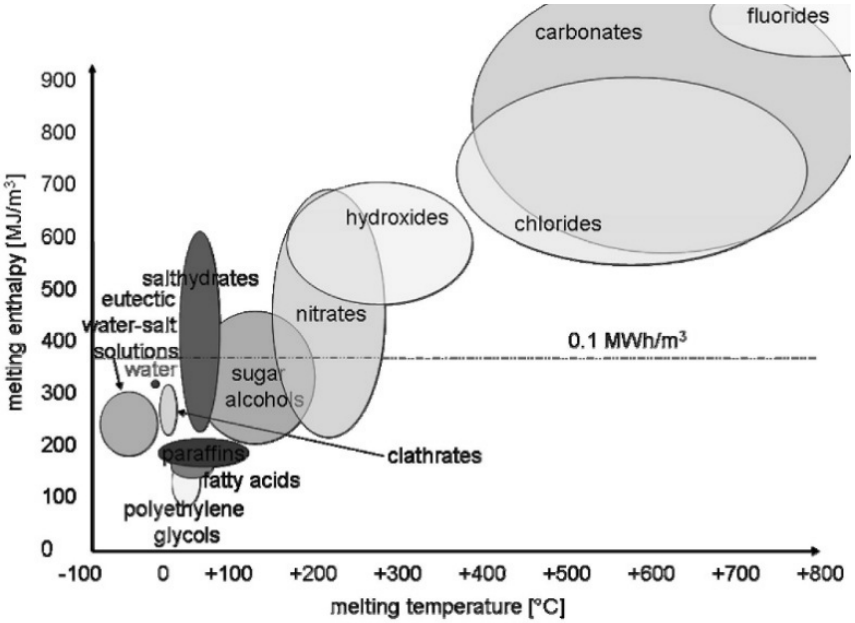

Figure 1.2: Typical Range of Melting Temperature and Melting Enthalpy for Different PCMs (ZAE Bayern)

The most common groups of PCMs are organic and inorganic compounds. Inorganic materials, as shown in Figure (1.2), cover a wide temperature range such as water at 0°C, aqueous salt solutions at temperature below 0°C, salt hydrate between about (5 - 130)°C and different salts at temperature above 150°C. Their density are usually larger than 1 g/cm^3 so their melting enthalpy per volume are larger than organic materials. On the other hand, organic materials cover a smaller temperature range from (0-150)°C. The popular example of organic materials is paraffins, fatty acids and sugar alcohols. Most organic PCMs are non-corrosive, chemically stable and do not subcool. Their disadvantages are low thermal conductivity and their flammability. Inorganic compounds have a higher latent heat per unit volume than organic PCMs, high thermal conductivity, are non-flammable and low in cost in comparison to organic compounds. However, they are corrosive to some metals and suffer from decomposition and subcooling, which can affect their phase change properties. The applications of inorganic PCMs require the use of nucleating and thickening agents to minimize subcooling and phase segregation. [79].

1.5.2 Applications

Potential fields of application for PCMs can be found directly from the basic difference between sensible and latent heat storage [2], as shown in Figure (1.3). Heat can be supplied or extracted from a latent heat storage material without significant temperature change. Therefore; PCMs can be applied to stabilize the indoor temperature in a building.

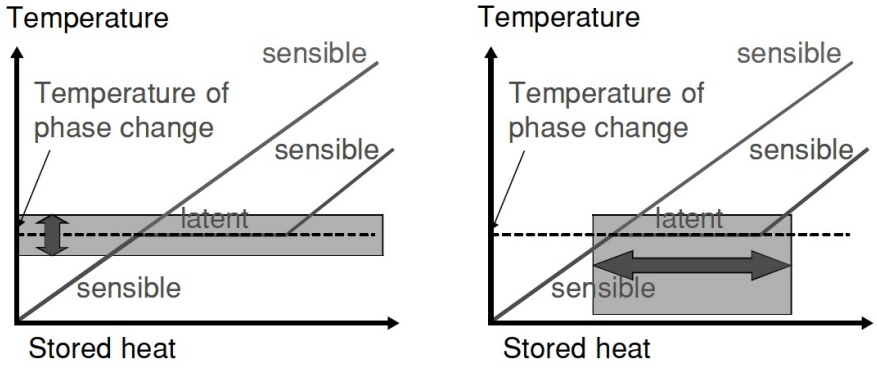

Figure 1.3: Potential Fields of PCM Applications: Temperature Stabilization (Left) and Storage of Heat or Cold with Small Temperature Change (Right) [2]

There are three goals of PCMs application in building; the first is reducing temperature swings of lightweight building by increasing their thermal mass, the second is using natural heat and cold sources (solar energy for heating or night cold for cooling), and the third is using manmade heat or cold sources. Accordingly, PCMs application in

building can be classified into two main systems; passive and active storage system. The passive storage system matches the first goal where the active storage system matches the second and third goals. These applications are summarized in Figure (1.4). This research will add new application (IESU) to this Figure which will be widely discussed in Chapter 5

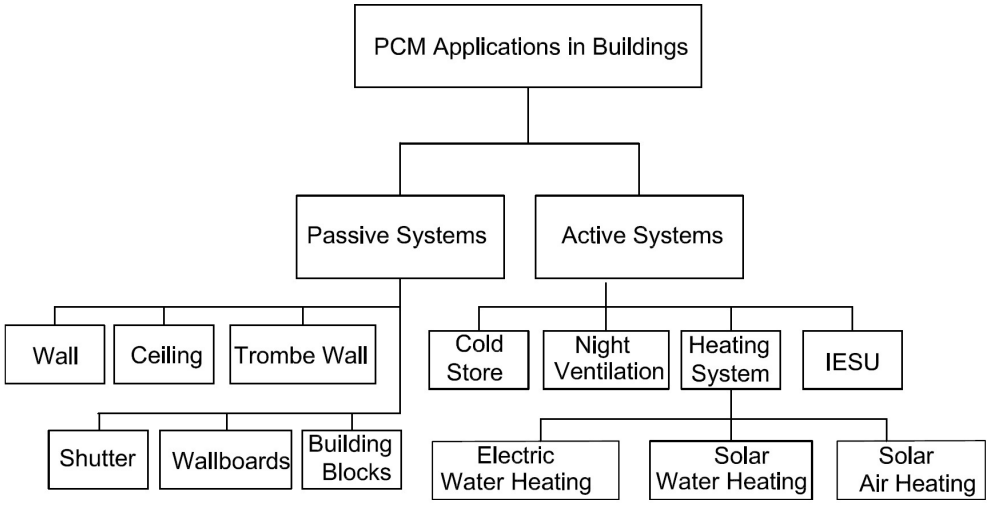

Figure 1.4: PCMs Applications in Buildings

1.5.3 Commercial PCMs

More than 50 PCMs are commercially available from the following companies:

- PCM Energy P. Ltd in India (http://www.pcmenergy.com/).
- RUBITHERM GmbH in Germany (http://www.rubitherm.de/).
- Climator AB in Sweden (http://www.climator.com/).
- CRISTOPIA Energy Systems in France (http://www.cristopia.com/).
- Dörken GmbH & Co. KG in Germany (http://www.doerken.de/).
- Mitsubishi Chemical in Japan.

Figure (1.5) shows an overview of commercial PCMs with their melting temperature and melting enthalpy per volume and mass. The prices of commercial PCM vary between 0.5 - 10 €/kg. For a rough estimate an energy price of 0.1 €/kWh for heat can be assumed. This means that 3600 kJ cost 0.1 €. From Figure (1.5), an average storage density of a PCM is 180 kJ/kg. Therefore 20 kg of PCM are necessary to store 1 kWh.

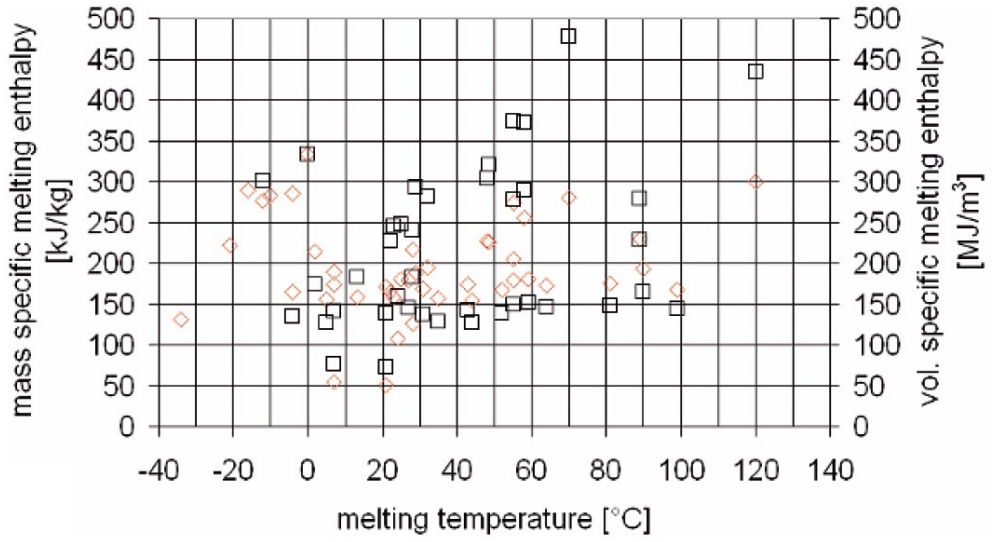

Figure 1.5: Phase Change Temperature and Enthalpy Per Volume (□) and Mass (⋄) of Commercial PCM (ZAE Bayern)

The initial cost of PCM (additional investment cost for the storage tank, heat exchanger and the stored heat, which is also never completely free, have not even been taken into account) needed to store required heat ranges between 10 - 200 €. So, a number of 100 - 2000 storage cycles are necessary. Therfore; seasonal storage using PCM is far from being economic at current energy prices. To be competitive in energy systems, one should try to charge and discharge a storage daily, or in even shorter periods.

1.6 Thermal Performance Calculation Methods

There are several methods that can be used for estimating thermal performance of buildings and systems, such as:

1.6.1 Simulation Methods

Simulations are numerical procedure which may give the same kind of thermal performance information as can physical experiments. In these methods, a mathematical model is established by using meteorological data, results are then considered to represent longer term performance. That model is then solved by a computer algorithm as a simulation process.
Simulations are uniquely suited to parametric studies and thus offer, to the process designer, the capability to explore the effects of design variables on long-term system performance [80]. They offer the opportunity to evaluate effects of system configuration and alternative system concepts. They have the advantage that the weather used to

drive them is reproducible, allowing parametric and configuration studies to be made without the uncertainties of variable weather. By the same token, a system can be operated by simulations in a wide range of climates to determine the effects of weather variation on its performance.
Simulation programs are research tools for exploring systems that are not well understood or that are too complicated to be described by short-cut methods. Many simulation software's are widely used such as, Carrier, DEROB-LTH, TRNSYS, Energy Plus, INSEL ... etc.

1.6.2 Short-Cut Method

Short-cut methods are ones of the design methods which include correlations of the results of a large number of detailed simulations. The results of many simulations are correlated in terms of easily calculated dimensionless variables.

1.7 Economic Evaluation Criteria

Several evaluation tools can be considered, to evaluate the cost-effectiveness of energy projects. Life Cycle Cost (LCC) and Payback Period (PbP) are the most common evaluation methods used in engineering projects.

1.7.1 Payback Period

This evaluation method measures the elapsed time between the point of an initial investment and the point at which accumulated savings are sufficient to offset the initial investment. PbP is the length of time it takes for an initial investment to be repaid out of the net cash inflows from a project [81]. At the end of PbP, the system has paid for the initial investment and any revenue produced thereafter is pure gain. Thus, PbP in years is equal to;

$$PbP = \frac{C_{i.c}}{C_s} \tag{1.1}$$

where;

$C_{i.c}$: initial cost (€)

C_s : annual saving (€).

PbP isn't the correct criterion for evaluating energy investments. It fails to account for system life, discount rate, fuel inflation, and benefits accrued during the remainder of the lifetime. Using payback period without any other economic tools can be misleading and economists have been unanimous in rejecting it.

1.7.2 Life Cycle Cost

Life Cycle Cost (LCC) is the sum of all costs associated with an energy delivery system over its lifetime in today's dollars and takes into account the time value of money [80] or;

$$LCC = \frac{Q_{aux.}P_c}{\eta_{aux}} \times PWF + C_{i.c} \tag{1.2}$$

where;

$Q_{aux.}$: annual auxiliary energy (kWh).

P_c : conventional energy price (€/kWh).

η_{aux} : auxiliary system efficiency (%).

PWF : Present Worth Factor.

When operating, maintenance and salvage values are taken into account, LCC can be written as [80];

$$LCC = \frac{Q_{aux.}P_c}{\eta_{aux}} \times PWF + C_{i.c}(1 + f_m PWF - (\frac{1+i}{1+r})^N f_{salv}) \tag{1.3}$$

where;

f_m : maintenance (%).

f_{salv} : salvage value (%).

i : inflation rate (%).

r : interest rate (%).

N : life time (year).

1.8 Optimization Method

The objective of optimization is to select the best possible decision for a given set of circumstances without having to enumerate all of the possibilities. The subject which formulates and explains this talent is a branch of applied mathematics known as optimization theory, a science that studies the best [82].
Three basic components are required to optimize building LCC. First, the mathematical model of the annual energy consumption as a function of energy systems variables, which can be manipulated and controlled. Second, an economic model of the building's

LCC is required. Finally, an optimization method must be selected which locates the values of the independent variables of the building's LCC to produce the minimum cost as measured by the economic model.

1.8.1 Graphical Optimization

Optimization problem can be solved by observing the way they are graphically represented. All constraint functions are plotted, and a set of feasible designs for the problem are identified. Objective function contours are then drawn and the optimum design is determined by visual inspection [83].

1.8.2 Numerical Methods

There are several methods can be used to solve constrained non-linear optimization problems numerically. The successful methods are; successive linear programming, successive quadratic programming and the Generalized Reduced Gradient (GRG) method [84].
In 1967, Wolfe developed the reduced gradient method based on a simple variable elimination technique for equality constrained problems [85]. GRG method is an extension of a reduced gradient method which is based on extending linear constraints method to apply to nonlinear constraints [86].
GRG method ranked best among 15 codes from industrial firms and universities in USA and Europe [87]. On the other hand, GRG ranked the second among 22 optimization programs and 180 test problems [88].
To find $\mathbf{x} = (x_1, x_2, \ldots, x_n)$, a design variable vector of dimension n, to minimize a cost function;

$$f(\mathbf{x}) = f(x_1, x_2, \ldots, x_n) \tag{1.4}$$

Subject to the m equality constraints

$$h_1(\mathbf{x}) \equiv h_1(x_1, x_2, \ldots, x_n) = 0 \tag{1.5}$$

.....

$$h_m(\mathbf{x}) \equiv h_m(x_1, x_2, \ldots, x_n) = 0 \tag{1.6}$$

GRG method uses a repeated sequence of steps that starts on the constraints, moves tangent to the constraints in a favorable direction with respect to f(x) and returns to the constraints. The individual steps for a problem of n variables and m constraints are as follows [83]:

1. Starts with trial point within the constraints, $\mathbf{x}^{(0)}$. Such a position may be located by arbitrarily n-m variables, substituting these variables into the m constraints and solving for the n variables by using analytical technique for constrains such as Newton-Raphson technique.

2. At the point on the constraints compute components of the gradient vector ∇f, $\nabla h_1 \ldots \nabla h_m$.

3. Apply the reduced gradient concept to move tangent to the constraints in a favorable direction with respect to f(x). If the step size chosen results in a less favorable value of f(x) than existed at the starting point, reduce the step size.

4. Return to the constraints by adjusting n of the variables through application of Newton-Raphson to the m simultaneous equations provided by the constraints.

5. If in the process of returning to the constraints the value of f(x) is degraded relative to its value at the starting point, return to Step 3 with a smaller step size.

6. If no improvement is possible with a sufficiently-small step size, terminate, otherwise, return to Step 2.

The central feature of the GRG method is Step 3, which determines the direction that is tangent to the constraints and at the same indicates a favorable direction for f(x). Newton-Raphson method is used to perform the direction of design change in multi-dimensional problems.
The basic idea of the Newton-Raphson method is to use second-order Taylor's series expansion of the function about the current design point. This gives a quadratic expression for the change in design $\nabla\mathbf{x}$. The necessary conditions for minimization of this function then give an explicit calculation for the direction of travel in the design space. Proper step length in this direction then completes one iteration of the method. The second-order Taylor series expansion for the function f($\mathbf{x}$);

$$f(\mathbf{x} + \nabla\mathbf{x}) = f(\mathbf{x}) + f(\mathbf{x})\nabla\mathbf{x} + 0.5\nabla^2 f(\mathbf{x})\nabla\mathbf{x}^2 \tag{1.7}$$

is minimized when $\nabla\mathbf{x}$ solves the linear equation;

$$f(\mathbf{x}) + \nabla^2 f(\mathbf{x})\nabla\mathbf{x} = 0 \tag{1.8}$$

The second derivative, $\nabla^2 f(\mathbf{x})$, is positive which provide that f($\mathbf{x}$) is a twice differentiable function. By reciprocal $\nabla^2 f(\mathbf{x})$ with the inverse of the Hessian matrix, H f($\mathbf{x}$),

the sequence $\mathbf{x}_n$ defined by;

$$\mathbf{x}^{(k+1)} = \mathbf{x}^{(k)} - [Hf(\mathbf{x})]^{-1}\nabla f(\mathbf{x})k \geqslant 0 \tag{1.9}$$

Equation (1.9) will have to be repeated to obtain improved estimates until the minimum is reached ($\mathbf{x}_n^*$). The geometric interpretation of Newton-Raphson method is that at each iteration one approximates f($\mathbf{x}$) by a quadratic function around $\mathbf{x}^{(k)}$, and then takes a step towards the minimum of that quadratic function.

1.9 Nonlinear Regression Analysis

Regression analysis gives information on the relationship between a response (dependent) variable and one or more (predictor) independent variables to the extent that information is contained in the data. The goal of regression analysis is to express the response variable as a function of the predictor variables. The duality of fit and the accuracy of conclusion depend on the data used.
Least Squares Method is the most popular method of parameter estimation for coefficients of regression models. It has well known probability distributions and gives unbiased estimators of regression parameters with the smallest variance [89].
Response of n data points (x_1, y_1), (x_2, y_2), ... (x_n, y_n) is predicted by a regression model given by

$$y = f(x) \tag{1.10}$$

where, the function *f(x)* is nonlinear and has regression constants that need to be estimated.
A measure of goodness of fit that is how the regression model *f(x)* predicts the response variable y is the magnitude of coefficient of determination (R^2) [89].

$$R^2 = 1 - \frac{\sum(f(x_i) - y_i)^2}{\sum(y_i - \bar{y_i})^2}, i = 1, 2, ...n \tag{1.11}$$

Ideally, R^2 equal to 1 means that an equation have been found in which all the points lie on a model.

1.10 Selected Tools for the Present Work

TRNSYS Simulation software is an acronym for a TRaNsient SYstem Simulation program. TRNSYS is a complete and extensible simulation environment for the transient

simulation of systems, including multi-zone buildings. It is to validate new energy concepts, from simple domestic hot water systems to the design and simulation of buildings and their equipment, including control strategies, occupant behavior, alternative energy systems and hydrogen systems [7]. The calculations are influenced by climatic factors such as outdoor temperature, solar radiation and relative humidity. Indoor climate properties of the building, annual heating and cooling energy and performance of Trombe wall system will be calculated by TRNSYS.
INSEL is an acronym for INtegrated Simulation Environment Language. It provides an integrated environment and a graphical programming language for the creation of simulation applications [4]. A full set of models for the simulation of ERS, which is implemented in the inselST toolbox, will be used to investigate the performance of ERS.
TRNSYS and INSEL softwares are coupled to each other. TRNSYS produces an hour per hour heating and cooling load files in addition to indoor climate properties files of the building. On the other hand, INSEL software produces the modified inlet air temperature due to introducing ERS or IEAC. Then, this temperature is used as input in TRNSYS to calculate the new hourly heating load, cooling load and indoor climate properties.
Since IESU is new unit in energy field; there is no research tool available in the open literature to simulate its performance. Thus, IESU software module will be developed using Visual Basic 6.0.
Finally, a complete economic equations for the LCC criterion will be formulated in order to calculate the optimum size of passive systems, ERS and IESU. Graphical and numerical method based on GRG method will be used to find the design parameters at minimum LCC. Moreover, PbP will be calculated beside LCC criterion.

1.11 Greenhouse Gas Emissions Reduction

The Kyoto protocol is one of the world's efforts to diminish Greenhouse Gas (GHG) emissions that contributes greatly to the global warming. There is a strong evidence for this, notably the correlation between CO_2 and the rise in global temperature and some argue that this is not an emissions problem, but rather a larger sustainable energy problem. Therefore, reducing the conventional energy consumption would likely lead to a reduction in CO_2 emissions and help slow global warming.
The calculated value of GHG emissions (kg-CO_2/year) is determined by multiplying the calculated energy savings by the emissions factor (kg-CO_2 /kWh). GHG emissions factor can be based upon the performance of an incremental generating unit (i.e. a natural gas-fired combined cycle power plant) or be based upon the average emissions

performance of a mix of utility and non-utility generating plants.
The emissions factor for diesel is assumed about 229.9 g-CO_2 /kWh, while for electricity is assumed about 588.3 g-CO_2 per kWh [90].

Chapter 2

Building Model

This chapter describes the typical residential building which will be thermally and economically designed to achieve lower energy consumption at reasonable cost.

2.1 Building Prototype

As mentioned by Department of Statistic (DOS), type of building called "Dar" in Jordan represents about 72% of the total residential building in Jordan [91]. Thus, the model in this study is considered as typical Jordanian residential building "Dar" and it can be described as follows:

- The building is a rectangular shape located in Amman region, well insulated according to Thermal Insulation Code [5].
- The floor area is about 154 m^2 and ceiling height is 3 m. It consists of three bedrooms, living room, guest room, kitchen and three bathrooms, as shown in Figure (2.1) and Figure (2.2).
- Number of occupants is 6 persons.
- The overall heat transfer coefficient (U) is 0.398 W/m^2K and 0.469 W/m^2K for wall and ceiling, respectively.
- All windows are aluminum-framed (U = 2.27 W/m^2K), sliding with tight double glazing (U = 2.83 W/m^2K and SHGC = 0.775).
- The specific energy consumption is 88.08 kWh/m^2.

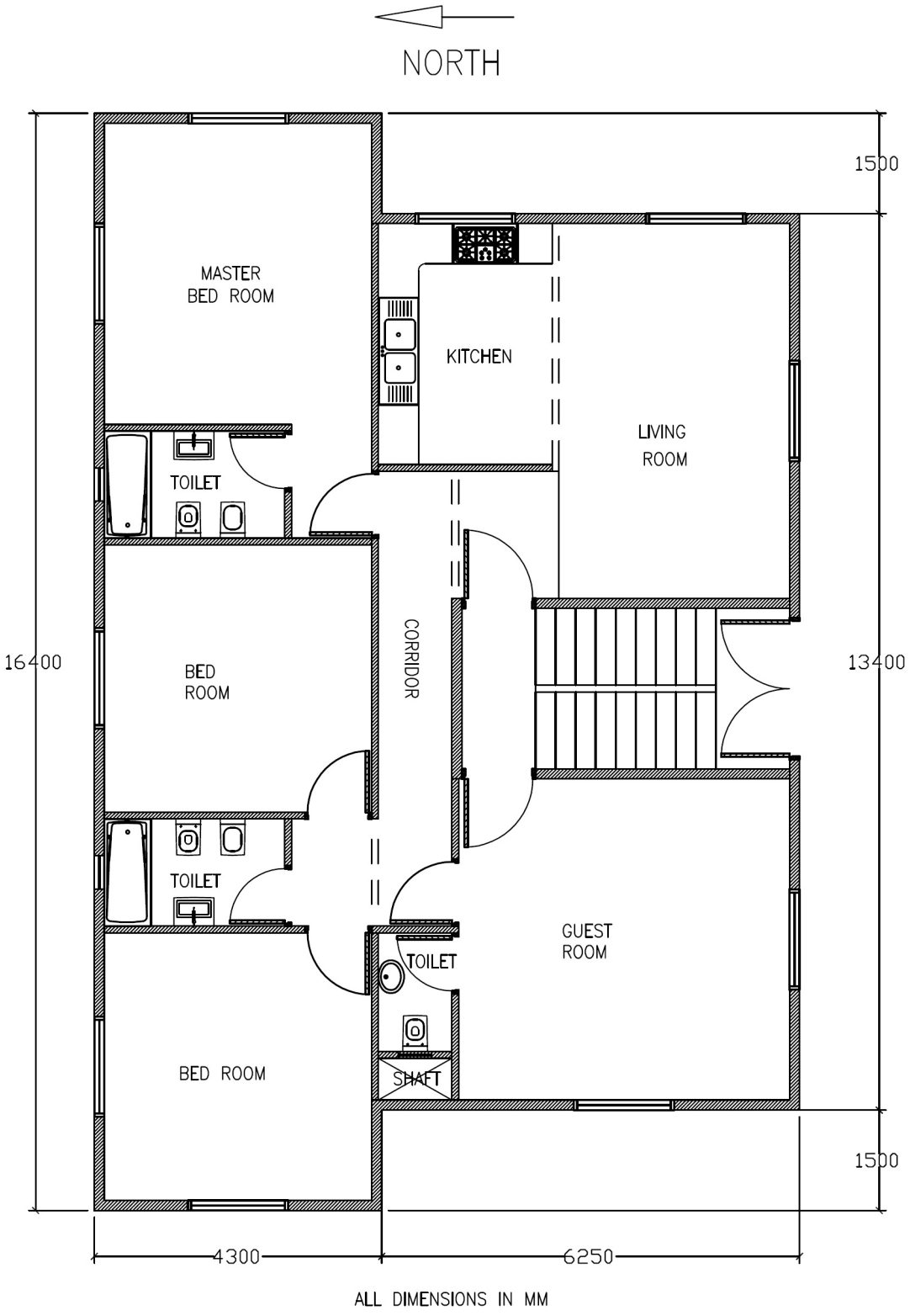

Figure 2.1: Selected Building Plan

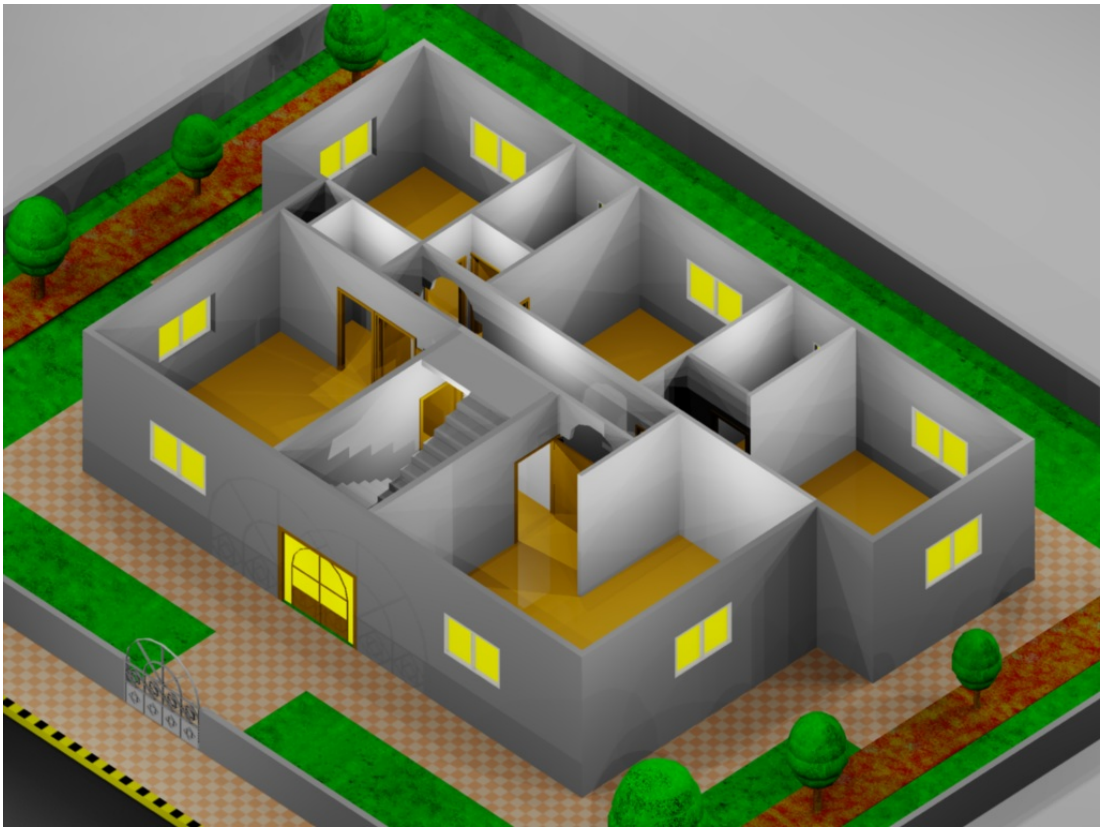

Figure 2.2: An Isometric View for the Selected Building

2.2 Design Conditions

The initial step in the load calculation is selecting indoor and outdoor design conditions. These conditions will be described in the following sections.

2.2.1 Indoor Design Conditions

Heating and cooling in buildings are strongly connected to human comfort requirements. The criteria considering the human comfort with respect to indoor climate relates to the heat exchange between the human body and the environment via thermal conduction, radiation, evaporation (sweating) and convection caused by temperature differences. Acceptable ranges of operative temperature and humidity for people in typical Summer and Winter clothing during primarily sedentary activity (Addendum ASHRAE 55a to ASHRAE Standard 55) [3] are shown in Figure (2.3).
Indoor conditions assumed for design purposes depend on building use, type of occupancy, and/or code requirements. ASHRAE Handbook of Fundamentals [3] and

ASHRAE Standards 55 and 55a [92; 93] define the relationship between indoor conditions and comfort. Typical practice indoor design conditions for cooling is 24°C dry bulb temperature and a maximum of 50-65% relative humidity. For heating, it is 20°C dry bulb temperature and 30% relative humidity [3]. These conditions will be used throughout this research.

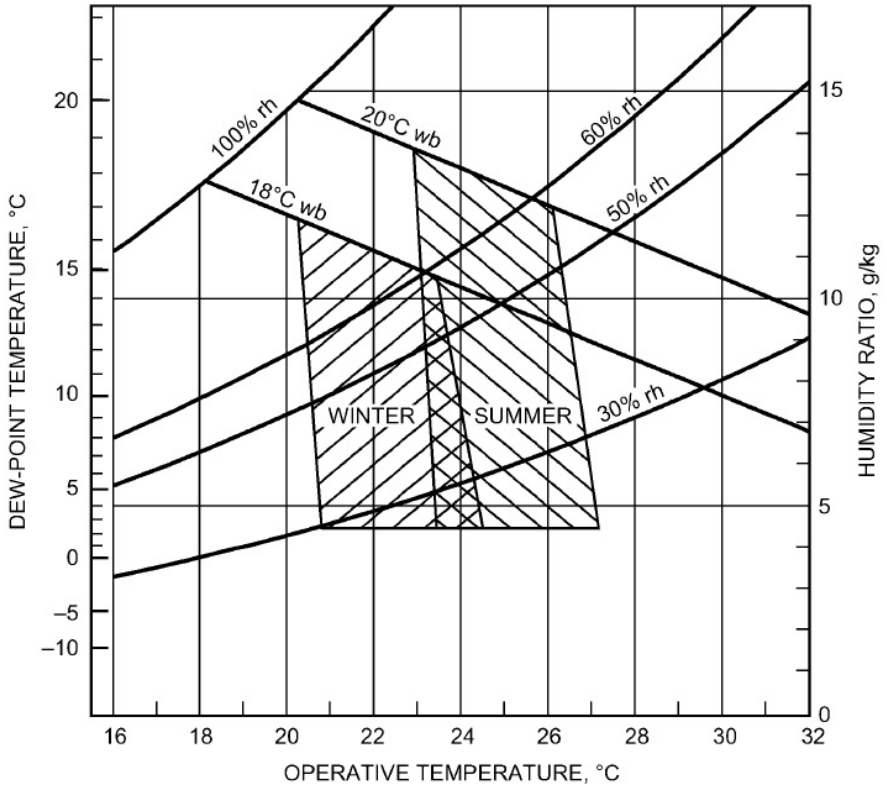

Figure 2.3: ASHRAE Summer and Winter Comfort Zones [3]

2.2.2 Outdoor Design Conditions

Amman capital of Jordan lies in the "global Sunbelt" at latitude of 32°C North and longitude of 36°C East which represents moderate weather with a mountainous topography. This location has abundant supplies of solar energy, with relatively high average daily solar radiation. The annual sunshine is more than 300 days [13].
The climate of Amman is predominantly of the Mediterranean type. It is marked by sharp seasonal variations in both temperature and precipitation. Climate can be cold to very cold in Winter and warm to hot in Summer. Summer starts around mid of May and Winter starts around mid of November, with two short transitional periods in between (autumn and spring). The demand for heating and cooling is strongly influenced by the outdoor air temperature and global solar radiation on horizontal

plate, around the building. In addition to relative humidity. These meteorological data have been obtained from INSEL library [4].
The yearly average of temperature is 17.2°C, with lowest mean temperature of 3.6°C in January and highest mean temperature of 32.6°C in August. Figure (2.4) represents hourly outdoor temperature profile all over the year which will be used in thermal performance calculations.

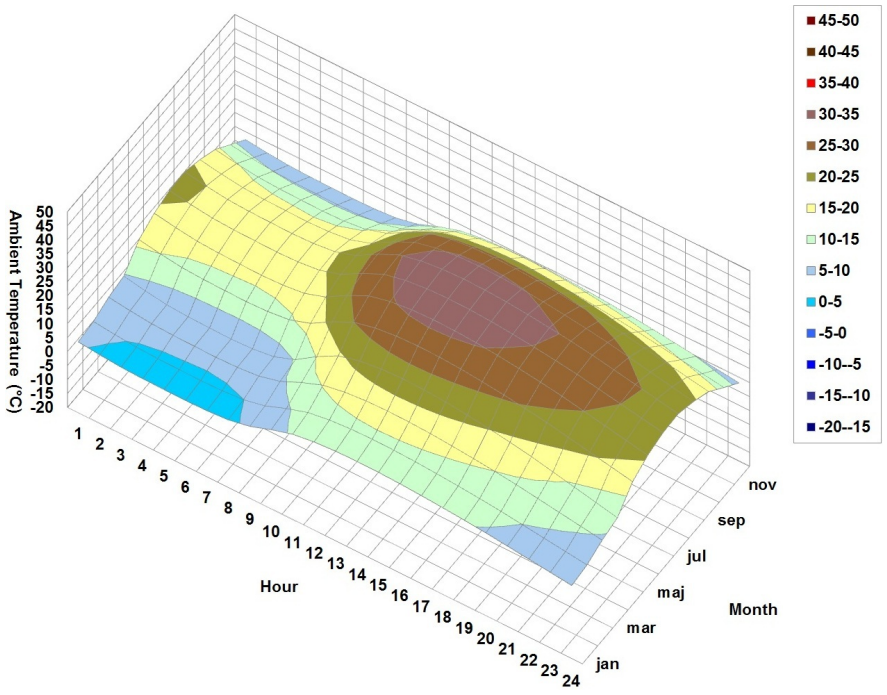

Figure 2.4: Outdoor Temperature Profile [4]

The mean relative humidity is varied from 39% in June to about 71% in January, as shown in Figure (2.5).
The highest solar radiation is 7.68 kWh/m^2.day in July, while the lowest solar radiation is 2.8 kWh/m^2.day in December. The daily average solar radiation is plotted in Figure (2.6). This hourly solar radiation data will be used to estimate the annual thermal performance.

2.3 Economic Model

Cost estimation of all measures and systems in addition to conventional energy systems do involve some basic assumption which can be summarized as follows:

- Life Cycle Cost criterion (LCC) and Payback Period (PbP) are the methods used in this research.

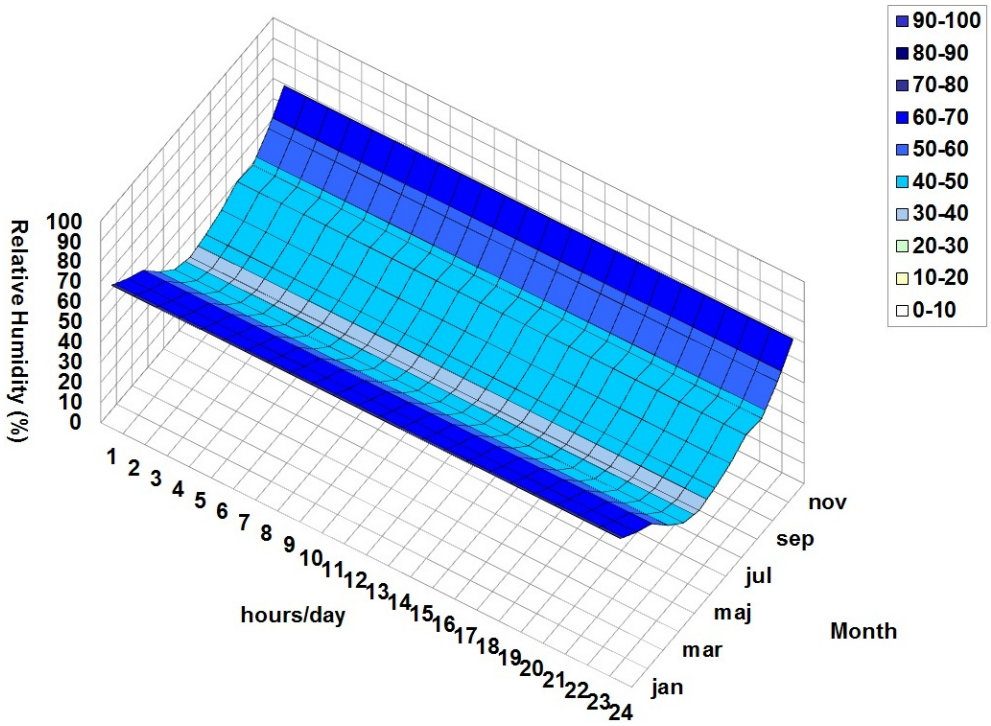

Figure 2.5: Outdoor Humidity Profile [4]

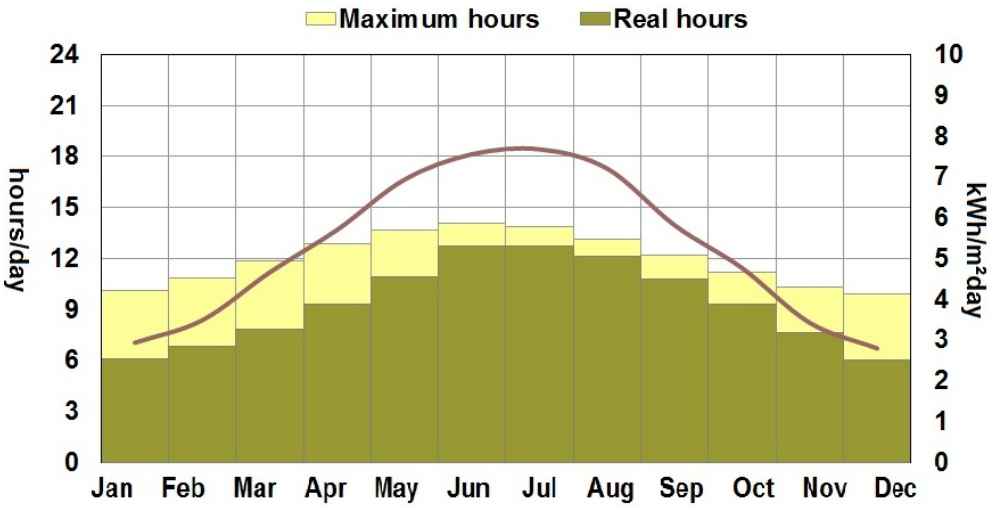

Figure 2.6: Outdoor Solar Radiation Profile [4]

- The life span of the building, auxiliary heating system and all passive systems used in this work is assumed to have 30 years.
- The auxiliary cooling system has 10 years life span.
- The Energy Recovery System (ERS) and Indirect Evaporative and Storage Unit (IESU) are assumed to have a 15 years life span.
- According to Jordanian market the inflation rate is around 8.9% and the interest rate is about 6.25% as mentioned by Central Bank of Jordan (CBJ).
- The auxiliary heating system has an efficiency of 65% [94].
- The auxiliary cooling system has Coefficient of Performance (COP) of 3 [94].
- The salvage factor is set at 10% of the capital cost for heating auxiliary system as well as ERS and IESU. on the other hand, it assumed to be 6% of the capital cost for auxiliary cooling system.
- Maintenance factor for the auxiliary heating and cooling systems is assumed to be 15%, and 10% of the capital cost, respectively.
- ERS and IESU are assumed to have a 6% as maintenance factor.
- Current fuel price is considered as current tariff in Jordan [95].
- The water cost is considered as current tariff in Jordan [96].

Chapter 3

Passive Solar Design

In this chapter the main important components in passive design will be thermally investigated. Thereafter, a complete economic equations for the Life Cycle Cost (LCC) criterion will be formulated and optimized as a function of thermal insulation thickness and Trombe wall area ratio .

3.1 Introduction

Climate often has a significant effect of building energy use, particularly in residences. Comfortable, beautiful, energy efficient and sustainable residential buildings can be designed after answered two questions; how and why buildings use energy? [12]. Steps of how residential buildings energy use can be reduced are summarized as follows;

- Designing the building passively taking into consideration the climate parameters in order to minimize the heating, cooling, dehumidification, lighting, equipment and hot water loads. This can be done by passive heating and cooling, indirect solar gain, best orientation, thermal mass, glazing ... etc.

- Improving the used mechanical and electrical equipment efficiency to meet remain loads.

- Supplying the needed primary energy with renewable rather than fuel, if needed.

Passive solar design was used long time ago. Throughout history, civilizations have learned how to adapt their architecture to their climatic conditions and in almost all cases primary importance was given to the relationships with the sun.
Passive solar systems can be identified as those systems in which heat is transferred by free convection and radiation modes. In passive solar systems the solar collection and storage subsystems are combined into one component [80].

Space heating and cooling loads have four major components; solar heat gain through apertures, heat conduction, ventilation/ infiltration, and internal loads. TRNSYS software is selected to simulate hourly heating and cooling load. Then technical effect of several passive design techniques; choosing the best façade orientation, effect of windows size, effect of Trombe wall and thermal insulation thickness to ceiling and walls will be investigated.

3.2 Heat Transfer through Building's Construction

Heat transfer through building's construction is the transient flow of thermal energy between outdoor and indoor air due to temperature difference between them. Heat transfer through walls, ceiling, door and windows are calculated in details in the following sections.

3.2.1 Thermal Resistance for Internal and External Air Films

Film thermal resistance, R_f, depends on the surface emissivity, surface exposure degree to the weather and the direction of heat flux. Materials can be classified into two types [97]:

- High emissivity: this includes general construction material such as cement blocks, stones, marbles, concrete, plaster, wood and glass.
- Low emissivity: this includes metallic materials such as aluminum and steel panels.

The external surfaces may be classified into three types depending on the exposure degree to the weather;

- Protected surfaces: this includes buildings with one or two floors and located in the center of the city.
- Normal exposure surfaces: this includes buildings with three, four or five floors and located in the city center and also includes buildings with one, two or three floors located near the city.
- Extensive exposure surfaces: this includes buildings with six floors or over located in the city center, buildings with four floors or over located near city and for buildings placed on hilly or seashores regions.

High emissivity and protected surfaces have been selected as the default case for the studied building. Corresponding; R_f would have the following values [5]:

$$walls = \begin{cases} R_{f,i} = 0.13 \\ R_{f,o} = 0.04 \end{cases}$$

$$ceiling = \begin{cases} R_{f,i} = 0.1 \\ R_{f,o} = 0.04 \end{cases}$$

$R_{f,i}$: inner film thermal resistance, (m^2K/W)

$R_{f,o}$: outer film thermal resistance, (m^2K/W).

3.2.2 Thermal Resistance Through External Walls

Heat conduction through opaque surfaces of the building envelop depends on the thermal properties of the material and on its effective heat capacity. Thermal conductivity and thickness of materials used in construction of the building are according to Jordanian Thermal Insulation Code [5]. Thermal properties of these materials are listed in Table (3.1).
Figure (3.1) shows the cross section of the used wall in this research. The thermal resistance for wall, R_w, can be calculated as follows:

$$R_w = R_{f,o} + (\frac{t}{k})_{stone} + (\frac{t}{k})_{concrete} + (\frac{t_w}{k})_{ins.} + (\frac{t}{k})_{brick} + (\frac{t}{k})_{plaster} + R_{f,i} \quad (3.1)$$

where;

t_w : thermal insulation thickness in walls (m).

k : materials thermal conductivity (W/m^2K).

t : materials thickness (m).

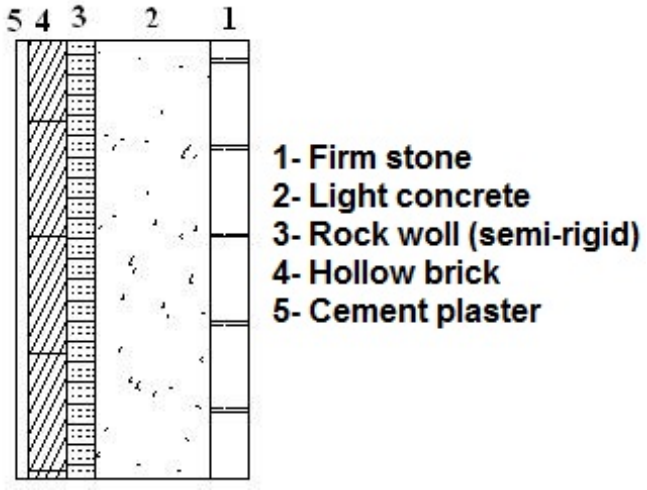

Figure 3.1: Wall Construction [5]

Table 3.1: Thermal Conductivity and Thickness of Materials Used in Construction [5]

Material	Density (kg/m^3)	Thermal conductivity (W/m^2K)	Thickness (m)	Thermal resistance (m^2K/W)	Specific heat (kJ/kg.K)
Firm stone	2250	1.7	0.07	0.0412	0.83
Light concrete	2300	1.75	0.2	0.1143	1.08
Rock wool (semi-rigid)	50	0.039	x	x/k	1.30
Rock wool (rigid panels)	130	0.036	x	x/k	1.30
Hollow brick	1400	0.9	0.07	0.078	0.90
Cement plaster	2000	1.2	0.02	0.017	1.01
Cement tiles	2100	1.1	0.03	0.027	0.86
Reinforced concrete	2300	1.75	0.06	0.034	0.94
Hollow concrete (rips)	1400	0.95	0.18	0.189	1.01
Sand	1800	0.7	0.02	0.0286	0.86

3.2.3 Thermal Resistance Through Ceiling

Ceiling with reinforced concrete and rips (hollow concrete block) will be used in this research. Figure (3.2) shows a cross sectional for this ceiling.

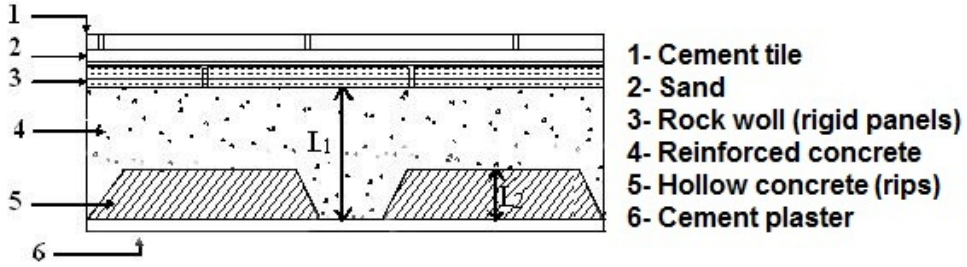

Figure 3.2: Ceiling Construction [5]

Since the construction for this type of ceiling is inhomogeneous, the following formulas will be used to calculate the ceiling thermal resistance:

$$R_1 = R_{f,o} + (\frac{t}{k})_{tile} + (\frac{t}{k})_{sand} + (\frac{t_c}{k})_{ins.} + (\frac{t}{k})_{concrete} + (\frac{t}{k})_{plaster} + R_{f,i} \tag{3.2}$$

$$R_2 = R_{f,o} + (\frac{t}{k})_{tile} + (\frac{t}{k})_{sand} + (\frac{t_1 - t_2}{k})_{concrete} + (\frac{t_2}{k})_{rips} + (\frac{t}{k})_{plaster} + R_{f,i} \tag{3.3}$$

Then, the overall heat transfer of ceiling, U_c, is;

$$U_c = \sum(\frac{U_i A_i}{A}) = \frac{U_1 A_1}{A} + \frac{U_2 A_2}{A} \tag{3.4}$$

Where $\frac{A_1}{A} = 20\%$ for non-rips ceiling and $\frac{A_2}{A} = 80\%$ for ceiling with rips.

3.2.4 Heat Transfer Through Windows and Doors

Thermal transmissions for windows and doors have been selected as follows [5]:

- Wooden doors, U = 3.5 W/m^{2}K.
- Double glaze windows with aluminum frame (15% frame(U = 2.27 W/m^{2}K)), U = 2.83 W/m^{2}K, SHGC = 0.775.

3.3 Orientation

In planning the building, it is just as important to design for protection from Summer sun as for access to Winter sun. The first step in designing a solar efficient structure is

the understanding of the geometrical relationship between earth and sun to orientate the building according to the sun [98].
In this study a passive façade, as shown in Figure (3.3), is set as a reference. Then the best building orientation is investigated by changing passive façade to face South, North, East and West in a consecutive manner in a purpose of allowing solar radiation to enter the building during Winter and protect it, as possible, during Summer. The annual auxiliary energy needed for heating and cooling for four different orientations have been hourly simulated by using Type 56 (multi-zone buildings) in TRNSYS software [7]. This component models the thermal behavior of a building divided into different thermal zones. Each thermal zone has one air node representing the thermal capacity of the zone air volume [7].
The simulation results are presented in Figure (3.4). This Figure shows that when passive façade facing North, the annual heating demand is the highest one due to prevent solar radiation from entering the building in Winter. The annual heating demand is around 5,045 kWh which means 5.53% more energy than South orientation case. On the other hand, the annual cooling demand is about 8,716 kWh, which is 0.78% less energy than South orientation case.

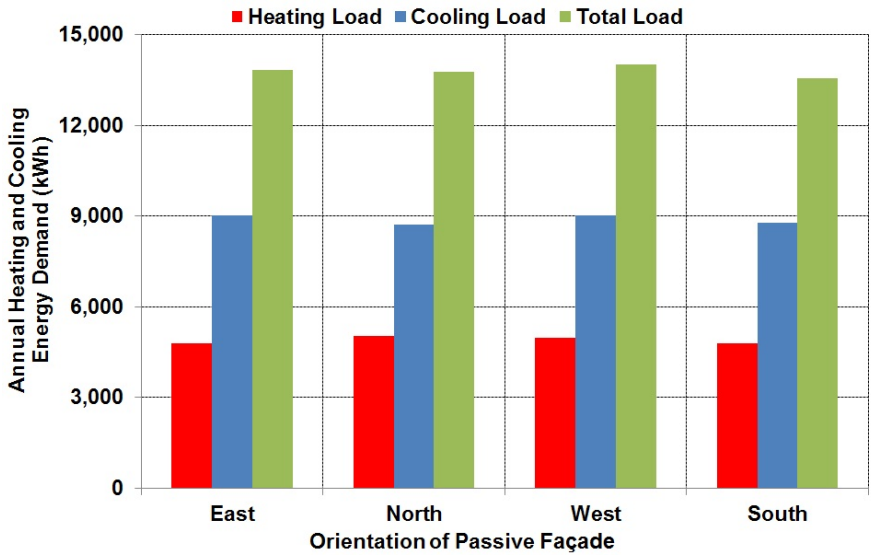

Figure 3.4: Annual Heating and Cooling Demand at Different Orientation

When orienting the passive façade to West the annual heating demand is about 4,970 kWh, as shown in Figure (3.4). This heating demand is more than South orientation case by 3.95%. The annual cooling demand is 9,032 kWh which uses 2.82% more energy than orientation to South case. This case has highest values for total annual energy demand as compared with other orientation cases.

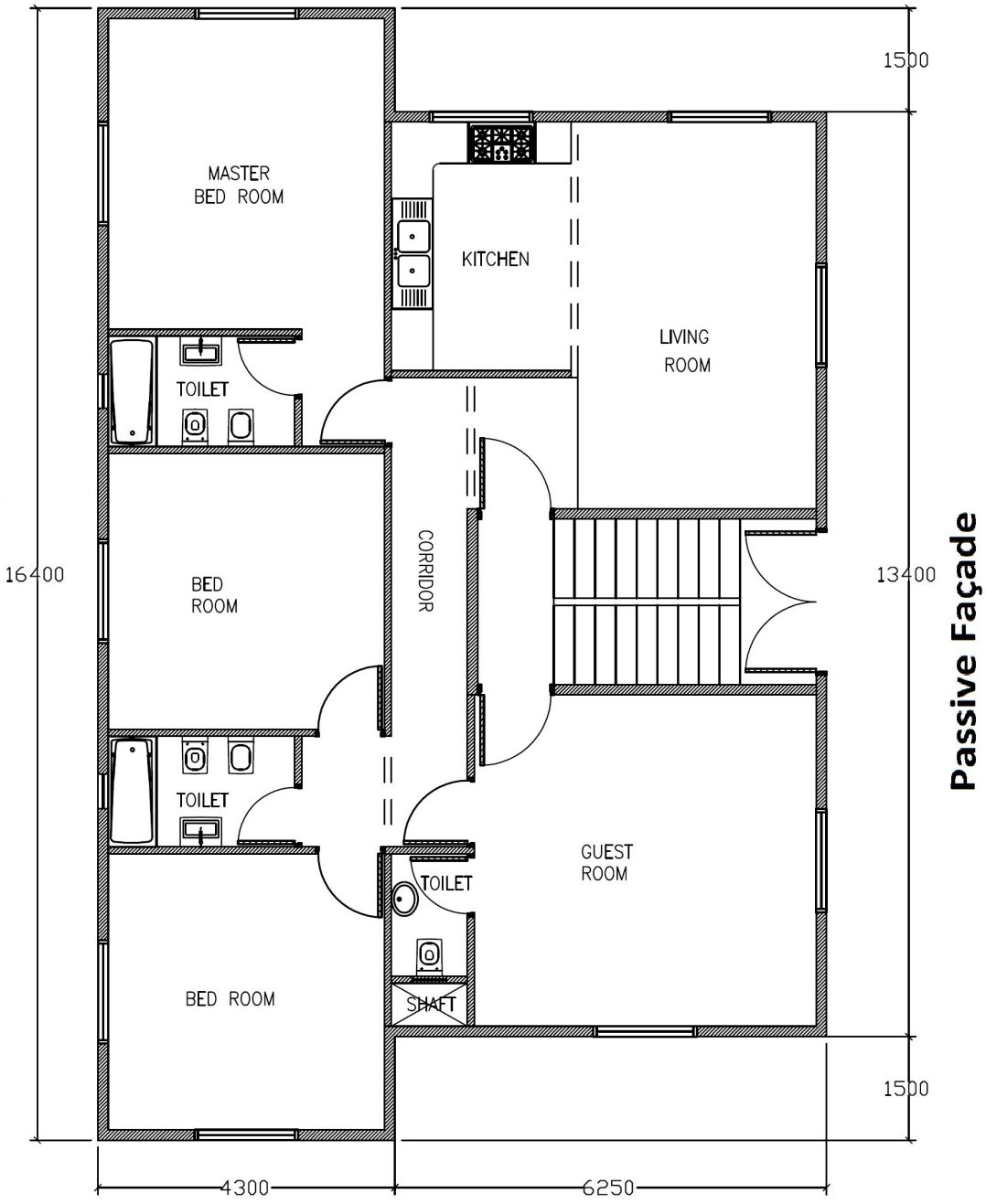

Figure 3.3: Reference Passive Façade

Also, it can be seen from Figure (3.4) that the annual heating and cooling energy are 4,796 kWh and 9,038 kWh, respectively once passive façade is facing East. That's using 0.30% and 2.89% more heating and cooling energy than South orientation case, respectively.
Furthermore, Figure (3.4) shows that the total energy needed to provide comfort throughout the year is 14,001 kWh, 13,833 kWh, 13,761 kWh, and 13,565 kWh for West, East, North, and South orientation, respectively. One can detect that the total annual energy needed in both heating and cooling is the lowest when the passive façade is oriented to South. Therefore; passive façade facing South is the best orientation from energy saving point of view.
As a result, the passive façade is orientated towards South to allow solar radiation to enter the building in cold weather is the best decision. This will be set as a base case for the following passive design measures. The hourly heating and cooling load is 4,781 kWh and 8,784 kWh, respectively. The maximum cooling load is 6.11 kW where the maximum heating load is 5.55 kW. The specific energy consumption is 88.08 kWh/m^2 and LCC equals to 78,698 €.

3.4 Windows' Size and Shading Device

Direct gain is the simplest passive solar building design technique [99]. Windows are very important component of passive design because heat loss and gain occurs mostly through windows. Windows not only provide interior light and view but also collect the sun's heat and they act as a collector, while the building itself provides some storage. Windows also provide a day-lighting which offer dramatic electrical energy savings and cooling load reductions. The minimum windows size is 10% from the façade area in order to reach human comfort [100; 101].
Shading is mainly for hot seasons thus linked to Summer comfort. The hottest hours of the day are between 10:00 AM - 4:00 PM. Thus, protection is needed from solar radiation at these times. In this work South windows are shaded with retractable shade to provide shading from direct solar radiation in Summer.

3.4.1 Thermal Optimization

The effect of windows' size on heating load is estimated for different windows' size technically by using TRNSYS software [7]. The results are plotted in Figure (3.5).

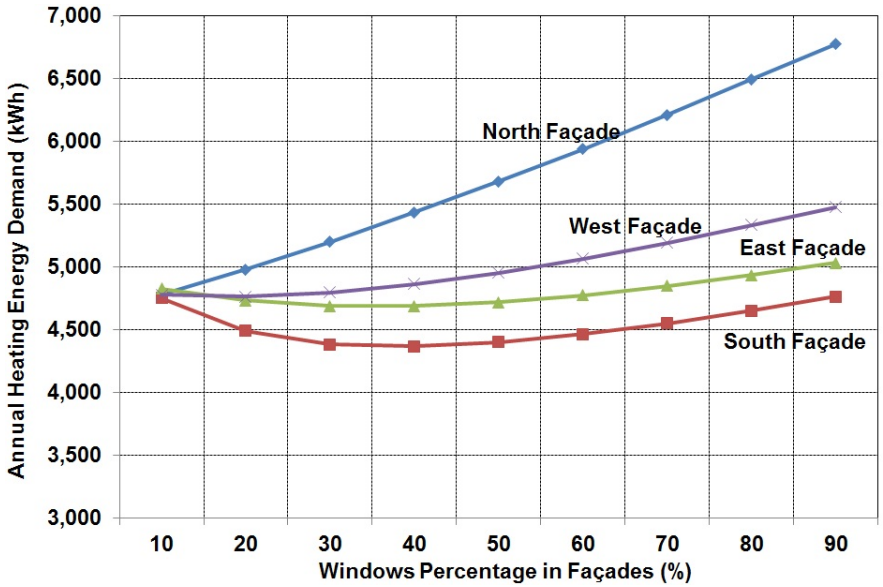

Figure 3.5: Annual Heating Energy at Different Windows' Size

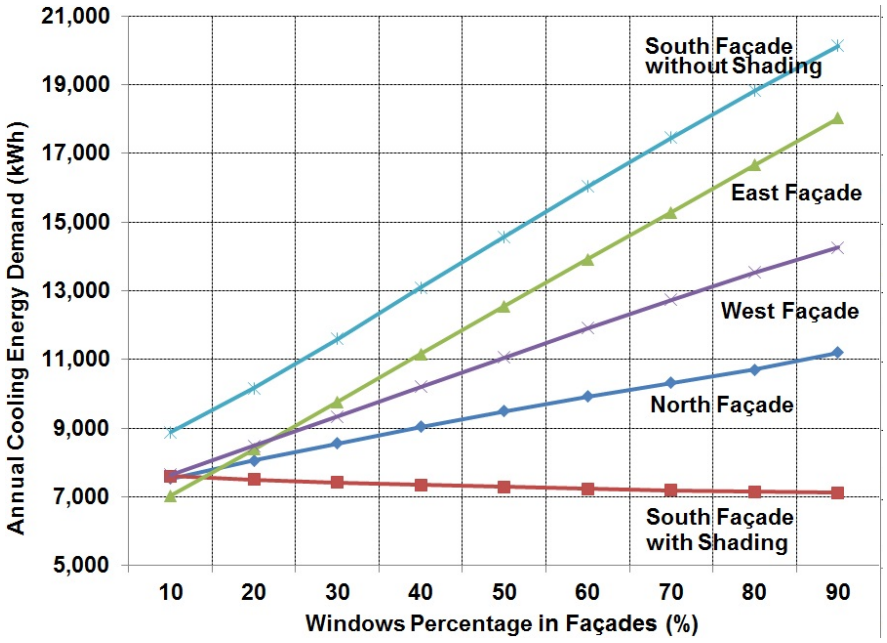

Figure 3.6: Annual Cooling Energy at Different Windows' Size

The heating load increases linearly as windows percentage at North façade increase, as shown in Figure (3.5). So, it is recommended to minimize windows' size at this façade for heating purpose. Furthermore, the heating load decreases with increasing South and East windows' area percentage till 40% from each façade area then it tends to increase. Therefore; the optimal percentage of windows' area for South and East façades is 40%

from the façade area. Moreover, it can be concluded from this Figure that the optimum windows' size is 20% for West façade. The thermal heat losses through windows become more than solar gain after this optimum percentage. This is happened when ambient temperature is lower than room temperature during Winter time that leads to increase the thermal heat losses.
Increasing of windows' size in all façades will increase the cooling load linearly, as shown in Figure (3.6). The highest cooling load occurs at South façade; thus proper shading device in Summer is installed on South façade. Shading device will take into consideration the latitude, climate, solar radiation transmittance, illumination levels and windows' size.
The curve fit equations of the required auxiliary energy during heating and cooling months, as a function of percentage windows' area from façade area (w), are listed in Table (3.2).

Table 3.2: Curve Fit Equations for Auxiliary Heating and Cooling Energy at Different Windows' Size

Auxiliary Energy (kWh)	R^2
Heating Mode	
Q = -0.001*w_N^3-0.114*w_S^3-0.054*w_E^3-0.033*w_W^3+0.339*w_N^2 + 7.846*w_S^2 +3.735*w_E^2 +2.696*w_W^2 + 36.061*w_N -147.186*w_S-60.031*w_E -28.145*w_W+5221.011	0.9995
Cooling Mode	
Q = -0.044*w_N^3-0.028*w_S^3+0.098*w_E^3-0.1*w_W^3 +2.875*w_N^2 +1.44*w_S^2 -2.888*w_E^2+3.504*w_W^2 + 47.191*w_N -35.703*w_S+421.59*w_E+245.764*w_W+5190.808	0.9985

3.4.2 Economic Optimization

The objective function which will be optimized is LCC function which equal to;
LCC = (auxiliary system cost + maintenance cost for auxiliary system - auxiliary system salvage cost) + base cost + windows cost + (annual auxiliary energy cost - annual cost of saved energy due to windows) or;

$$\begin{aligned} LCC = {} & C_{aux.,h}(w_W, w_E, w_S, w_N)[1 + f_m PWF - f_{salv}(\frac{1+i}{1+r})^N] \\ & + C_{aux.,c}(w_W, w_E, w_S, w_N)[1 + f_m PWF - f_{salv}(\frac{1+i}{1+r})^N] + C_b \\ & + C(w_W, w_E, w_S, w_N) + [Q_{aux.,h}(0) - Q_{aux.,h}(w_W, w_E, w_S, w_N)] \\ & \frac{p_d}{\eta_{aux.}} PWF + [Q_{aux.,c}(0) - Q_{aux.,c}(w_W, w_E, w_S, w_N)] \frac{p_e}{COP} PWF \end{aligned} \tag{3.5}$$

where;

w : percentage of windows' area from total façade area (%).

C_b : basic cost. (€).

$C(w_W, w_E, w_S, w_N)$: windows cost (€).

$C_{aux.,h}$: auxiliary heating system cost (€).

$C_{aux.,c}$: auxiliary cooling system cost (€).

$Q_{aux.,h}(0)$: annual auxiliary heating energy consumption (base load) (kWh).

$Q_{aux.,c}(0)$: annual auxiliary cooling energy consumption (base load) (kWh).

$Q_{aux.,c}(w_W, w_E, w_S, w_N)$: annual cooling energy saved due to windows (kWh).

$Q_{aux.,h}(w_W, w_E, w_S, w_N)$: annual heating energy saved due to windows (kWh).

f_m : maintenance fraction.

PWF : Present Worth Factor.

$$PWF = \sum_{j=1}^{N} (\frac{1+i}{1+r})^j = \frac{1+i}{1+r}(1 - (\frac{1+i}{1+r})^N) \tag{3.6}$$

f_{salv} : salvage fraction.

i : inflation rate.

r : interest rate (equivalent to discount rate).

N : life time (years).

p_d : thermal energy price (€/kWh).

p_e : electrical energy price (€/kWh).

$\eta_{aux.}$: auxiliary heating system efficiency (%).

COP : Coefficient Of Performance.

LCC is subjected to five constraint equations as follows;

$$z = C_w(w_W, w_E, w_S, w_N) \tag{3.7}$$

$$10\% \leq w_W \leq 90\% \tag{3.8}$$

$$10\% \leq w_E \leq 90\% \tag{3.9}$$

$$10\% \leq w_N \leq 90\% \tag{3.10}$$

$$10\% \leq w_S \leq 90\% \tag{3.11}$$

The Microsoft Excel "solver add-in" which uses GRG algorithm is used in estimating the minimum LCC. The results show that the minimum LCC is occurred when the windows size is set as 30% of the South façade area, 20% of the East façade, 10% of North façade and 10% of West façade. The LCC is reduced by about 1.63% from the base LCC while the additional cost is raised by 4.47%. The new energy consumption in Winter season is reduced by 5.06% while in Summer season is reduced by 8.61% from the base case. The specific energy consumption is 81.6 kWh/m^2.

3.5 Thermal Insulation

The internal mass is the key to a successful thermal environment and the proper thickness of insulation is the tool for achieving this key.
The annual heating and cooling load is estimated for different insulation thickness for walls and ceiling, by using TRNSYS software [7]. Then the optimum thermal insulation thickness is calculated by optimizing the objective function LCC which equals to;
LCC = (auxiliary system cost + maintenance cost for auxiliary system - auxiliary system salvage cost) + base cost + thermal insulation cost + (annual auxiliary energy cost - annual cost of saved energy due to thermal insulation thickness), or;

$$\begin{aligned} LCC = {} & C_{aux.,h}(t_c,t_w)[1+f_m PWF - f_{salv}(\frac{1+i}{1+r})^N] + C_{aux.,c}(t_c,t_w) \\ & [1+f_m PWF - f_{salv}(\frac{1+i}{1+r})^N] + C_b + C_{ins.}(t_c,t_w) + [Q_{aux.,h}(0) \\ & - Q(t_c,t_w)]\frac{p_d}{\eta_{aux.}}PWF + [Q_{aux.,c}(0) - Q_{aux.,c}(t_c,t_w)]\frac{p_e}{COP}PWF \end{aligned} \tag{3.12}$$

where;

t_w : thermal insulation thickness in wall (m).

t_c : thermal insulation thickness in ceiling (m).

$C_{ins.}$: thermal insulation cost (€).

$Q_{aux.,h}(0)$: annual auxiliary heating energy consumption after windows' optimum design (kWh).

$Q_{aux.,c}(0)$: annual auxiliary cooling energy consumption after windows' optimum design (kWh).

$Q_{aux.,c}(t_c,t_w)$: annual cooling energy saved due to thermal insulation (kWh).

$Q_{aux.,h}(t_c,t_w)$: annual heating energy saved due to thermal insulation (kWh).

LCC is subjected to three constraint equations as follows;

$$z = C_{ins.}(t_c, t_w) \tag{3.13}$$

$$0.06 \leq t_c \leq 0.6 \tag{3.14}$$

$$0.06 \leq t_w \leq 0.6 \tag{3.15}$$

Three scenarios will be studied in order to find minimum LCC as follows;

3.5.1 First Scenario

In this scenario, the thermal insulation in ceiling is set constant (0.06 m) and varies in the walls. Then the opposite has been done (i.e the thermal insulation in walls is set constant and varies in the ceiling).
The percentage of annual saving at different insulation thickness has been simulated and plotted in Figure (3.7). Once the ceiling is insulated with 0.18 m and the walls with 0.06 m, about 20.44 % will be saved from the base case annually. The specific energy consumption is 70.08 kWh/m^2. Also, about 11.93% energy saving will be achieved when the ceiling is insulated with 0.06 m and walls with 0.13 m. The specific energy consumption is 77.58 kWh/m^2.

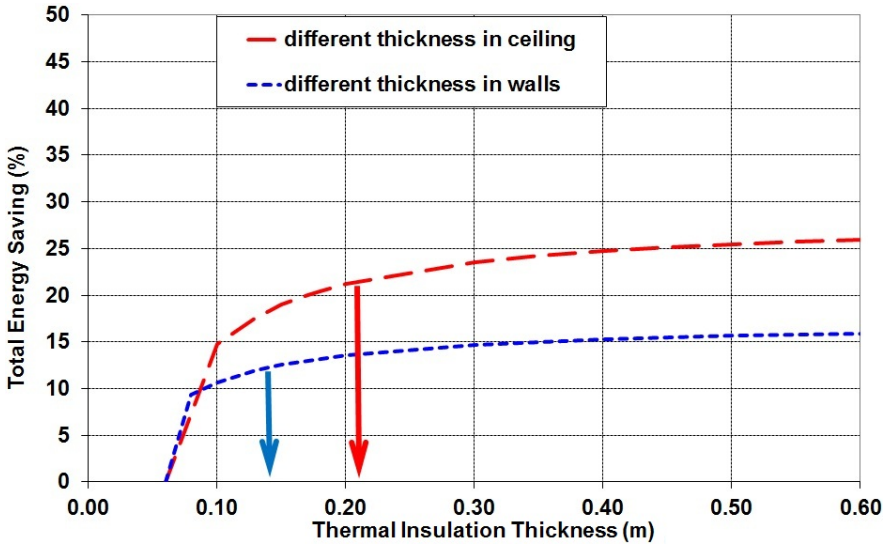

Figure 3.7: Energy Saving at Different Insulation Thickness (First Scenario)

Once the thermal insulation thickness of 0.18 m is used for ceiling and 0.06 m for walls, the initial cost is increased by 22.06%. On the other hand, LCC is reduced by 7.88%, as shown in Figure (3.8).
Figure (3.9) shows that the optimum insulation thickness is 0.13 m for walls when

thermal insulation thickness is set 0.06 m for ceiling. The LCC is reduced by 4.33% and the initial cost needed is increased by 7.57%.

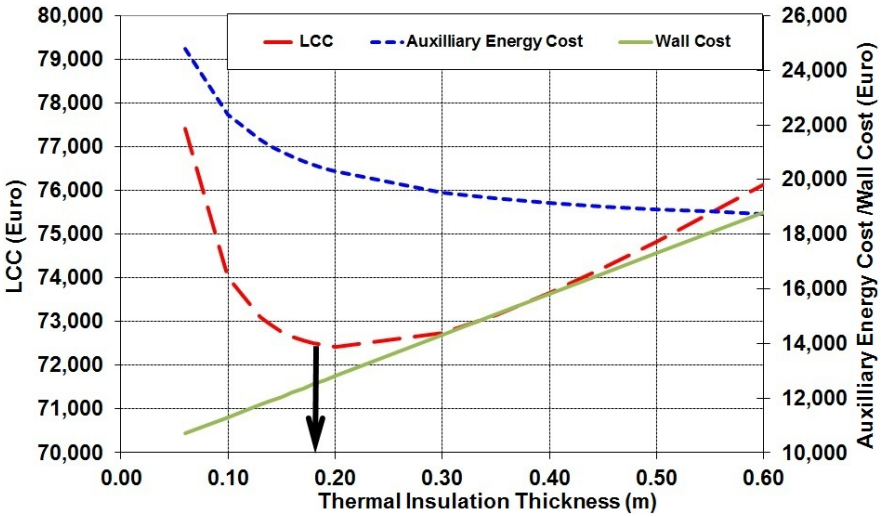

Figure 3.8: Optimum Thermal Insulation Thickness (t_w = 0.06 m)

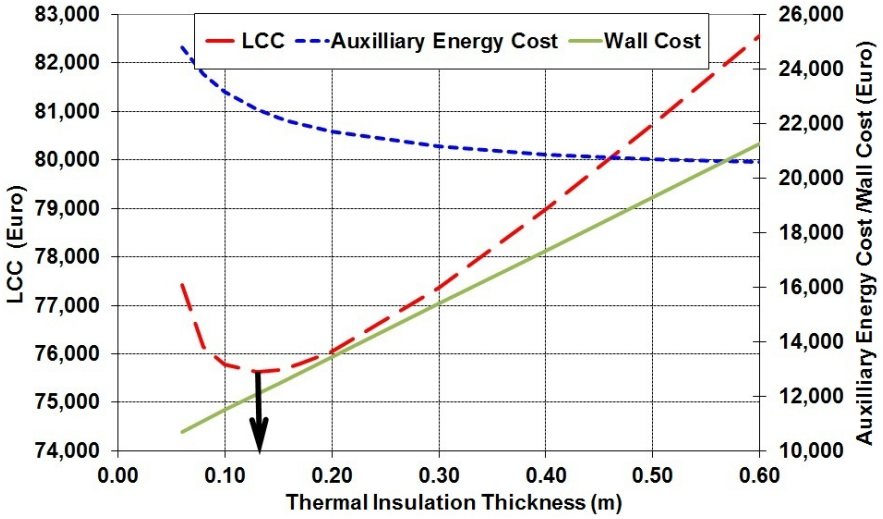

Figure 3.9: Optimum Thermal Insulation Thickness (t_c = 0.06 m)

3.5.2 Second Scenario

In this scenario, both ceiling and walls are insulated with the same thickness. The optimum insulation thickness tends to annually save about 50.81% and 14.95% from annual heating and cooling energy demand, respectively. The specific energy consumption is 63.79 kWh/m^2. These outcomes are shown in Figure (3.10).

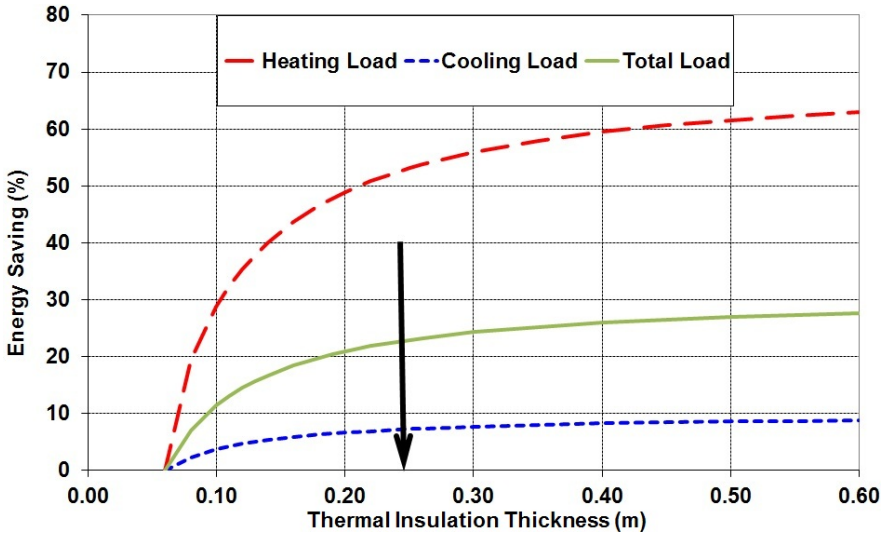

Figure 3.10: Energy Saving at Different Insulation Thickness (Second Scenario)

LCC of the conventional heating and cooling system over selected building life time is about 69,612 €, as shown in Figure (3.11). Investment of 13,832 €is needed, once an investor tend to install insulation thickness of 0.22 m for both walls and ceiling. That means, about 11.55% will be saved over the life cycle of the building with an extra investment of 35%.

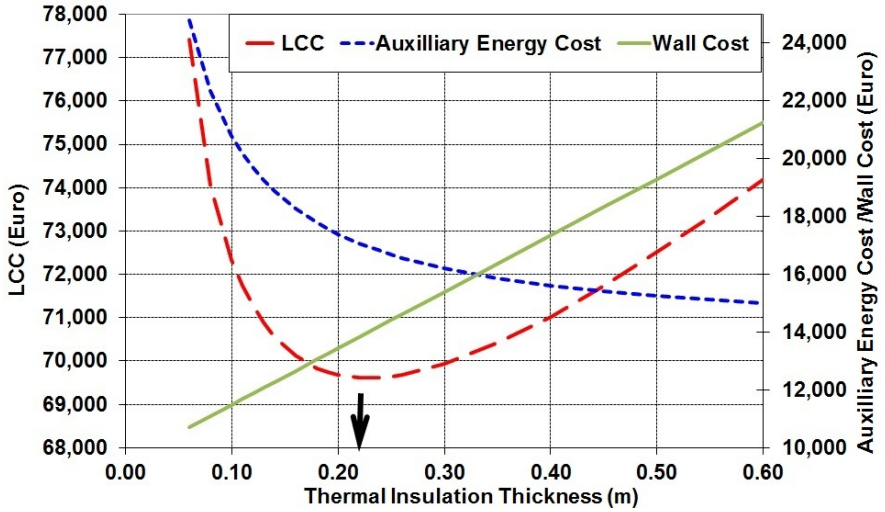

Figure 3.11: Economic Effect at Different Insulation Thickness for Both Walls and Ceiling

3.5.3 Third Scenario

The last scenario is a combination between thermal insulation thickness of 0.13 m for walls and 0.18 m for ceiling. This scenario saves annual energy consumption by 24.58% and reduces LCC by 10.65%. The annual specific energy consumption per square meter is 66.44 kWh/m^2.
The curve fit equations of the required auxiliary energy during heating and cooling months, as a function of thermal insulation thickness are listed in Table (3.3) .

Table 3.3: Curve Fit Equations for Auxiliary Heating and Cooling Energy at Different Insulation Thickness

Auxiliary Energy (kWh)	R^2
Heating Mode	
Q = -8213.3 x_c^2 - 8392.7 x_w^2 + 20068.6 x_c + 20077.3 x_w - 17384.6 $\sqrt{x_w}$ - 17616.7 $\sqrt{x_c}$ + 10701.6	0.9977
Cooling Mode	
Q = 4914.8 x_w^3 - 5788.2 x_c^2 -5020.6 x_w^2 + 14427.8 x_c + 1983 $\sqrt{x_w}$ -12741.4 $\sqrt{x_c}$ + 9806.4	0.9983

3.6 Trombe Wall

Trombe wall was first developed by American named Edward Morse in 1881 [102] and recently revived by the French inventor Felix Trombe [80]. Trombe wall is made of a material that absorbs a lot of heat, such as concrete or masonry and it is coated with a dark color [80]. It will be placed behind South facing glass to increase the thermal mass to receive high amounts of solar gain. The heat absorbed from the sun is conducted slowly through the storage mass to the inner surface. The air heated by convection rises and passes into the heated space. During the period of no sunlight, heat stored in the thermal mass wall is radiated and convected into space to be heated. Energy can be transferred to the room by air circulating through the gap between wall and glazing through openings at the top and bottom of the wall. Circulation can be natural convection controlled by dampers on the vent openings or by forced circulation by fans [80]. Properly sized overhangs should be used to shade Trombe wall during Summer when the sun is high in the sky. Shading Trombe wall can prevent the wall from getting hot during the time of the year when the heat is not needed [33; 103]. Trombe wall system is shown in Figure (3.12).

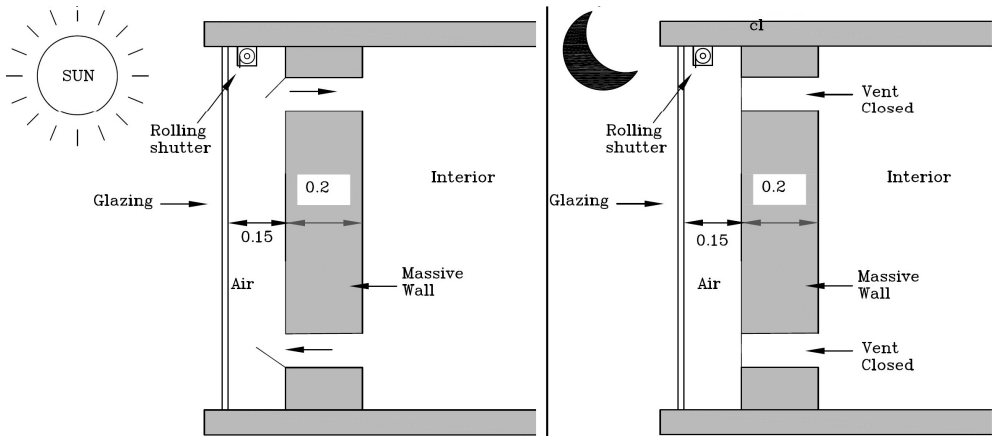

Figure 3.12: Trombe Wall [6]

3.6.1 Theory

Trombe wall system can be considered as a set of nodes connected together by a thermal network, each with a temperature and capacitance as shown in Figure (3.13). The wall is divided into N nodes across its thickness [80].

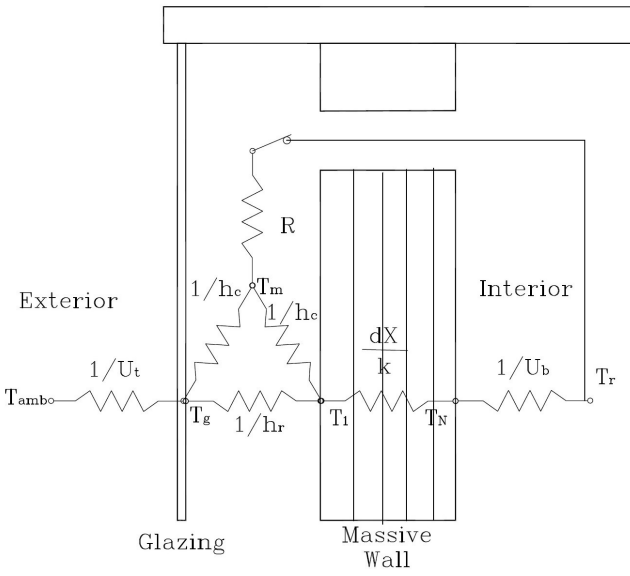

Figure 3.13: Thermal Scheme of Trombe Wall [7]

The thermosyphon mass flow of air in this model has been determined by applying Bernoulli's equation to the entire air flow system. For simplicity, it is assumed that the density and temperature of the air in the gap varies linearly with height. The average

air velocity through the gap ($\bar{V}$) is [80];

$$\bar{V} = [\frac{2gh}{C_1(\frac{A_g}{A_v})^2 + C_2}\frac{T_m - T_r}{T_m}] \tag{3.16}$$

where;

$C_1(\frac{A_g}{A_v})^2 + C_2$: represents the pressure drop in the gap and vents, and C_1 and C_2 are dimensionless empirical constants. Values of C_1 and C_2 have been determined by Utzinger [104] to be 8.0 and 2.0, respectively.

h : wall height (m).

T_m : mean air Temperature in the gap (°C).

g : gravity acceleration (m/s^2).

T_r : room air temperature (°C).

The thermal resistance (R) to energy flow between the gap and the room when mass flow rate of air in the gap is finite is given by [7];

$$R = \frac{A[(\frac{\dot{m}C_p}{2h_cA})(exp(-\frac{2h_cA}{\dot{m}C_p}) - 1) - 1]}{\dot{m}C_p(exp(-\frac{2h_cA}{\dot{m}C_p}) - 1)} \tag{3.17}$$

where;

$\dot{m}$: mass flow rate of air in the gap (kg/s).

C_p : specific heat of air (kJ/kg.K).

h_c : gap air heat transfer coefficient (kJ/m^2K).

A : Trombe wall area (m^2).

Heat is transferred by radiation across the gap and by convection between air flowing in the gap and the absorbing surface and the inner glazing. The heat transfer coefficient between air in the gap and the wall and glazing depends on whether the vents are open or closed. If the vents are closed, the heat transfer coefficient is calculated by solving natural convection and infrared radiation exchange between gray surfaces problems for vertical collectors.If vents are open and there is flow through the gap, the following equation can be used for flow in the turbulent region [80];

$$Nu = 0.0158\,Re^{0.8} \tag{3.18}$$

where;

Nu : Nusselt number.

Re : Reynolds number

In the laminar region the following correlation can be used [80];

$$Nu = \frac{0.0606(RePrD_h/L)^{1.2}}{1 + 0.0909(RePrD_h/L)^{0.7}Pr^{0.17}} \tag{3.19}$$

where;

Pr : Prandtl number.

L : length (m).

D_h : hydraulic diameter (m).

A heat loss coefficient (U_t) is based on the inner glazing temperature. It can be estimated by standard methods of Chapter 6 in "Solar Engineering of Thermal Processes" book [80]. Finally, heat transfer from the room side of the wall to the room (U_b) is calculated by conventional methods [80].
Type 36 in TRNSYS is chosen to simulate the performance of Trombe wall. This model is directly coupled to the room. Absorbed solar radiation reaches the room by either of two paths. One path is conduction through the wall. From the inside wall surface, the energy is convected and radiated into the room. The second path is convection from the hot outer wall surface to air in the gap. Room air flowing through the gap is heated, carrying energy into the room. The wall also loses energy by conduction, convection and radiation to the environment through the glazing covers [7].

3.6.2 Thermal Optimization

A masonry wall of 0.2 m thickness, coated with a dark, heat absorbing material and covered by a single layer of glass, placed from about 0.15 m away from the masonry wall is selected, as shown in Figure (3.12). The detailed parameters of Trombe wall are listed in Table (3.4).
The hourly heating energy demand as well as hourly energy gain conducted through the wall and convected by air flow into the heated space is simulated at different Trombe wall sizes. The calculation procedure assumes that the heat from the wall offsets the heating load whenever the building temperature is below the maximum temperature limit. Whenever the building temperature exceeds this maximum value, the excess energy is dumped. Practically, this is done by installing roller shutters insulation curtains between glass and masonry wall layer, as shown in Figure (3.12).

Table 3.4: Trombe Wall Parameters

Parameters		Unit
Orientation	South	-
Trombe wall area ratio (a)	0 - 51.83	%
Windows shading coefficient	0.9	-
Wall height	3	m
Wall thickness	0.2	m
Wall thermal conductivity	1.75	W/m^2K
Wall specific heat × density	1932	kJ/m^3K
Wall solar absorbance	0.9	-
Glazing emittance	0.9	-
Window R-value	0.333	m^2K/W
Space between wall and glazing	0.15	m
Number of glazing	1	-

The annual energy consumption in Winter season for the selected residential building, before adding Trombe wall, is 2,352 kWh where the maximum load is 3.78 kW. Trombe wall firstly is added to the two bed rooms which facing South façade. That means Trombe wall ratio (a), the percentage of Trombe wall to the total South wall, is 18.29%. The results of the annual Trombe wall flux and heating energy demand are presented in Figure (3.14).

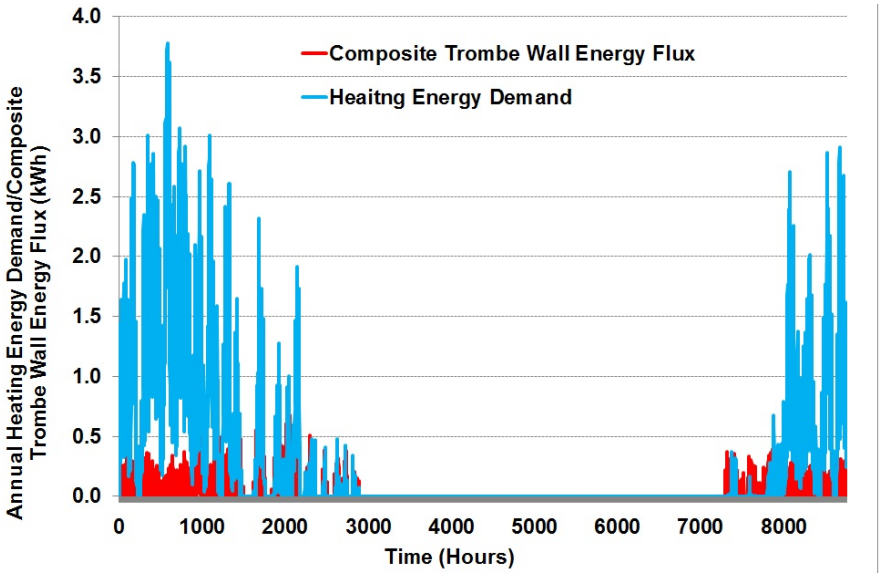

Figure 3.14: Trombe Wall Integrated to Bed Rooms

Figure (3.14) shows that the annual heating load is 1,862 kWh when Trombe wall area ratio is 18.29% where the maximum load is 3.78 kW. That means about 20.9% of the total heating load can be saved. The annual specific heating energy consumption of

the building is 12.09 kWh/m^2.
Once Trombe wall is added to the two bed rooms and guest room that facing South façade (a = 27.44%) about 27% can be saved from the base load as shown in Figure (3.15). This Figure shows that the maximum load and the annual heating load is 3.78 kW and 1,716 kWh, respectively. Moreover, the annual specific heating energy consumption for the building is 11.14 kWh/m^2.

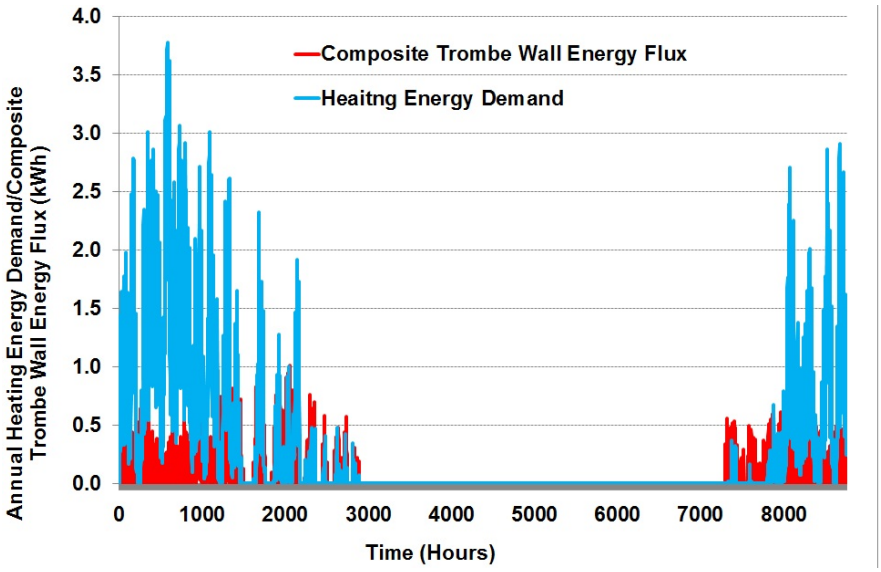

Figure 3.15: Trombe Wall Integrated to Bed and Guest Rooms

The effect of increasing Trombe wall area ratio to 36.59% is also studied. This time Trombe wall is integrated with two bed rooms, guest room and living room. The results are presented in Figure (3.16). The energy saving can be reached up to 32.1% of the annual heating load. The annual specific heating energy consumption is 10.36 kWh/m^2. The energy saving of 32.4% and 32.5% is achieved once extra area of Trombe wall is added to living room and guest room, respectively. The annual specific heating energy consumption can be reached up to 10.31 kWh/m^2, if Trombe wall ratio is 51.83%. Table (3.5) shows a summary of thermal analysis at different Trombe wall area ratio.

Table 3.5: Summary of Trombe Wall Thermal Analysis

Trombe wall area ratio (a)	0	18.19	27.44	36.59	45.73	51.83
Annual heating load (kWh)	2,352	1,862	1,716	1,596	1,591	1,587
Max. heating load (kW)	3.78	3.78	3.78	3.78	3.78	3.78
Specific energy consumption (kWh/m^2)	15.27	12.09	11.14	10.36	10.33	10.31
Energy saving (%)	-	20.85	27.04	32.16	32.36	32.53

It is concluded from Table (3.5) that Trombe wall doesn't reduce the maximum load. On the other side it reduces the annual heating energy consumption. That is because

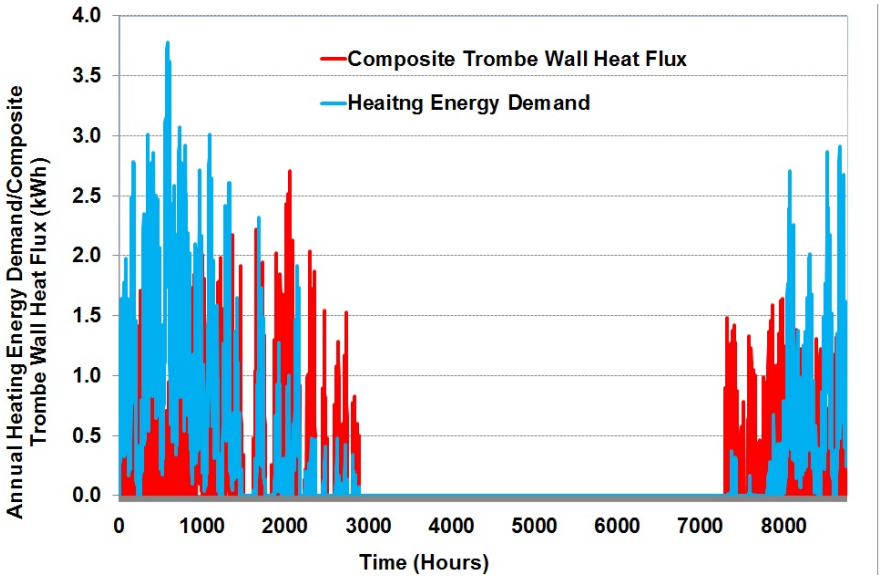

Figure 3.16: Trombe Wall Integrated to Bed, Guest and Living Rooms

Trombe wall depends on the availability of solar radiation; when there is high solar radiation a less heating demand is required and vice versa.
The effect of Trombe wall area ratio on building heating demand is presented in Figure (3.17). The ability of Trombe wall in covering the annual heating load after ratio of 37% is becoming negligible. That means the technical optimal Trombe wall area ratio is 36.59%. Moreover, it is clear from Figure (3.17) that the relationship that describes the heating load over different Trombe wall area ratio of nonlinear type, it is second order equation. The curve fit equation for the auxiliary energy needed after installing Trombe wall is presented in Table (3.6)

Table 3.6: Regression Equations of Auxiliary Energy as a Function of Trombe Wall Area Ratio

Auxiliary Energy Regression (kWh)	R^2
Q = 3620.3 a^2 - 3347.4 a + 2352.8	0.9988

3.6.3 Economic Optimization

The objective function which will be optimized is LCC function which equal to;
LCC = (auxiliary system cost + maintenance cost for auxiliary system - auxiliary system salvage cost) + base cost + Trombe wall cost + (annual auxiliary energy cost

- annual cost of saved energy due to Trombe wall), or;

$$LCC = C_{aux.,h}(a)[1 + f_m PWF - f_{salv}(\frac{1+i}{1+r})^N] + C_{aux.,c}(a)[1 + f_m PWF - f_{salv}(\frac{1+i}{1+r})^N] + C_b + C_{T.W}(a) + [Q_{aux.,h}(0) - Q(a)]\frac{p_d}{\eta aux.}PWF + Q_{aux.,c}\frac{p_e}{COP}PWF] \tag{3.20}$$

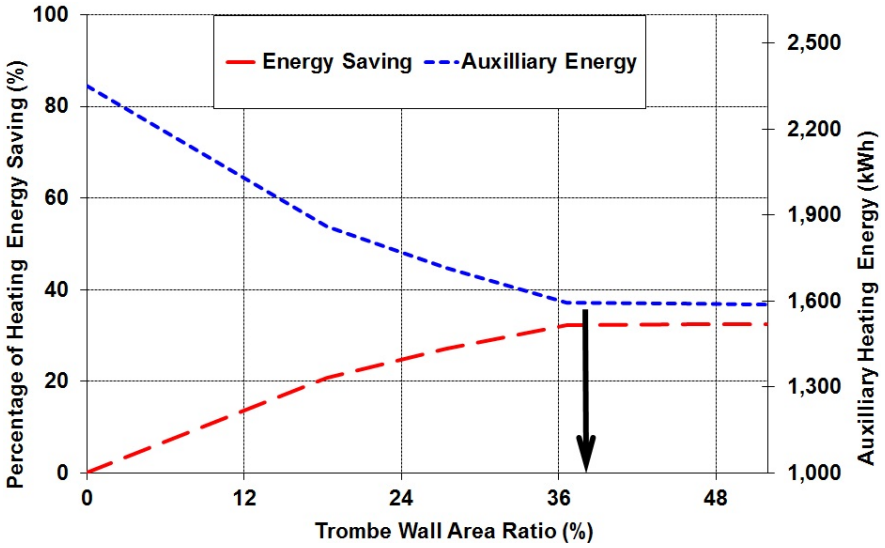

Figure 3.17: Annual Auxiliary Energy due to Trombe Wall

where:

a : Trombe wall area ratio.

$C_{T.W}$(a) : cost of the Trombe wall (€).

Q(a) : annual heating energy saved due to Trombe wall (kWh).

$Q_{aux.,h}(0)$: Annual auxiliary heating energy consumption after optimal thermal insulation (€).

$Q_{aux.,c}$: Annual auxiliary cooling energy consumption after optimal thermal insulation (€).

LCC is subjected to two constrain equations as follows;

$$z = C_{TW}(a) \tag{3.21}$$

$$0 \leq a \leq 51.83\% \tag{3.22}$$

The economic analysis of employing Trombe wall is presented in Figure (3.18). This Figure shows Trombe wall cost, auxiliary energy needed after installing Trombe wall and LCC of the building as a function of Trombe wall area ratio.

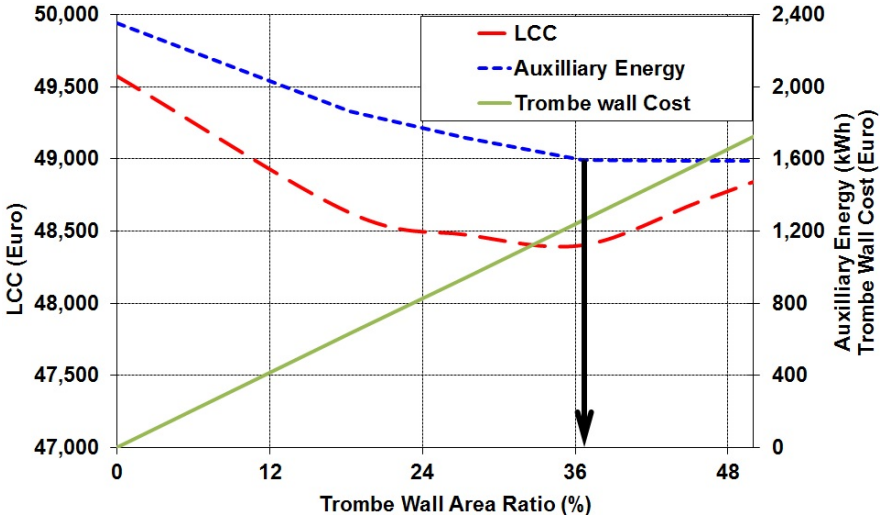

Figure 3.18: Trombe Wall System Economic Analysis

The results show that the economic optimal point is occurred at Trombe wall area ratio of 36.59%. LCC will be reduced by 13.03% over the life span of the building.

3.7 Thermal Insulation and Trombe Wall Optimization

Thermal performance of a combination of Trombe wall and thermal insulation in walls and ceiling have been investigated and reported in Figure (3.19).
A multiple regression analysis for the heating and cooling load have been estimated and reported in Table (3.7). It is obvious that the relationship which describes the heating load over different Trombe wall area ratio and thermal insulation thickness is non-linearly proportioned.

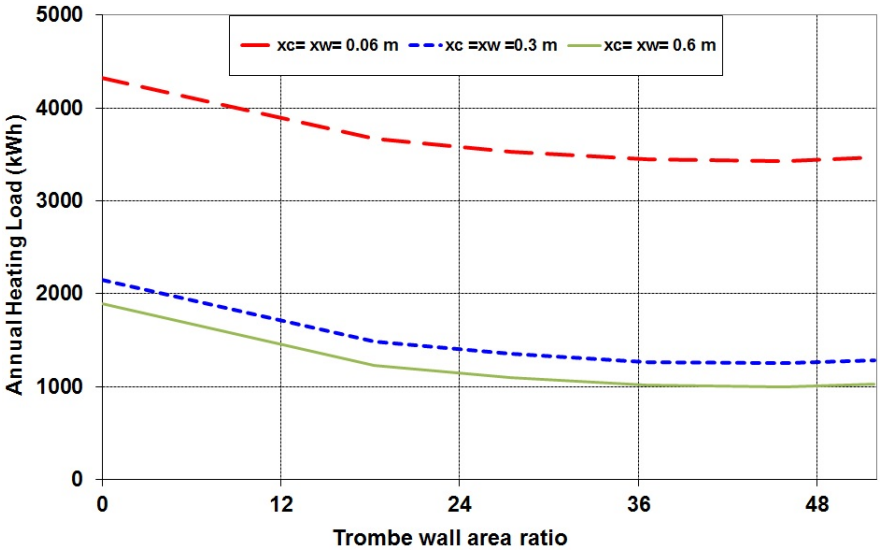

Figure 3.19: Annual Heating Load due to Trombe Wall and Thermal Insulation

Table 3.7: Regression Equation of Heating Load as a Function of Trombe Wall Ratio and Thermal Insulation Thickness

Auxiliary Energy (kWh)	R^2
Heating Mode	
Q = 3592.5 a^4 - 9959.2 x_w^2 + 7084.5 x_c + 21432 x_w - 1559.6 $\sqrt{a}$ - 9443.7 $\sqrt{x_c}$ -17524.2 $\sqrt{x_w}$ + 9259.2	0.9849
Cooling Mode	
Q = 4914.8*x_w^3-5788.2*x_c^2-5020.6*x_w^2+14427.8*x_c -12741.4*$\sqrt{x_c}$+1983*$\sqrt{x_w}$ + 9806.4	0.9983

An optimization of thermal insulation and Trombe wall is estimated using economic figures from local markets. The objective function which will be optimized is LCC function which equal to;
LCC = (auxiliary system cost + maintenance cost for auxiliary system - auxiliary system salvage cost) + (base cost + thermal insulation cost + Trombe wall cost) + (annual auxiliary energy cost - annual cost of saved energy due to thermal insulation and Trombe wall), or;

$$\begin{aligned} LCC = {} & C_{aux.,h}(a,t_c,t_w)[1+f_m PWF - f_{salv}(\frac{1+i}{1+r})^N] + C_{aux.,c}(t_c,t_w)[1+f_m PWF \\ & - f_{salv}(\frac{1+i}{1+r})^N] + C_b + C_{ins.}(t_w,t_c) + C_{T.W}(a) + [Q_{aux.,h}(0,0,0) \\ & - Q_{aux.,h}(a,t_c,t_w)]\frac{p_d}{\eta_{aux.}} \times PWF + [Q_{aux.,c}(0,0) - Q_{aux.,c}(t_c,t_w)]\frac{p_e}{COP}PWF] \end{aligned} \tag{3.23}$$

where:

$Q_{aux.,h}(0,0,0)$: annual auxiliary heating energy consumption (base load) (kWh).

$Q_{aux.,c}(0,0,0)$: annual auxiliary cooling energy consumption (base load) (kWh).

$Q_{aux.,h}(a,t_c,t_w)$: annual heating energy saved due to thermal insulation and Trombe wall (kWh).

$Q_{aux.,c}(t_c,t_w)$: annual cooling energy saved due to thermal insulation (kWh).

LCC is subjected to four constraint equations as follows;

$$z = C_{ins}(t_c,t_w) + C_{T.W}(a) \tag{3.24}$$

$$0\% \leq a \leq 0.52\% \tag{3.25}$$

$$0.06 \leq t_c \leq 0.6 \tag{3.26}$$

$$0.06 \leq t_w \leq 0.6 \tag{3.27}$$

Three design variables have been optimized namely; thermal insulation thickness in ceiling (t_c), thermal insulation thickness in wall (t_w) and Trombe wall area ratio (a). The Microsoft Excel "solver add-in" which uses Generalized Reduced Gradient (GRG) algorithm was used in estimating the optimum variables at minimum LCC.
The results of the economical analysis at different investment levels are presented in Table (3.8). The thermal insulation and Trombe wall have a considerable benefit in Amman region. The calculated benefits are due to both reduction in auxiliary energy system size and reduction in fuel consumption.

Table 3.8: Minimum LCC of a Combination of Thermal Insulation and Trombe Wall at Different Investment Levels

z	t_c	t_w	a	LCC
€	m	m	%	€
Base	Case			78,698
12,000	0.11	0.15	4.95	70,715
14,000	0.19	0.21	20.37	68,285
15,000	0.23	0.24	28.60	68,022
15,093	0.23	0.24	29.24	68,019
15,500	0.25	0.25	31.78	68,046
16,000	0.27	0.27	34.34	68,158
18,000	0.30	0.60	36.82	69,026
20,000	0.42	0.60	42.01	70,428
22,000	0.55	0.60	43.37	72,324
23,327	0.60	0.60	60.00	74,149

It is clear from above Table that minimum LCC occur at (x_w = 0.24 m, x_c = 0.23 m, a = 29.24%) which will reduce LCC by 13.57%. In fact, Trombe wall area ratio of 29.24% is refused from architectural point of view. Thus Trombe wall area ratio will be increased to 36.59%.

As a conclusion, the optimum size for thermal insulation and Trombe Wall is (U_w = 0.123 W/m^{2}K, U_c = 0.143 W/m^{2}K, a = 36.59%). This will reduce annual energy consumption by 33.5% annually by extra initial cost by 49.77%. The specific energy consumption is 58.58 kWh/m^2. On the other hand, LCC will be reduced by 13.55% and 41% of annual CO_2 emission will be saved annually. The new building model is shown in Figure (3.20).

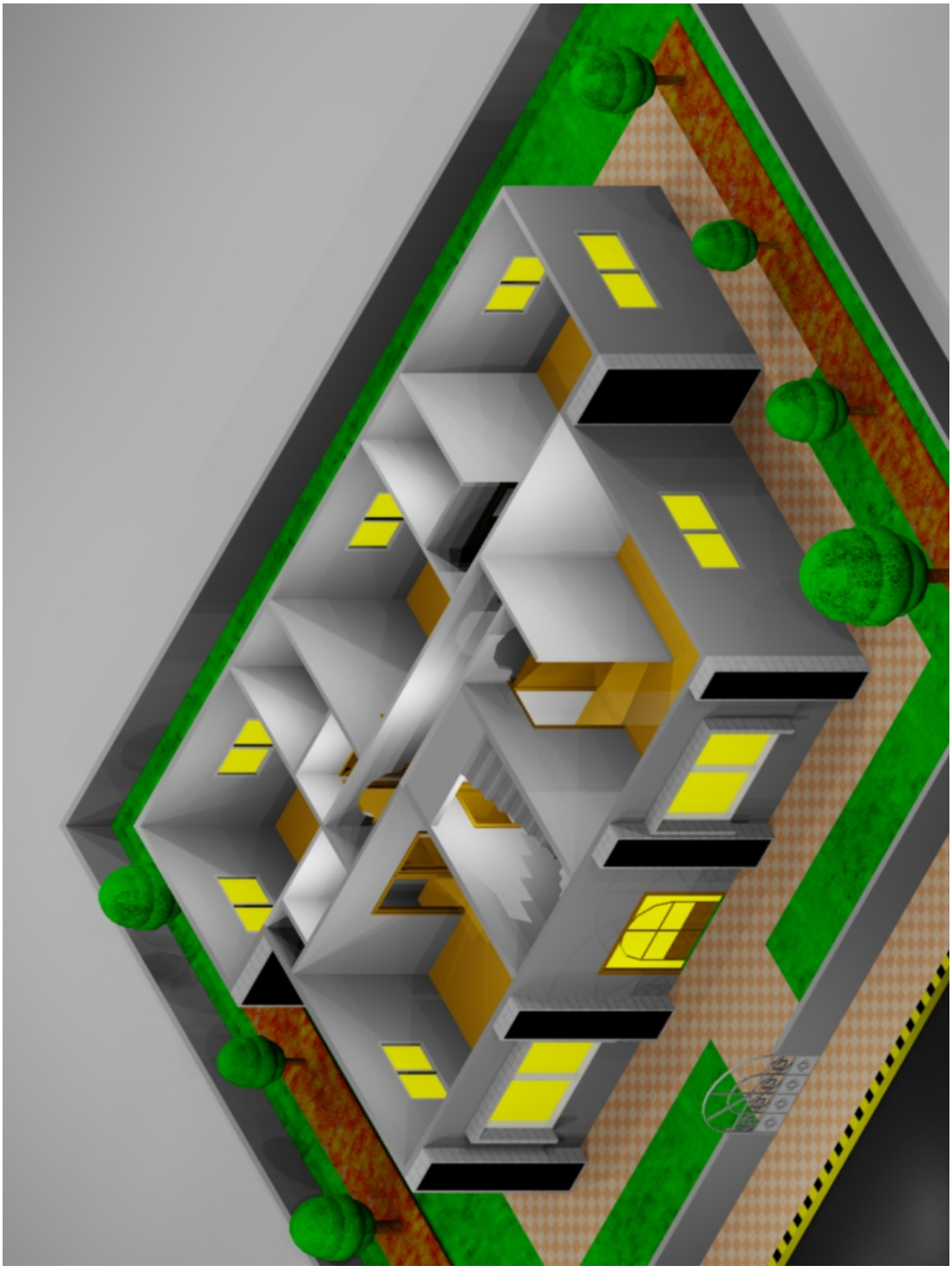

Figure 3.20: New Building Model

Chapter 4

Energy Recovery System

4.1 Introduction

Due to concerns over Indoor Air Quality (IAQ) and occupants health, HVAC-related organizations have set standards that specify the minimum required ventilation rate depending on the type of buildings and occupancy [105; 106]. Higher ventilation rates improve the IAQ by diluting pollutants such as airborne particles and volatile organic compounds. On the other hand, studies have shown that higher ventilation rates increase the building energy consumption in a majority of cases, especially during heating season [107; 108; 109]. In this chapter Energy Recovery System (ERS) will be designed technically and economically to ensure a healthy environment for the occupants and reduce energy loss due to ventilation.

4.2 Energy Recovery System Design

ERS has two fans and two duct systems. One duct introduces fresh air (supply duct system) while the other one exhausts indoor polluted air (exhaust duct system). Exhaust duct system works by depressurizing the building by reducing the inside air pressure below the outdoor air pressure, while supply duct system works by pressurizing the building by using a fan to force outside air into the building.
Exhaust air is taken from the kitchen and bathrooms to ensure that there is no air move from bathrooms and kitchen to the other places in the building by making negative pressure in these areas. On the other hand, fresh air is supplied to the bedrooms, guest and living rooms.
According to ASHRAE standards 62.2-2004, the ventilation air requirement is 21 l/s at all times, in addition to 5 Air Changes per Hour (ACH) from the kitchen and 10 l/s per each bathroom as continuous exhaust ventilation [105]. Thus, the total ventilation

rate for the building is 92.17 l/s. The fresh air in this study is considered at the same conditions of the ambient, while the exhaust air is considered at the same conditions of the inside air.
Cross flow heat exchanger is a major component in ERS. This type of exchanger is less likely to become blocked with contaminants and is more easily cleaned. Maintenance is also minimized because there are no moving parts. This heat exchanger is made of Aluminum and its geometry is shown in Figure (4.1).

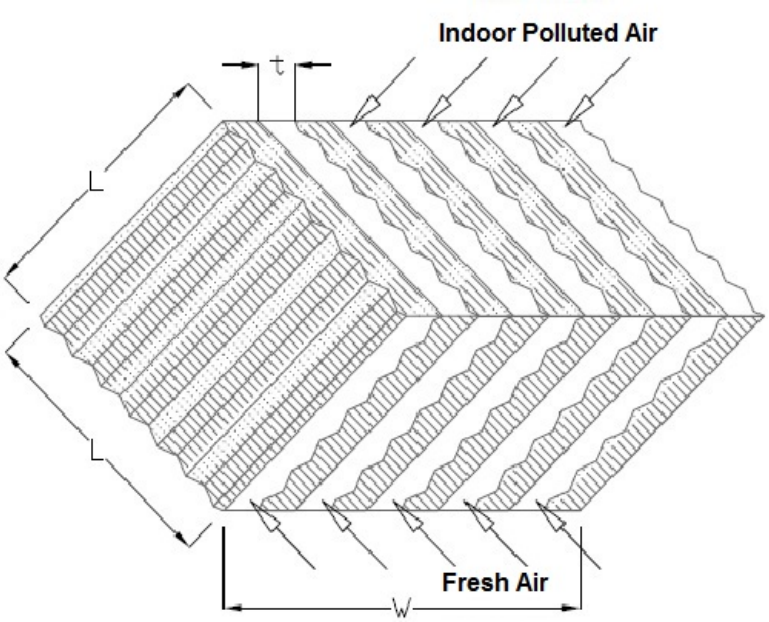

Figure 4.1: Cross Flow Heat Exchanger Geometry

The heat exchanger width (W) varies between 30 - 130 mm. The heat exchanger length (L) varies between 200 - 500 mm. The heat transfer area varies between 0 - 50 m^2.
Heat transfer effectiveness (ε) for cross flow heat exchanger (unmixed) is independent of exchanger temperatures. It can be expressed as [3];

$$\varepsilon = 1 - exp(\frac{e^{-NTU\gamma\dot{C}_r} - 1}{\dot{C}_r\gamma}) \tag{4.1}$$

where;

γ= NTU$^{-0.22}$, $\dot{C}_r = \frac{\dot{C_{min}}}{\dot{C_{max}}}$

NTU : Number of Transfer Units.

Also ε is defined as the actual heat transfer ($\dot{Q}_{HX}$) divided by the maximum possible

heat transfer ($\dot{Q}_{max}$) [3],

$$\varepsilon = \frac{\dot{Q}_{HX}}{\dot{Q}_{max}} \tag{4.2}$$

Assuming that there is no leakage flow, no heat loss and no phase change. Thus, the enthalpy differences across the supply and exhaust air streams are equal. Hence, the heat transfer can be expressed as;

$$\dot{Q}_{HX} = \dot{C}_s(T_{s,o} - T_{s,i}) = \dot{C}_e(T_{e,i} - T_{e,o}) = UA\Delta T_{lm} \tag{4.3}$$

where;

$\dot{C}_s$: supply air capacity rate (kJ/K.s).

$\dot{C}_e$: exhaust air capacity rate (kJ/K.s).

$T_{s,o}$: outlet temperature of supply air (°C).

$T_{s,i}$: inlet temperature of supply air (°C).

$T_{e,o}$: outlet temperature of exhaust air (°C).

$T_{e,i}$: inlet temperature of exhaust air (°C).

A : heat exchanger area (m^2).

U : overall heat transfer coefficient (W/m^2K).

ΔT_{lm} : log mean temperature difference.

Since supply and exhaust capacity rate are equal ($\dot{C}_s = \dot{C}_e = \dot{C}$), Therefore;

$$\dot{Q}_{HX} = \dot{C}(T_{s,o} - T_{s,i}) = \dot{C}(T_{e,i} - T_{e,o}) \tag{4.4}$$

The maximum heat exchange is given by the product of the lower capacity rate ($\dot{C}_{min}$) and the inlet temperature difference, i.e.;

$$\dot{Q}_{max} = \dot{C}_{min}|(T_{e,i} - T_{s,i})| \tag{4.5}$$

By substituting equations (4.4) and (4.5) into (4.2) equation; ε can be computed as;

$$\varepsilon = \frac{(T_{s,i} - T_{s,o})}{(T_{s,i} - T_{e,i})} \tag{4.6}$$

Then, the outlet temperature of supply air can be calculated as;

$$T_{s,o} = T_{s,i} + \varepsilon(T_{e,i} - T_{s,i}) \tag{4.7}$$

The heat transferred is calculated by substituting T_{so} into equation (4.4). Then, the outlet temperature of the exhaust air is;

$$T_{e,o} = T_{e,i} + \frac{\dot{Q}_{HX}}{\dot{C}} \tag{4.8}$$

Hourly outlet temperatures of supply and exhaust streams have been simulated by using INSEL simulation software [4]. Then, hourly outlet supply temperatures are used as inlet air temperature to TRNSYS software [7] to calculate hourly cooling and heating load required for indoor comfort. Outlet supply temperature profile as compared with ambient temperature profile for the whole year is simulated and plotted in Figure (4.2)

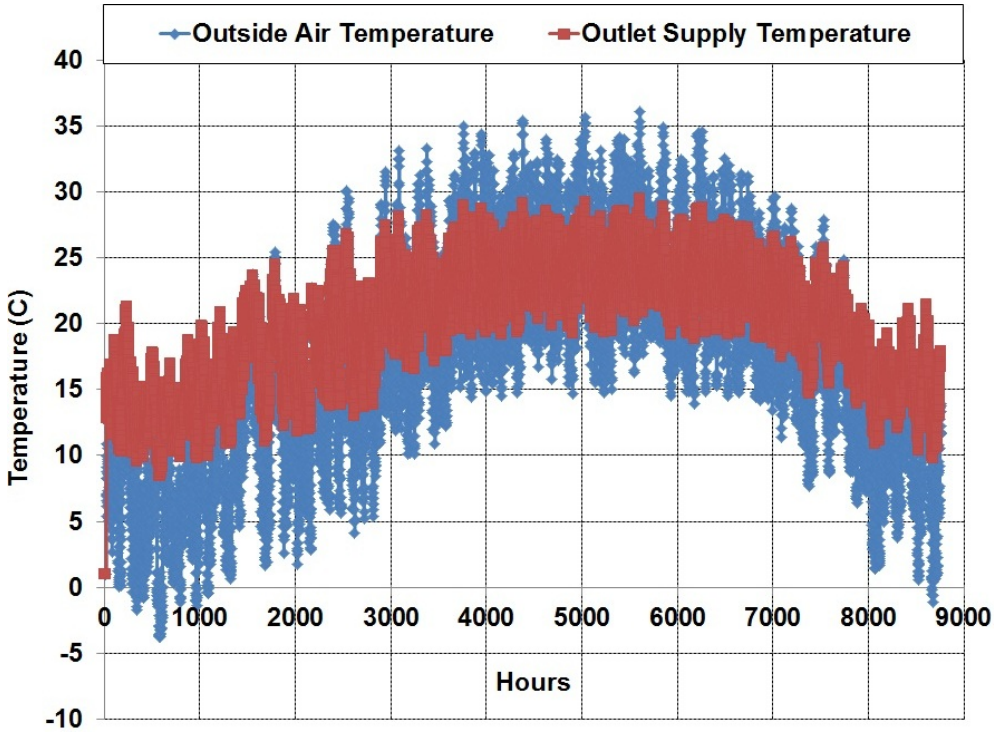

Figure 4.2: Temperature Variation due to ERS

Outlet supply temperature profiles for the coldest day (January 22) in Winter and the hottest day (August 26) in Summer are shown in Figure (4.3) and Figure (4.4). These Figures show that ERS is used during the whole day in winter while it's used in summer only after 8:00 AM.

The relationships which describe annual energy demand at different heat transfer ar-

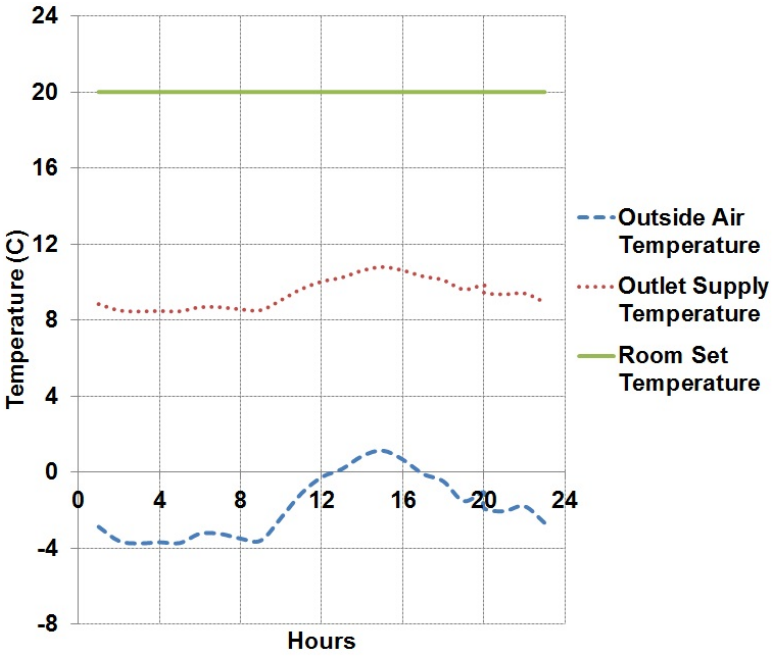

Figure 4.3: Temperature Variation due to ERS (Jan. 22)

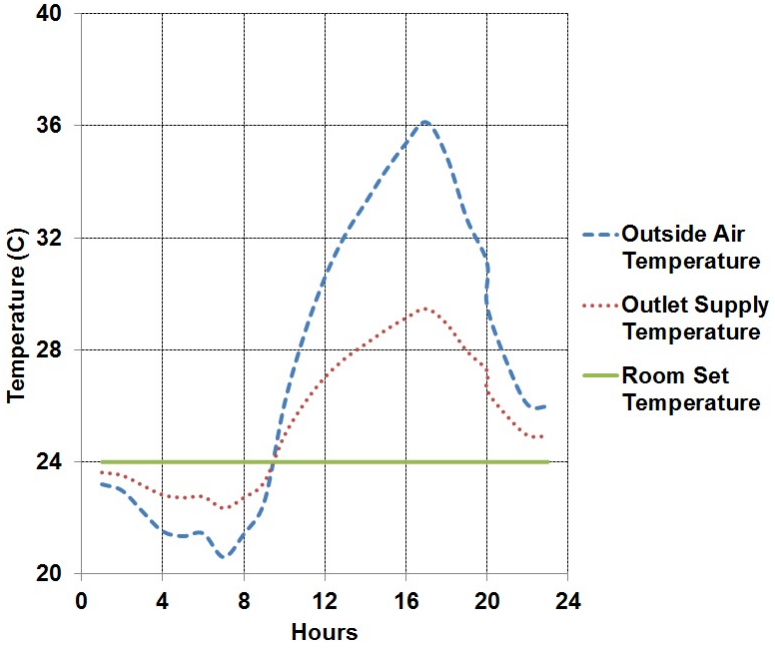

Figure 4.4: Temperature Variation due to ERS (Aug. 26)

eas are non-linearly proportioned. A multiple regression equations for annual energy demand as a function of heat transfer areas are presented in Table (4.1).

Table 4.1: Regression Equations of Auxiliary Energy as a Function of Heat Transfer Area

Auxiliary Energy (kWh)	R^2
Heating Mode	
$Q = -1\times10^{-4}A^5+1.44\times10^{-2}A^4-0.7661A^3+19.234A^2-239.25A+1563.1$	0.9972
Cooling Mode	
$Q = -1.2\times10^{-3}A^5+7.6\times10^{-2}A^4-1.8A^3+22.54A^2-145.19A+7469.1$	0.9972

Hours of using ERS for heating and cooling modes has been determined based on outside and inside conditions. The annual operation hours of ERS in Winter, where the outside temperature is lower than 20°C, is 2,666 hours. The annual operation hours in Summer, where the outside temperature is higher than 24°C, is 1,417 hours.
Figure (4.5) shows energy saving due to ERS. It is noticed that heat transfer area of 2.4 m^2 is sufficient to reduce about 32.65% and 1.85% from annual heating and cooling energy load, respectively. Also, heat transfer area of 50 m^2 will save 89.64% and 6.90% from heating and cooling energy consumption, respectively.

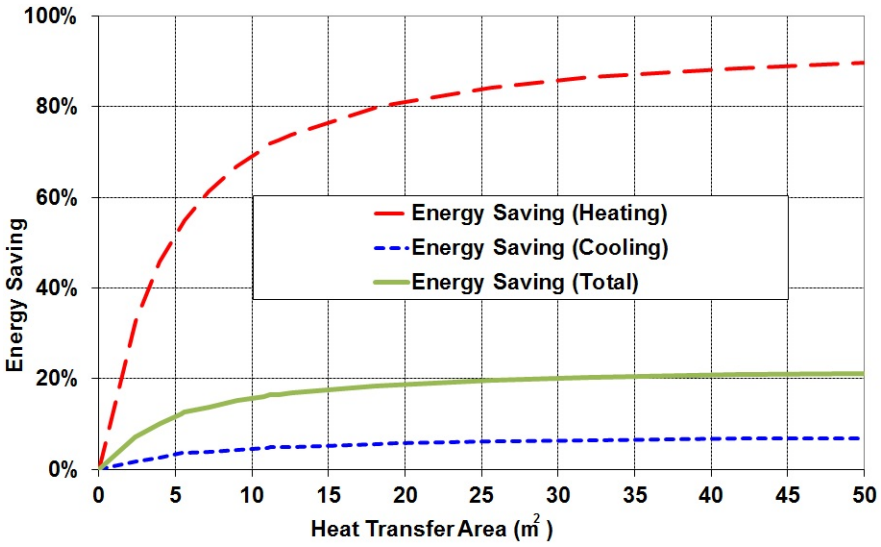

Figure 4.5: Energy Saving due to ERS

It is clear from the Figure above that ERS in Winter is more effective than in Summer. The energy saving is slightly increased after heat transfer area of 10 m^2 in Winter where it is slightly increased after area of 4 m^2 in Summer.

4.3 Energy Recovery System Optimization

In order to perform optimum size of ERS, it is necessary to obtain building Life Cycle Cost (LCC). Then, LCC is minimized by using economic figures from local markets. The objective function equals to;
LCC = (auxiliary system cost + maintenance cost for auxiliary system - auxiliary system salvage cost) + (ERS cost + maintenance cost - salvage cost) + base cost + (annual auxiliary energy cost - annual cost of saved energy due to ERS + ERS running cost) or;

$$\begin{aligned} LCC = {} & C_{aux.,h}(A)[1 + f_m PWF - f_{salv}(\frac{1+i}{1+r})^N] + C_{aux.,c}(A)[1 + f_m PWF \\ & - f_{salv}(\frac{1+i}{1+r})^N] + C_{ERS}(A)[1 + f_m PWF - f_{salv}(\frac{1+i}{1+r})^N] + C_b + [Q_{aux.,h}(0) \\ & - Q_{ERS,h}(A)]\frac{p_d}{\eta aux.} PWF + [Q_{aux.,c}(0) - Q_{ERS,c}(A)]\frac{p_e}{COP} PWF + Q_{r.e} PWF \end{aligned} \tag{4.9}$$

where:

A : ERS heat transfer area (m^2).

C_b : base cost (€).

C_{ERS} : ERS cost (€).

$C_{aux.,h}$: auxiliary heating system cost (€).

$C_{aux.,c}$: auxiliary cooling system cost (€).

$Q_{aux.,h}$ (0) : annual auxiliary heating energy consumption after applying optimum passive design techniques (kWh).

$Q_{aux.,c}$ (0) : annual auxiliary cooling energy consumption after applying optimum passive design techniques (kWh).

Q_{ERS} : annual cooling energy saved due to ERS (kWh).

$Q_{r.e}$: annual running energy due to ERS (kWh).

f_m: maintenance fraction (%)

PWF: Present Worth Factor

$$PWF = \sum_{j=1}^{N} (\frac{1+i}{1+r})^j = \frac{1+i}{1+r}(1 - (\frac{1+i}{1+r})^N) \tag{4.10}$$

f_{salv}: salvage fraction (%).

i : inflation rate (%).

r : interest rate (equivalent to discount rate) (%).

N : life time (Years).

p_d : thermal energy price (€/kWh).

p_e : electrical energy price (€/kWh).

$\eta_{aux.}$: auxiliary heating system efficiency (%)

COP : auxiliary cooling system Coefficient Of Performance.

LCC is subjected to two constrain equations as follows;

$$z = C_{ERS}(A) \tag{4.11}$$

$$2.4 \leq A \leq 50 \tag{4.12}$$

The running cost of ERS is the summation of supply and exhaust fans electricity cost. The fan power required is estimated from [110];

$$P = (\dot{V} * \triangle p)/(\eta_{f,m} * 1000) \tag{4.13}$$

where;

P : fan power (W).

$\dot{V}$: volume flow rate of supply air (l/s).

$\triangle p$: pressure drop of air caused by fluid friction (pa).

$\eta_{f,m}$: overall efficiency of fan and motor.

Energy saving, LCC and Payback Period (PbP) results at different heat transfer areas are calculated and summarized in Table (4.2). Moreover, ERS initial cost, annual auxiliary energy (heating and cooling) and LCC are plotted in Figure (4.6).

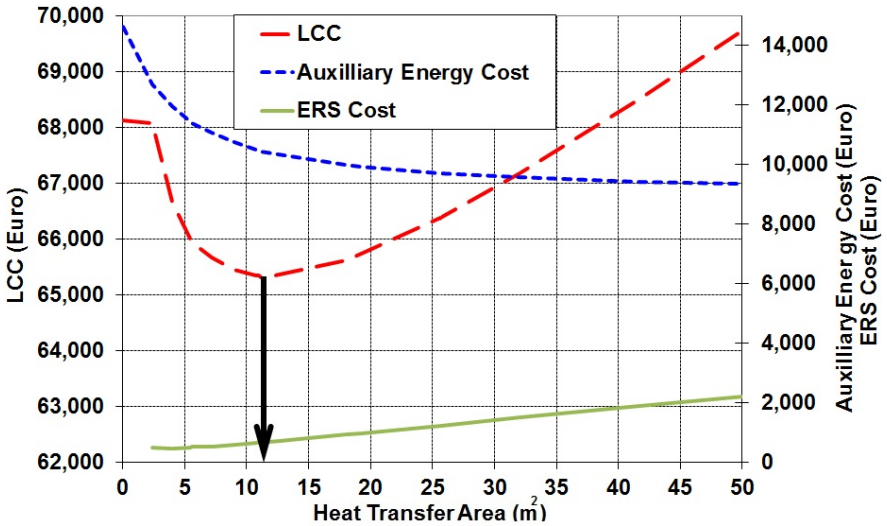

Figure 4.6: Economical Analysis of ERS

Table 4.2: Summary of Economic Benefits

A m^2	Saving %	PbP Years	LCC €
Base	Case	-	78,698
0	33.5	-	68,037
2.4	38.26	12.33	68,070
4.0	40.24	7.94	66,671
5.6	41.87	7.30	65,937
7.2	42.69	6.90	65,665
9.0	43.57	7.06	65,442
10.8	44.24	7.40	65,353
11.2	44.43	7.44	65,320
12.6	44.75	7.80	65,356
18.0	45.78	9.23	65,614
19.2	45.93	9.60	65,729
25.6	46.59	11.55	66,378
32.0	47.01	13.55	67,175
41.6	47.43	16.60	68,496
50.0	47.58	19.34	69,729

It is shown from Figure (4.6) and Table (4.2) that as initial cost increases the annual auxiliary energy needed to cover the annual energy demand is decreased. The results show that minimum LCC over 30 years is occurred at heat transfer area of 11.2 m^2. The LCC of the building is reduced by 17% from the basic case by applying optimum passive design techniques in addition to introducing ERS. This will reduce annual

energy consumption by 44.43% annually by extra initial cost by 56.31%. The specific energy consumption is 48.95 kWh/m^2. On the other hand, annual CO_2 emissions by 54.8% will be saved annually. The payback period of ERS initial cost from the achieved saving is 7.44 years.

Chapter 5

Indirect Evaporative and Storage Unit

Phase Change Materials (PCMs) are received increasing interest, which have been recognized as one of effective approaches to reduce energy consumption in buildings. This chapter will focus on a novel application of PCM for cooling purpose.

5.1 Evaporative Cooling

5.1.1 Direct Evaporative Air-Conditioning

Direct Evaporative Air-Conditioning (DEAC) is the simplest, the oldest, and the cheapest system of air-conditioning. This system typically consists of large porous wetted pads, a sump at the bottom, an electric motor driven fan, a water pump and a water distribution. In this system, air is drawn through porous wetted pads and its sensible heat evaporates some water; the heat and mass transfer between the air and water lowers the air dry-bulb temperature and increases the humidity at a constant wet-bulb temperature. The heat and mass transfer stops when the dry-bulb temperature of the nearly saturated air approaches the ambient air's wet-bulb temperature [110]. The amount of cooling provided is determined by efficiency of the wetting medium, the fan, and the overall design and construction of the unit. This system is well suited for climates where the air is hot and humidity is low. The disadvantages of such system are: the noise, difficult in controlling the interior temperature, and the quality of conditioned air due to adding moisture to the air. To improve the comfort level of conditioned air Indirect Evaporative Air-Conditioning (IEAC) is introduced [41; 42; 43; 44].

5.1.2 Indirect Evaporative Air-Conditioning

Indirect Evaporative Air-Conditioning (IEAC) is similar to DEAC, but uses heat exchanger. The cooled moist air never comes in direct contact with the conditioned air. The indirect process is a sensible cooling process on the psychometric chart. This process follows a line along a constant humidity ratio since no moisture is introduced in IEAC.
The performance of IEAC is measured by Wet-Bulb Depression Efficiency (WBDE). This is calculated as follows [110]:

$$WBDE = \frac{T_{amb} - T_{si}}{T_{amb} - T_{wb}} \tag{5.1}$$

where;

WBDE : Wet-Bulb Depression Efficiency (%).

T_{si} : inlet temperature of secondary air (°C).

T_{amb} : ambient temperature (°C).

T_{wb} : wet-bulb temperature (°C).

Two models of IEAC were simulated by Jaber and Ajib [111]. The performance of these models were investigated by using INSEL and TRNSYS Softwares. INSEL produces the modified inlet air temperature (supply air temperature to the building) due to introducing IEAC. Then, this temperature is used as input to TRNSYS software to calculate hourly cooling load required for indoor comfort [111].
The schematic of first model is shown in Figure (5.1). The inlet primary stream comes from the room while the inlet secondary stream comes from outside air at ambient temperature. The cooling due to ventilation (hot air entering the building) is calculated in TRNSYS software.
The second model considers the outside and room air as inlet primary and inlet secondary stream, respectively. The cooling due to ventilation is set to be zero in TRNSYS software because it is already included in INSEL software. The schematic of this model is shown in Figure (5.2).
The results show that first model of IEAC behaves technically better than the second model [111]. Figure (5.3) shows the psychometric process for both models at ambient temperature of 35°C and 22°C. Even the new model behaves technically better but it's still not sufficient to work at peak cooling load.

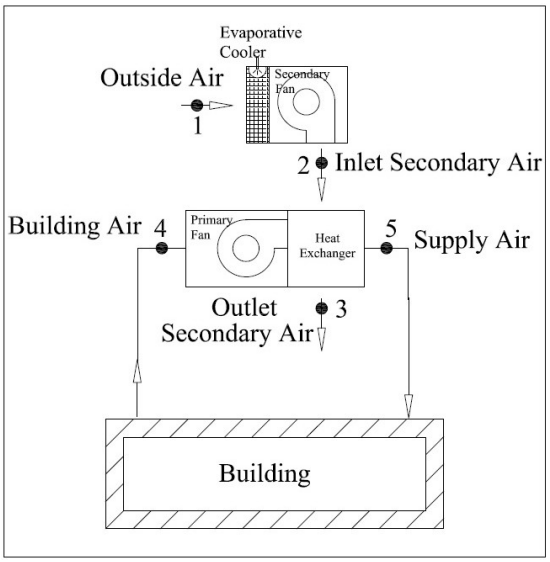

Figure 5.1: First Model of IEAC

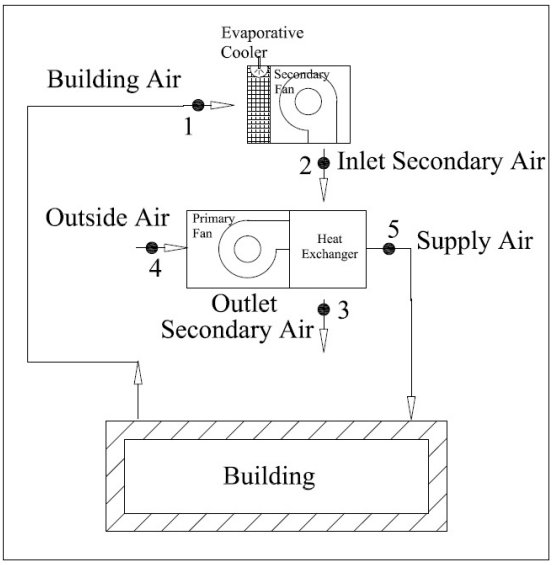

Figure 5.2: Second Model of IEAC

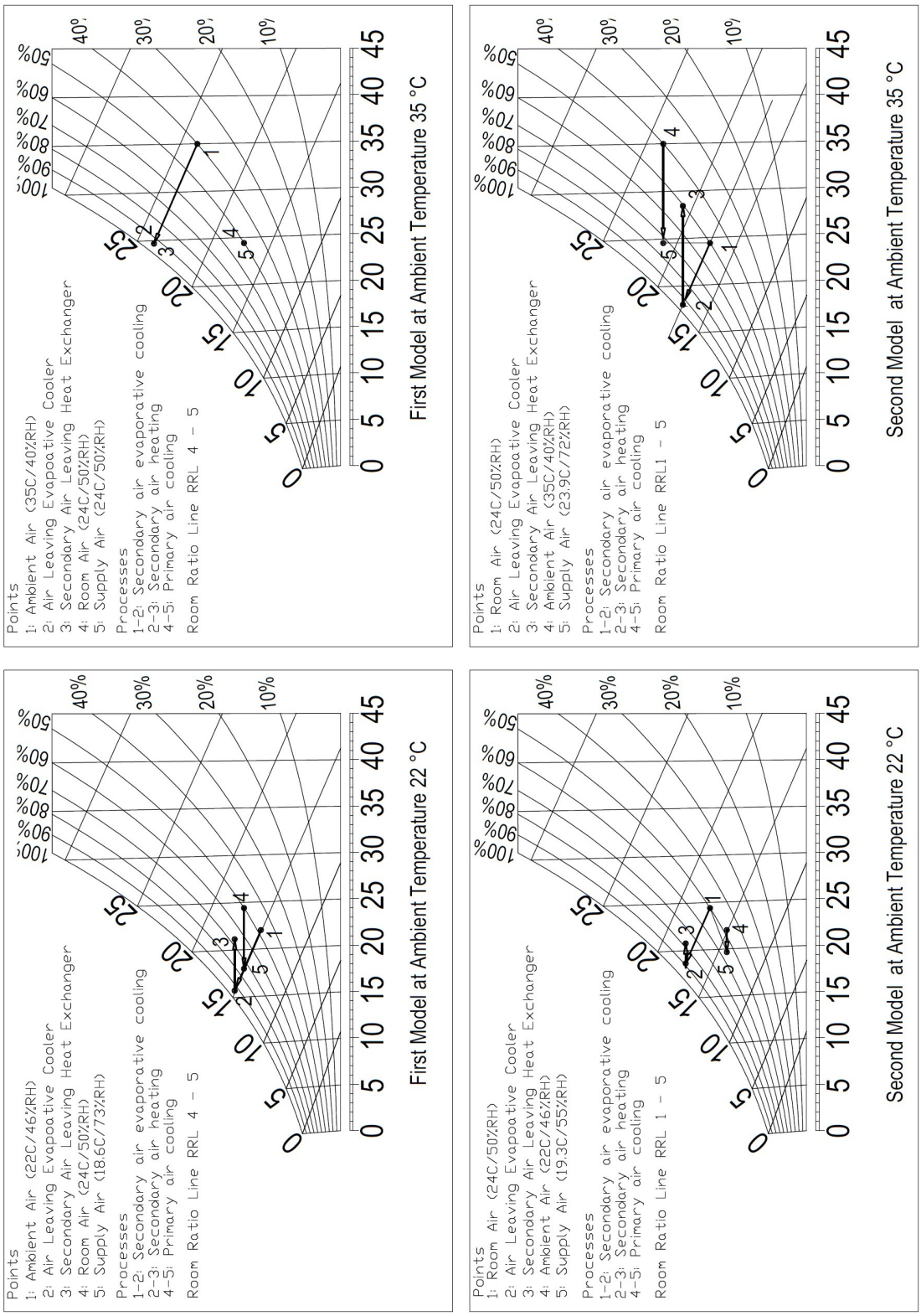

Figure 5.3: Psychometric Chart of First and Second Model at Ambient Temperature of 35°C and 22°C

5.2 Mathematical Model

Indirect Evaporative and Storage Unit (IESU) consists of IEAC and PCM heat exchanger, as shown in Figure (5.4). This model is treated as a forced convection problem.

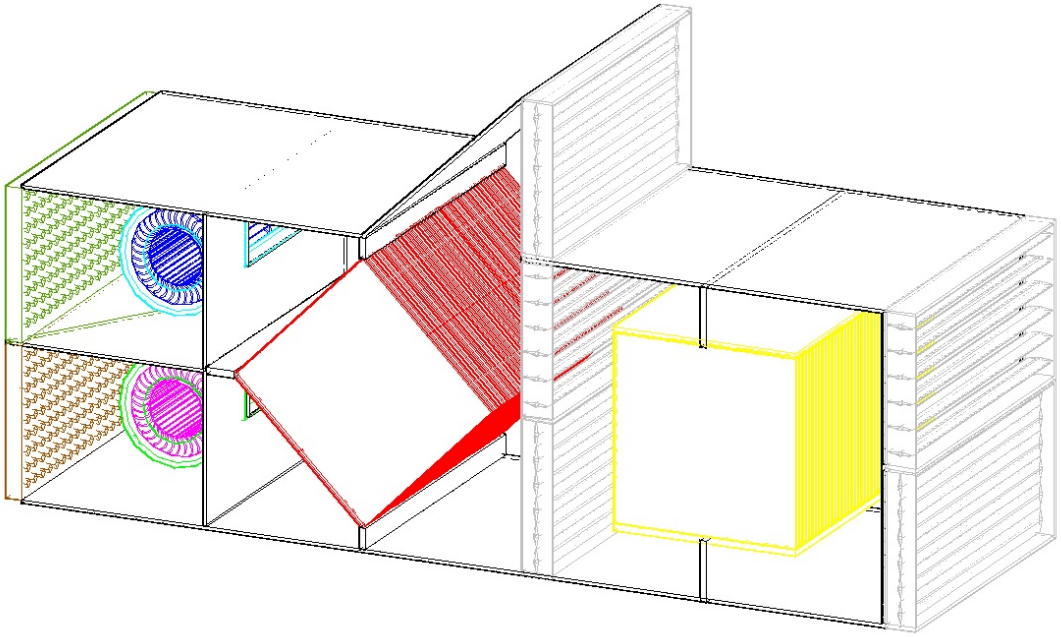

Figure 5.4: Indirect Evaporative and Storage Unit Model

5.2.1 Indirect Evaporative Air-Conditioning

The outlet temperatures for both primary and secondary air at each time step i can be calculated from the following equations [110];

$$\begin{aligned} T_{po,i} &= T_{pi,i} - \varepsilon * (T_{pi,i} - T_{si,i}) \\ T_{so,i} &= T_{si,i} - \varepsilon * (T_{pi,i} - T_{si,i}) \end{aligned} \tag{5.2}$$

where;

ε : heat exchanger effectiveness (%).

T_{pi} : inlet temperature of primary air (°C).

T_{po} : outlet temperature of primary air (°C).

T_{so} : outlet temperature of secondary air (°C).

Effectiveness in equations (5.2) is independent of exchanger temperatures. For cross flow heat exchanger (unmixed) the dimensionless exchanger heat transfer effectiveness is computed from equation 4.1 on page 55.
Then; cooling capacity at each time step i can be calculated from the following equation [3];

$$\dot{Q}_{IEAC,i} = \dot{m} * C_p * (T_{pi,i} - T_{po,i}) \tag{5.3}$$

where;

$\dot{Q}_{IEAC}$: IEAC cooling capacity (kJ/s).

$\dot{m}$: air flow rate (kg/s).

C_p : air specific heat (kJ/kg.K).

5.2.2 PCM Heat Exchanger

The schematic of the heat exchanger filled with PCM is shown in Figure (5.5). The air flows through the passages between PCM layers. The thermal losses through the outer wall of the PCM heat exchanger are negligible.

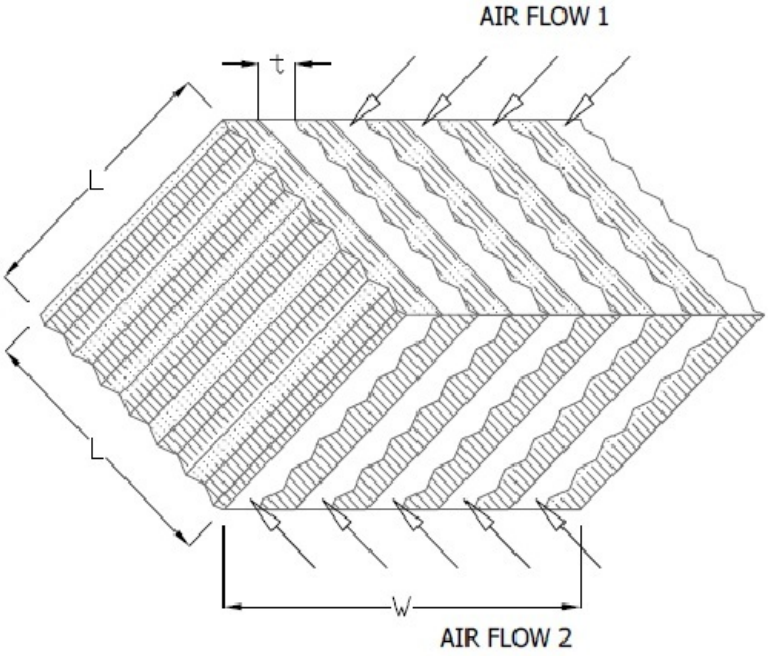

Figure 5.5: Heat Exchanger Model

PCM heat exchanger is modeled as rectangular corrugated flat tube with constant airflow temperature in Y-direction. The air temperature in X direction is varied through

over the year every 6 minutes. PCM is initially solid and its temperature is assumed at ambient temperature. The capacity of the PCM heat exchanger at each time step i is given by [53];

$$\dot{Q}_{p,i} = \alpha_p * P * L * (T_{a,i} - T_{pcm,i}) \tag{5.4}$$

where;

$\dot{Q}_p$: PCM heat exchanger capacity (kJ/s).

T_a : air temperature (°C).

P : heat exchanger perimeter (m).

L : heat exchanger length (m).

T_{pcm} : PCM temperature (°C).

α_p : fictive convective heat transfer coefficient (W/m^2K).

The fictive convective heat transfer coefficient depends on the geometry of the heat exchanger, the airflow and perimeter of the exposed material. It can be calculated from the following formula [53];

$$\alpha_p = \frac{v * A * \rho * C_p * (1 - e^{-\frac{P*U}{v*A*\rho*C_p}L})}{P * L} \tag{5.5}$$

where;

v : air velocity (m/s).

A : cross sectional area (m^2).

ρ : air density (kg/m^3).

U : heat transfer coefficient between middle of the PCM and air (W/m^2K)

The physical properties of PCM that used in this research are presented in Table (5.1).

Table 5.1: PCM Physical Properties [9]

Latent heat of fusion (λ)	175	kJ/kg
Specific heat (C_p)	2	kJ/kg.K
Thermal conductivity (k)	1	W/m.K
Density (ρ)	671	kg/m^3

5.2.3 Indirect Evaporative and Storage Unit

The schematic of IESU model is shown in Figure (5.6). This unit will be optimally designed from both technical and economic point of view.
Mathematical model for IESU has been developed. This mathematical model is based on the phase change process involving either melting or solidification. A change of material phase refers to change of material state between the phases solid and liquid. The heat absorbed or released as a result of phase change is referred to as latent heat. This change of phase occurs at constant temperature called melting temperature (T_m). The heat absorbed or released, at time step i, can be calculated from the following equation;

$$\dot{Q}_{p,i} = \alpha_p A(T_{a,i} - T_{pcm,i}) \tag{5.6}$$

where;

$\dot{Q}_p$: PCM heat exchanger capacity (kJ/s).

α_p : fictive convective heat transfer coefficient (W/m^2.K).

A : heat exchanger area (m^2).

T_{pcm} : PCM temperature (°C).

T_a : air temperature (°C).

If PCM temperature doesn't equal the melting temperature, that means sensible heat will be absorbed or released. In this case PCM temperature will change accordingly until reaching the melting temperature. The new PCM temperature ($T_{pcm,i+1}$) can be calculated from the following equation in this case;

$$T_{pcm,i+1} = T_{pcm,i} + \frac{\dot{Q}_i}{\dot{m}C_{p,pcm}} \quad , \quad T_{pcm,i} \neq T_m \tag{5.7}$$

If PCM temperature is equal the melting temperature, That means only latent heat will be absorbed or released. In this case PCM temperature will not change (i.e $T_{pcm,i+1}$ = $T_{pcm,i}$) until reaching the maximum capacity of PCM. Maximum latent heat stored can be calculated as follows;

$$Q_{max} = m\lambda \quad , \quad T_{pcm} = T_m \tag{5.8}$$

where;

Q_{max} : maximum latent heat stored during transition state (kJ).

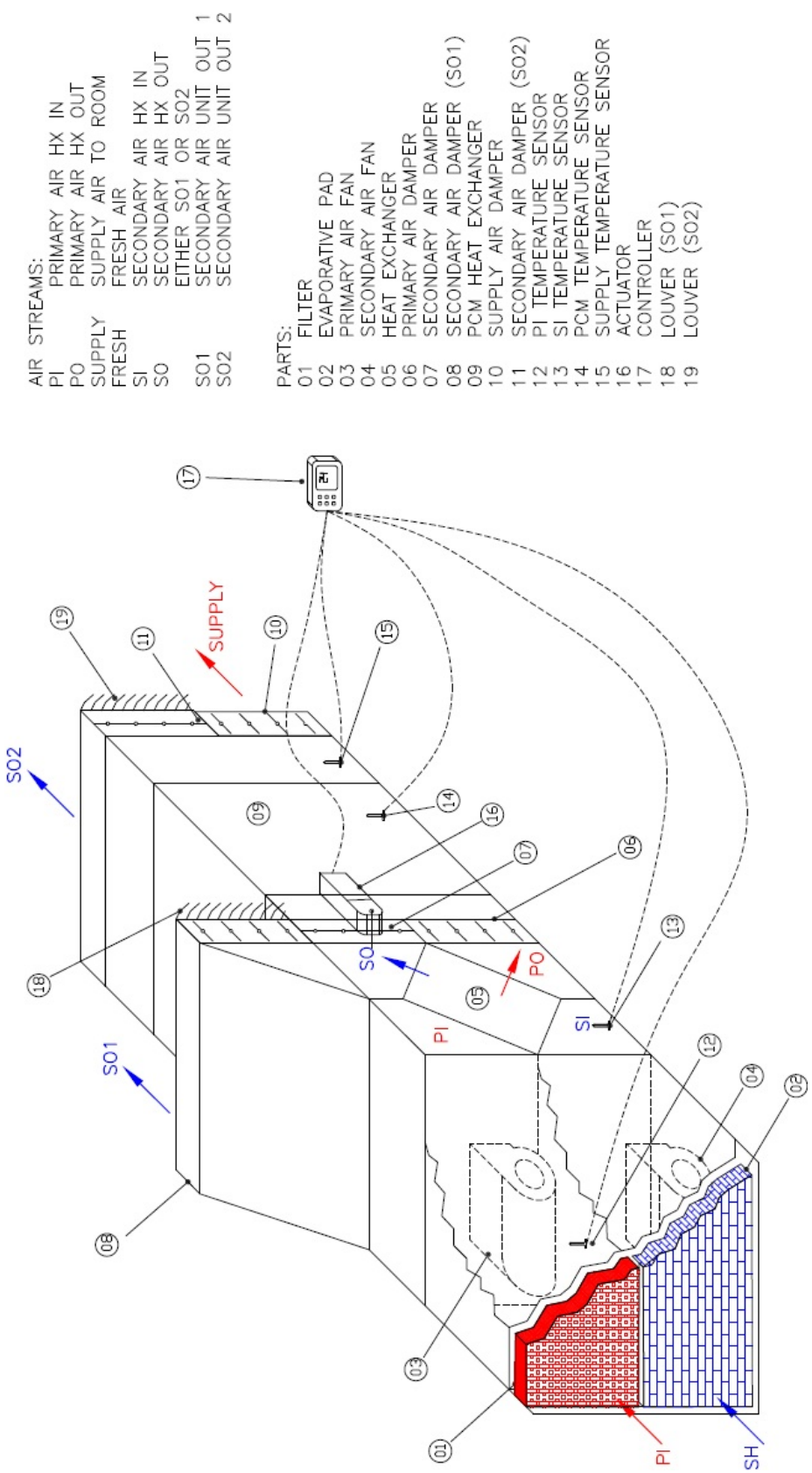

Figure 5.6: Schematic of Indirect Evaporative and Storage Unit Model

m : PCM mass (kg).

λ : latent heat of fusion (kJ/kg).

The heat transfer coefficient is calculated from the following equation [112];

$$h = \frac{Nu.k}{D_h} \tag{5.9}$$

where;

h : heat transfer coefficient (W/m^{2}K).

Nu : Nusselt number.

k : thermal conductivity (W/m.K).

D_h : hydraulic diameter (m).

Nusselt number (Nu) is calculated for a rectangular corrugated flat tubes from Hausen empirical relation [112];

$$Nu = 0.036.Re^{0.8}Pr^{1/3}(\frac{D_h}{L})^{0.055} \tag{5.10}$$

where;

Re : Reynolds number.

Pr : Prandtl number.

L : heat exchanger length (m).

IESU software module has been developed by using Visual Basic 6. This software simulates IESU performance every 10 minutes during the whole year. IESU's software is easy to use, contains 24 inputs and 59 outputs, as shown in Appendix. The user can chose the output styles which are save data to file or plot output data or view output data directly in the software screen. Furthermore, The hourly output temperatures at different locations can be monitored. These temperatures are T_{pi}, T_{po}, T_{si}, T_{so}, T_s, T_{pcm}. Moreover, in order to facilitate the optimization analysis the user can select 8 parameters and do multi-simulations for 8 parameters (L_e, W_e, t_e, L_p, W_p, t_p, $\dot{m}$, T_m). Flow chart of the IESU simulation software is shown in Figure (5.7).
IESU has four modes of operation namely; cooling by PCM plus IEAC, cooling by PCM, charging and OFF mode, as shown in Figure (5.7).
Once first mode (cooling by PCM plus IEAC) happens dampers number 6, 8 and 10 will be opened automatically where both dampers 7 and 11 will be closed, as shown in Figure (5.8). Moreover, both primary and secondary air fans will be operated.

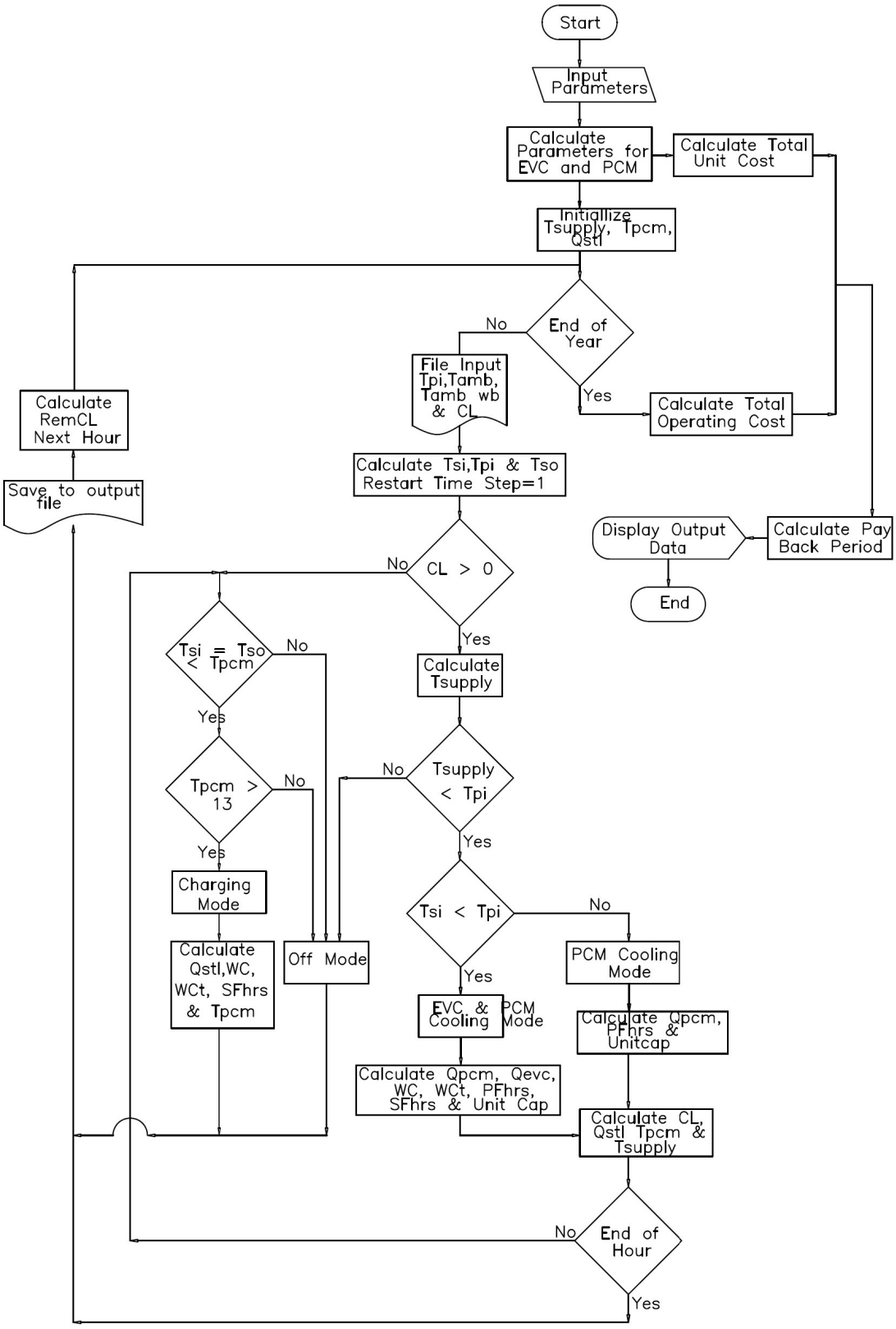

Figure 5.7: Sequence of Operation

In case secondary air temperature is higher than primary air temperature (i.e IEAC is adding heat to the primary air), the air will pass only by PCM heat exchanger while IEAC fan will be off. In this case both dampers 6 and 10 will be opened while dampers 7, 8 and 11 will be closed automatically, as shown in Figure (5.6). The secondary air fan will be switched off.
In charging mode, the secondary air fan will be switched on while the primary fan will be switched off. Furthermore, dampers 7 and 11 will be opened and dampers 6, 8 and 10 will be closed, as shown in Figure (5.9). This mode will occur once there is no cooling load demand and availability of good weather conditions to operate IEAC. This will be a good chance to store cooling energy in PCM for later use.
The last mode is OFF which will happen in three cases. The first case when IESU supplies temperature higher than leaving temperature from the building. The second when there is no cooling demand and PCM temperature is lower than secondary air temperature. That means IEAC will increase PCM temperature. The last case will be once there is no cooling load and PCM temperature is less than 13°C. This temperature insures that supply air temperature to the building will not be too cold [113].
The supply temperature from this unit to the building at each time step i is calculated with the following equation;

$$T_{s,i} = T_{pcm,i-1} + (T_{po} - T_{pcm,i-1}) * e^{-\frac{P*U}{v*A*\rho*C_p}L} \tag{5.11}$$

T_s : supply temperature (°C).

A : cross sectional area (m^2).

The running cost of IESU is the summation of the water cost, primary and secondary fans electricity cost. The fan power required is estimated from equation 4.13 on page 61. The water consumption of IESU can be calculated from the following equation;

$$m_w = 3600 \times \dot{m}(w_{si} - w_{amb})t \tag{5.12}$$

where;

$\dot{m}$: air flow rate (kg/s).

w_{si} : humidity ratio at inlet secondary air conditions (kg_w/kg_a).

w_{amb} : humidity ratio at ambient conditions (kg_w/kg_a).

t : time period (hour).

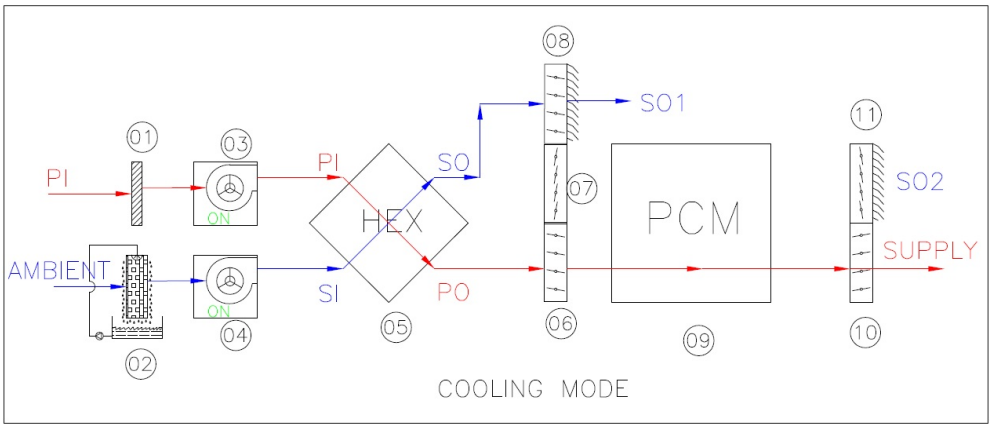

Figure 5.8: IESU's Cooling Mode

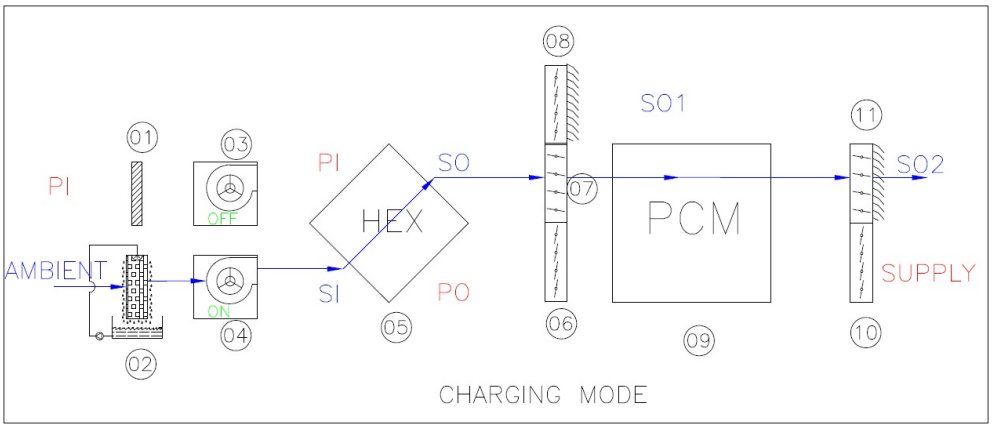

Figure 5.9: IESU's Charging Mode

5.3 Thermal Analysis

Energy storage components improve the energy efficiency of IESU by reducing the mismatch between supply and demand. There are eight parameters highly affect the performance of IESU namely; PCM melting temperature (T_m), PCM heat exchanger thickness (t_p), PCM heat exchanger length (L_p), PCM heat exchanger width (W_p), IEAC heat exchanger thickness (t_e), IEAC heat exchanger length (L_e), IEAC heat exchanger width (W_e), flowrate ($\dot{V}$). The range of investigated parameters are shown in Table (5.2).

Table 5.2: Range of Investigated Parameters

Parameter	Quantity	Unit
T_m	14 - 26	°C
	Default 20	°C
t_p	0.002 - 0.018	m
	Default 0.005	m
L_p	0.2 - 0.8	m
	Default 0.8	m
W_p	0.2 - 0.8	m
	Default 0.5	m
t_e	0.002 - 0.01	m
	Default 0.005	m
L_e	0.2 - 0.8	m
	Default 0.8	m
W_e	0.2 - 0.8	m
	Default 0.5	m
$\dot{V}$	200 - 800	l/s
	Default 540	l/s

5.3.1 PCM Melting Temperature

In order to find optimum design of PCM melting temperature, two heat transfer processes have to be taken into consideration. The first is the heat transfer from primary air to PCM. This heat transfer will increase as the melting temperature decreases. The second is the heat transfer from secondary air to PCM; as the melting temperature decreases the heat transfer from secondary air decreases. Therefore; an optimum has to be selected to gain more useful energy as well as increase charging period. Several heat exchanger sizes are simulated at different melting temperature and presented in Figure (5.10). It is clear from Figure (5.10) that the optimum melting temperature is 20°C at any heat exchanger dimensions.

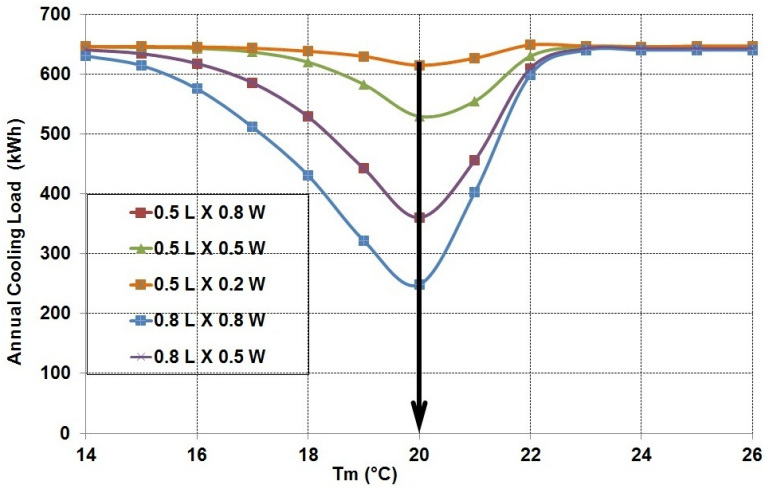

Figure 5.10: Effect of PCM Melting Temperature on Annual Cooling Load

5.3.2 Heat Exchanger Thickness

The effect of heat exchanger thickness, distance between plates, has been investigated through repeated simulations. Figure (5.11) shows that the annual cooling load is increased as distance between plates increased for both IEAC and PCM heat exchangers. This is due to decreasing number of modules.

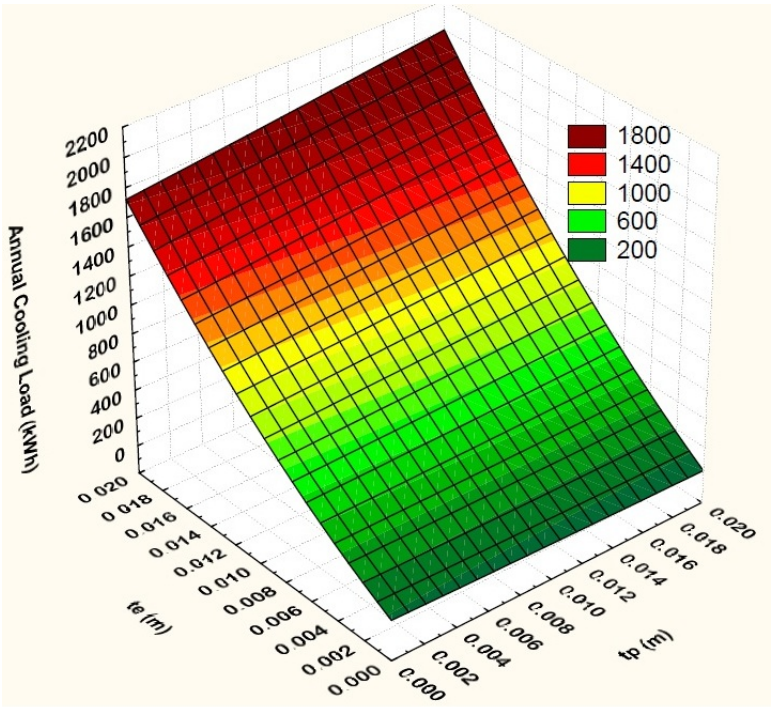

Figure 5.11: Effect of Heat Exchanger Thickness on Annual Cooling Load

5.3.3 Heat Exchanger Width

Figure (5.12) shows the effect of heat exchanger width on annual cooling load. As both IEAC and PCM heat exchangers' width is increased the annual cooling energy decreased. This is due to increasing the effective heat transfer area.

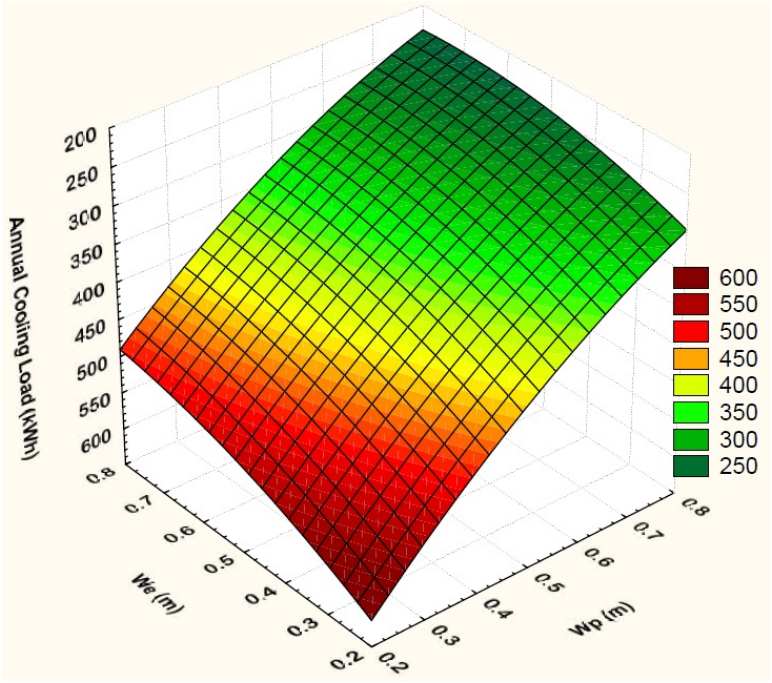

Figure 5.12: Effect of Heat Exchanger Width on Annual Cooling Load

5.3.4 Heat Exchanger Length

The annual cooling load is decreased as both L_p and L_e increased due to increasing the number of modules, as shown in Figure (5.13).
It can be concluded from Figures (5.12 and 5.13) that the effect of heat exchanger length is more than it's width. Actually this is because the heat transfer area is equal to quadratic length multiply by number of modules.

5.3.5 Volumetric Flowrate

The impact of volumetric flowrate ($\dot{V}$) is also investigated for different heat exchanger size. The results are shown in Figure (5.14). The results show that after volumetric flowrate of 500 l/s the cooling load is slightly decreased.

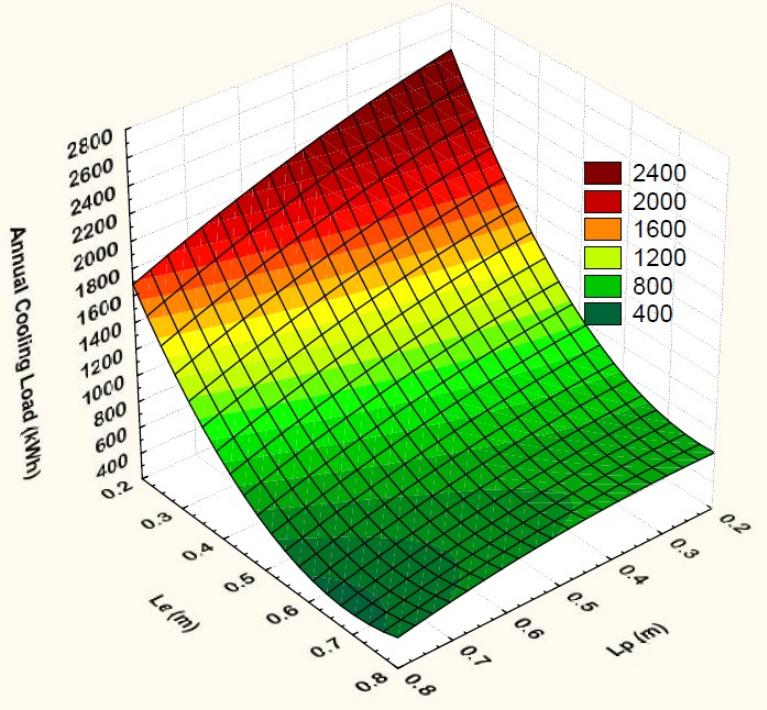

Figure 5.13: Effect of Heat Exchanger Length on Annual Cooling Load

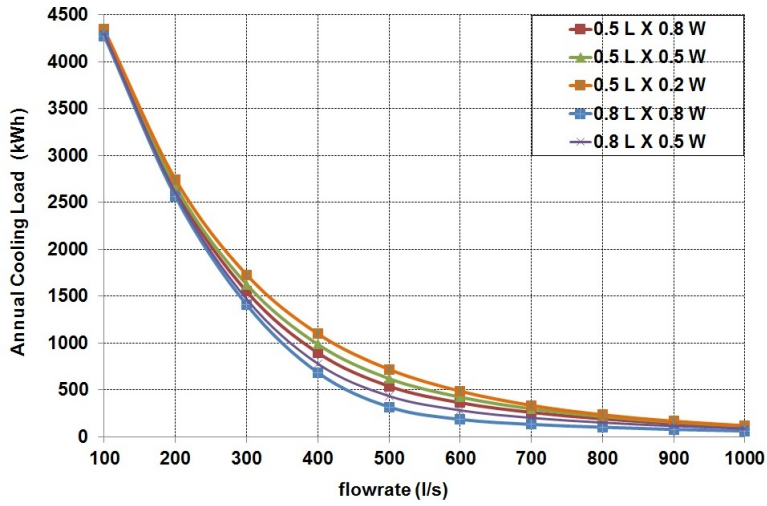

Figure 5.14: Effect of Volumetric Flowrate on Annual Cooling Load

5.4 Economic Optimization

Traditional air-conditioning with annual electricity consumption of 2,367 kWh is needed to cover the current annual cooling load. This costs around 201 €annually.
In order to cover current cooling load, from technical point of view, IESU with initial

cost of 5,671 €is needed. The dimension of IESU is ($L_p = L_e = W_p = W_e = 0.8$ m, $t_p = t_e = 0.002$ m, $\dot{V} = 800$ l/s, $T_m = 20°$C). The annual running cost is more than the annual energy saving. That means this size isn't economically feasible.
Simulation has been done for more than 6,000 cases; each case has different IESU's size. Then Life Cycle Cost (LCC) equation has been built which equals to;
LCC = (auxiliary system cost + maintenance cost for auxiliary system - auxiliary system salvage cost) + (IESU cost + IESU maintenance cost - IESU salvage cost) + base cost + (annual auxiliary energy cost - annual cost of saved energy due to IESU + IESU running cost) or;

$$\begin{aligned} LCC = {} & C_{aux.,c}(\dot{V}, L_p, L_e, W_p, W_e, t_p, t_e, T_m)[1 + f_m PWF - f_{salv}(\frac{1+i}{1+r})^N] + C_b \\ & + C_{aux.,h}[1 + f_m PWF - f_{salv}(\frac{1+i}{1+r})^N] + C_{IESU}(\dot{V}, L_p, L_e, W_p, W_e, t_p, t_e, T_m) \\ & [1 + f_m PWF - f_{salv}(\frac{1+i}{1+r})^N] + [Q_{aux.,c}(0,0,0,0,0,0,0,0) \\ & - Q_{IESU}(\dot{V}, L_p, L_e, W_p, W_e, t_p, T_m)]\frac{p_e}{COP}PWF + Q_{r.e}PWF + Q_{aux.,h}\frac{p_d}{\eta}aux.PWF \end{aligned} \tag{5.13}$$

where:

C_b : base cost (€).

C_{IESU} : IESU cost (€).

$C_{aux.,c}$: auxiliary cooling system cost (€).

$C_{aux.,h}$: auxiliary heating system cost (€).

$Q_{aux.,c}$ (0,0,0,0,0,0,0,0) : annual auxiliary cooling energy consumption after applying optimum passive design techniques and ERS (kWh).

$Q_{aux.,h}$: annual auxiliary heating energy consumption after applying optimum passive design techniques and ERS (kWh).

Q_{IESU} : annual cooling energy saved due to IESU (kWh).

$Q_{r.e}$: annual running energy due to ERS (kWh).

f_m: maintenance fraction (%)

PWF: Present Worth Factor

$$PWF = \sum_{j=1}^{N}(\frac{1+i}{1+r})^j = \frac{1+i}{1+r}(1 - (\frac{1+i}{1+r})^N) \tag{5.14}$$

f_{salv}: salvage fraction (%).

i : inflation rate (%).

r : interest rate (equivalent to discount rate) (%).

N : life time (Years).

p_e : electrical energy price (€/kWh).

$\eta_{aux.}$: auxiliary heating system efficiency (%)

p_d : thermal energy price (€/kWh).

COP : auxiliary cooling system Coefficient Of Performance.

LCC is subjected to nine constrain equations as follows;

$$z = C_{IESU}(\dot{V}, L_p, L_e, W_p, W_e, t_p, t_e, T_m) \tag{5.15}$$

$$14 \leq T_m \leq 26 \tag{5.16}$$

$$0.002 \leq t_p \leq 0.018 \tag{5.17}$$

$$0.2 \leq L_p \leq 0.8 \tag{5.18}$$

$$0.2 \leq W_p \leq 0.8 \tag{5.19}$$

$$0.002 \leq t_e \leq 0.01 \tag{5.20}$$

$$0.2 \leq L_e \leq 0.8 \tag{5.21}$$

$$0.2 \leq W_e \leq 0.8 \tag{5.22}$$

$$200 \leq \dot{V} \leq 800 \tag{5.23}$$

LCC results at different IESU's sizes are calculated and presented in Figure (5.15). The minimum LCC occurred at IESU's size of (L_e = 0.6 m, W_e = 0.8 m, $W_p = L_p$ = 0.4 m, t_p = 0.014 m, t_e = 0.006 m, $\dot{V}$ = 400 l/s, T_m = 20°C). This IESU's optimum size is sufficient to save 80.03% of the annual cooling energy. LCC is reduced by 2.66%. Payback Period (PbP) of each unit size is calculated and plotted in Figure (5.16). PbP of IESU's optimum size is 7.8 years. The initial cost is about 1,195 €. The annual electricity consumption (primary and secondary fans) is 443 kWh. Since Jordan is one of the ten most water-deprived countries in the world; the water consumption of IESU should be considered. The calculation yields that the annual water consumption is about 16.54 m^3. Therefore; the payback period of IESU from energy saving occurred due to replacing electricity-driven air-conditioning is 7.8 years.

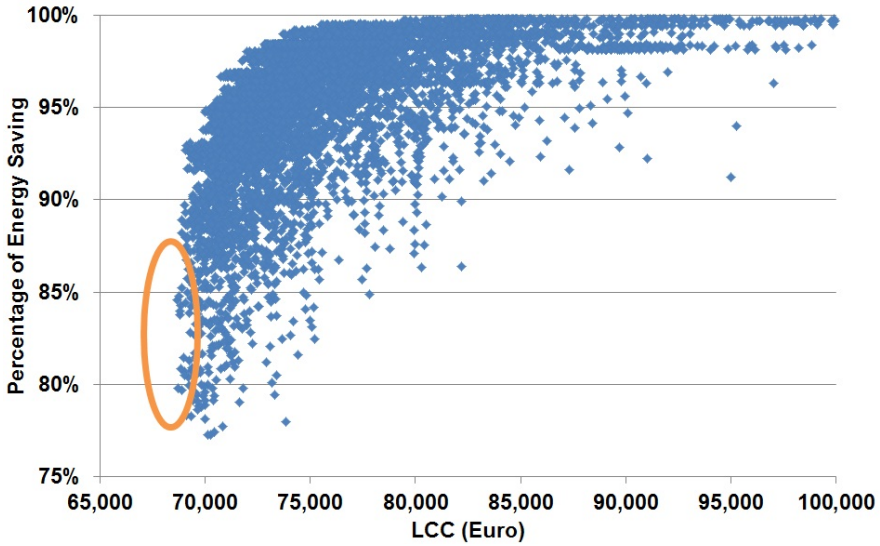

Figure 5.15: LCC at Different IESU's Sizes

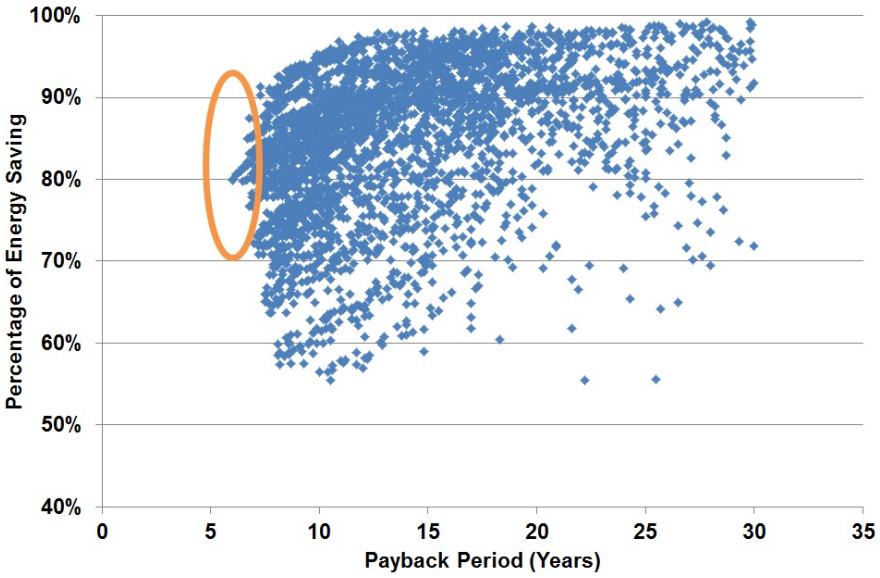

Figure 5.16: PbP at Different IESU's Sizes

The hourly energy behavior during the peak load day (July, 2) for the optimum size is shown in Figure (5.17). The Figure at top shows the hourly cooling load before and after installing IESU for three sequent days; the peak day, one day after and one day before the peak load day. Figure at bottom illustrates the charging, discharging and stored energy in PCM profiles for the same period. It is clear from this Figure that IESU will store cooling energy to use it whenever there is cooling load and IEAC isn't sufficient to cover the required cooling load.

5.5 Software Module Verification

IESU software module aims to simulate the hourly performance of cold storage in PCM as well as the hourly cooling supply to the building. The source of cold is cheap source comes from IEAC. It may be interesting to investigate the performance of flat plate heat exchanger and IEAC and compare it to available softwares.
Effectiveness of different flat plate heat exchanger dimensions are simulated by Klingenburg software and IESU software. Klingenburg software is based on a theoretical approach as well as on internal measurements. Thus the results can be considered as real flat plate heat exchanger performance [114]. Formulas for Nusselt numbers are corrected according to the measurements results. The results show that the maximum percentage of error is 1.6% while the average percentage error between real flat plate heat exchanger effectiveness and theoretical effectiveness is 0.4%. On the other hand, there are many points typically give the same effectiveness of real flat plate heat exchanger. Some of effectiveness results are presented in Figure (5.18). This Figure presents the effectiveness of flat plate heat exchanger with 800 mm length, 500 mm width and 9 mm plate thickness (Figure at top) and flat plate heat exchanger with 500 mm length, 500 mm width and 9 mm plate thickness (Figure at bottom).
The difference between IESU software results and Klingenburg real case is a result of the plate geometry especially surface enlargement factor, which has influence on the flow conditions, Nusselt numbers and efficiencies. As well as Nusselt numbers correlation itself.
A comparison of annual cooling load due to IEAC by both INSEL and IESU softwares has been done. As may seen in Figure (5.19), good agreement is obtained with INSEL software. The error ranges between (0.54 - 7.31)%. The average error occurred is 3.63%. This error could happen because of different Nusselt number correlation which will affect the heat transfer between air streams.
Another comparison of annual water consumption has been done and plotted in Figure (5.20). This comparison has been done between IESU and INSEL softwares. The percentage of error doesn't exceed 7.29%. The average in percentage of error is 5.01%. The differences between these two softwares happen due to the differences in annual cooling load.

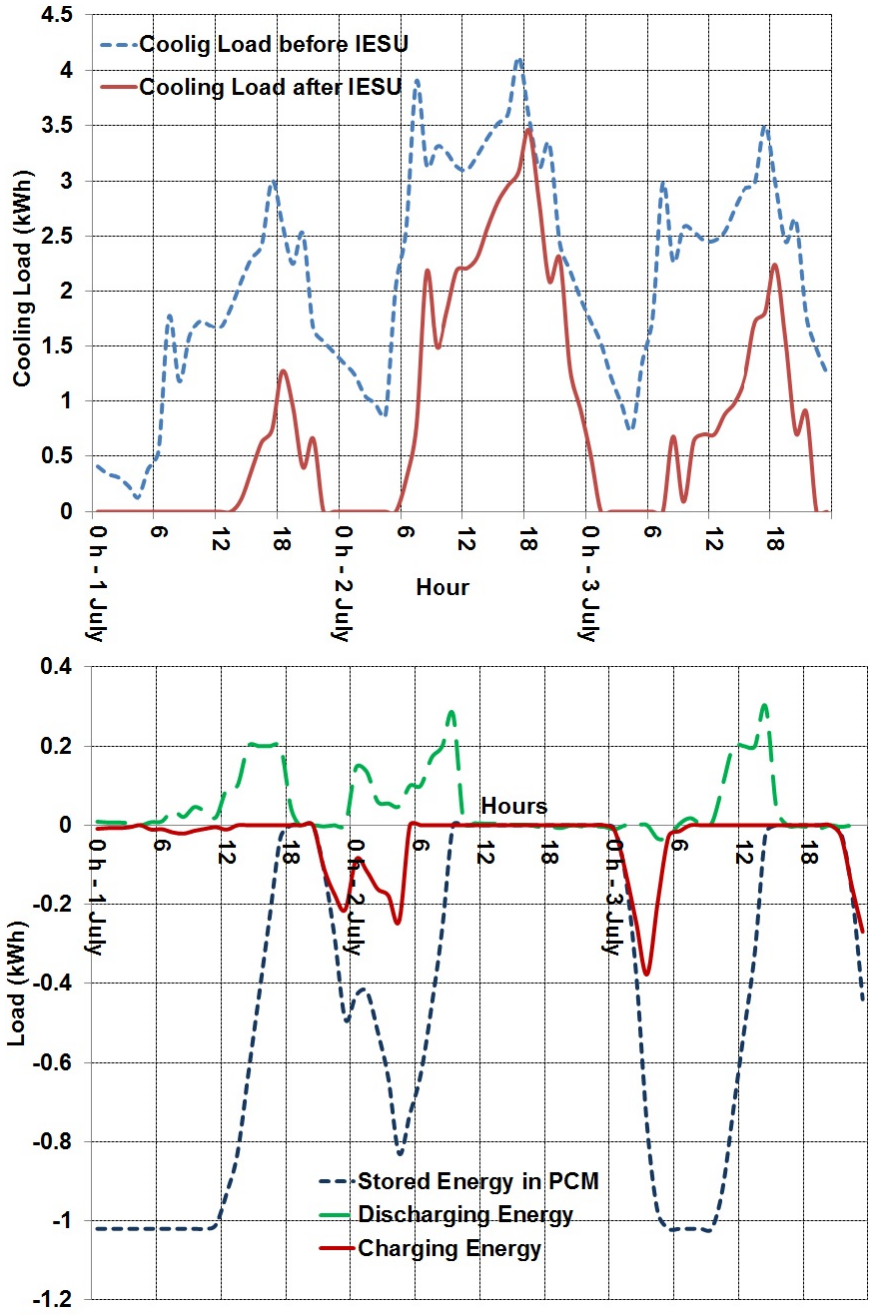

Figure 5.17: Performance of IESU's Optimum Size at Peak Period

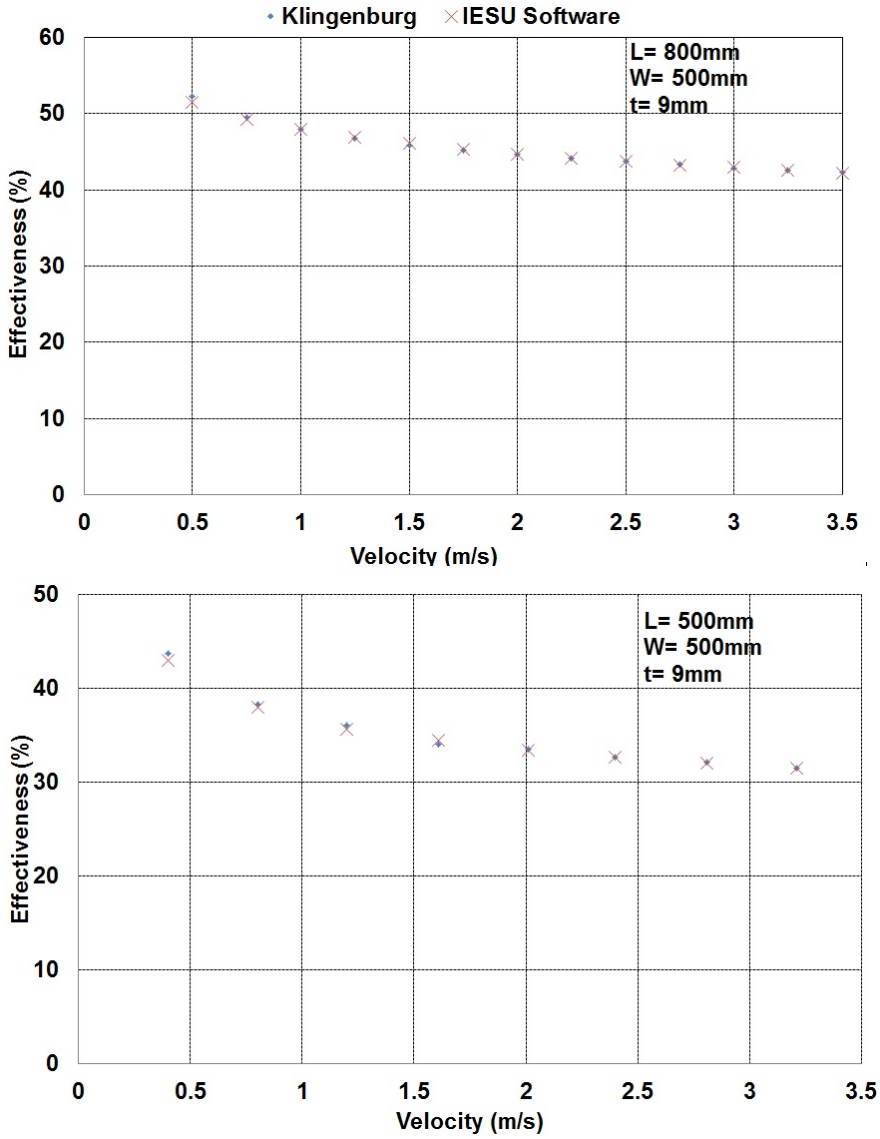

Figure 5.18: Comparison of Effectiveness Between Klingenburg and IESU Softwares

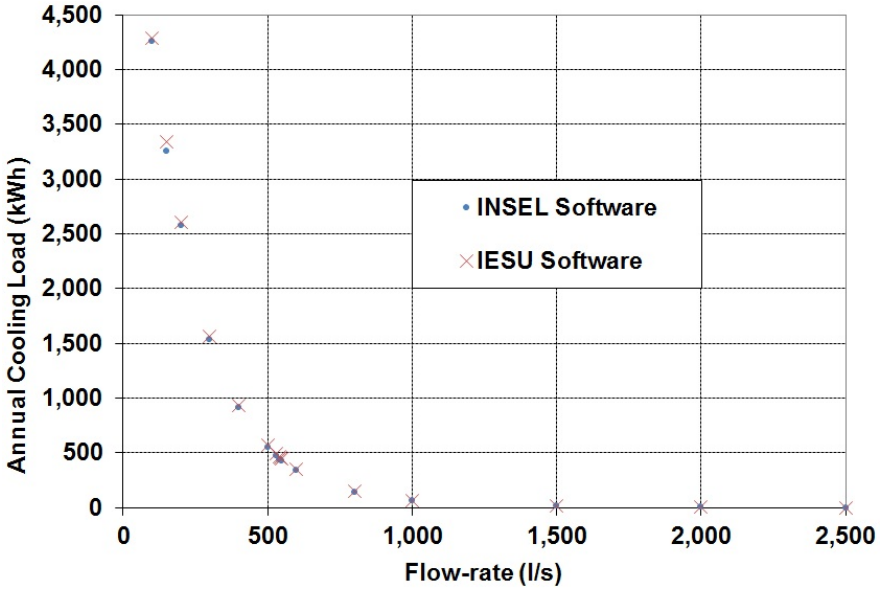

Figure 5.19: Comparison of Annual Cooling Load Between INSEL and IESU Softwares

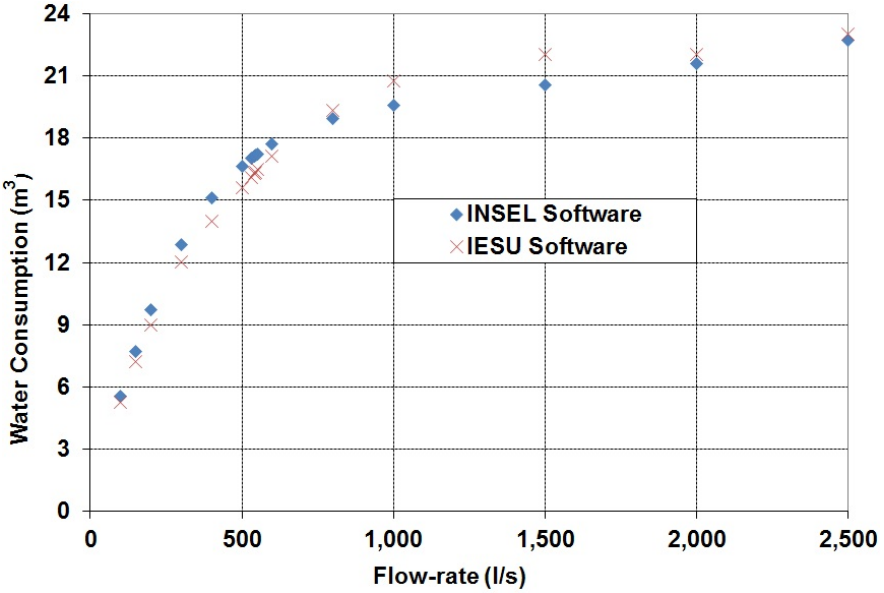

Figure 5.20: Comparison of Annual Water Consumtion Between INSEL and IESU Softwares

Chapter 6

Comparison Between Europe and Mediterranean Climate Zones

This chapter compares the feasibility of all discussed systems in previous chapters in three different climates. Two locations have been selected from Middle East and one from Europe.

6.1 Design Conditions

The climate of Jordan is predominantly of the Mediterranean type. It is marked by sharp seasonal variations in both temperature and precipitation. Climate can be cold to very cold in Winter and warm to hot in Summer. Two climate zones have been selected in Jordan; Amman capital of Jordan and Aqaba located South of Jordan.
Aqaba city is characterized by very hot and dusty weather in Summer; Summer temperatures rise above 46°C [4]. Winter is mild therefore there is little need for heating with extremely little amount of precipitation. The mean annual daily average temperature is estimated at around 24.1°C [4].
In Amman, Summer starts around mid of May and Winter starts around mid of November, with two short transitional periods in between (autumn and spring). In Summer, high temperatures reach 35°C on most days in June, July and August [4]. Nights are comfortable with average low temperatures of 14.4°C in June, 14.7°C in July and 14.8°C in August [4]. Amman gets absolutely no rainfall during an average Summer. Winter is Amman's wettest season. The coldest month in Winter is January. Frosty mornings are common in Amman and snow falls once or twice during the season.
The city of Berlin stands on the eastern side of Germany and enjoys characterized by mild Summer weather. The maximum temperature in Summer is 30.3°C in August [4]. Berlin is also characterized by its cold Winter. December, January and February are

the coldest during the year. The lowest temperature in Winter is -11.5°C in December [4]. The annual daily average temperatures in Berlin is around 8.8°C [4].
The demand for both heating and cooling is strongly influenced by the outdoor air temperature and global solar radiation on horizontal plate around the building. These data are listed in Table (6.1) for different locations [4].

Table 6.1: Daily Average Weather Data for Different Location

	Amman		Aqaba		Berlin	
Month	T_{db} °C	G_h kWh/m^2	T_{db} °C	G_h kWh/m^2	T_{db} °C	G_h kWh/m^2
Jan.	6.5	2.9	15.5	3.5	-2.3	0.6
Feb.	7.5	3.5	17.0	4.0	0.6	1.0
Mar.	12.3	4.7	21.0	5.1	4.0	2.5
Apr.	15.0	5.7	22.3	5.7	7.9	3.5
May	19.7	6.9	27.8	6.8	14.4	4.9
June	23.4	7.6	30.1	7.4	15.8	5.4
July	24.6	7.7	31.8	7.5	17.1	5.4
Aug.	24.3	7.2	30.4	7.1	19.0	4.8
Sep.	23.2	5.8	28.5	6.0	14.5	3.1
Oct.	20.6	4.8	26.0	5.1	10.2	1.7
Nov.	15.4	3.4	22.7	3.8	4.9	0.8
Dec.	9.1	2.8	15.7	3.2	-0.1	0.5
Average	16.8	5.2	24.1	5.4	8.8	2.8

An optimization of passive solar systems, Energy Recovery System (ERS) and Indirect Evaporative and Storage Unit (IESU) is estimated using economic figures from local markets for each location using Life Cycle Cost (LCC) criterion. The estimation costs of these systems in addition to conventional energy systems do involve some basic assumption which can be summarized as follows:

- The life span of the building, auxiliary heating system and all passive systems used in this work is assumed to have 30 years. The auxiliary cooling used in this work is assumed to have life span of 10 years.

- The ERS and IESU are assumed to have a 15 years life span.

- According to Jordanian market the inflation rate is around 8.9% and the interest rate is about 6.25% as mentioned by Central Bank of Jordan (CBJ). Thus, Present Worth Factor, PWF, which is a function of interest rate and inflation rate is 44.96 and 11.48 at 30 and 10 years, respectively.

- According to German market the inflation rate is around 1.90% and the interest rate is about 1.00% as mentioned by Deutsche Bundesbank. Thus, Present Worth

Factor, PWF, which is a function of interest rate and inflation rate is 34.52 and 10.50 at 30 and 10 years, respectively.

- The auxiliary heating system has an efficiency of 65% in all locations.
- The auxiliary cooling system has Coefficient of Performance (COP) of 3 in all locations.
- The salvage factor is set at 10% of the capital cost for heating auxiliary system as well as ERS and IESU. on the other hand, it assumed to be 6% of the capital cost for auxiliary cooling system in all locations.
- Maintenance factor for the auxiliary heating and cooling systems is assumed to be 15%, and 10% of the capital cost, respectively in all locations.
- The ERS and IESU are assumed to have a 6% maintenance factor.
- Current fuel price is 0.455 €/l where the electricity price is 0.085 €/kWh in Jordan [95].
- Current fuel price is 0.653 €/l [115] where the electricity price is 0.250 €/kWh [116] in Germany.

6.2 Passive Solar Design

Windows' size and type, Trombe wall and thermal insulation thickness in both ceiling and walls will be optimized technically and economically in three climate zones; Amman, Aqaba and Berlin. The optimum size of all parameters will be done by Life Cycle Cost (LCC) economic criterion. Numerical method based on Generalized Reduced Gradient (GRG) method will be used to find the design parameters at minimum LCC. Moreover, Payback Period (PbP) will be calculated beside LCC criterion.

6.2.1 Windows' Optimization

Window's performance in terms of energy efficiency can be assessed mainly by looking at its U-value and Solar Heat Gain Coefficient (SHGC) [117]. U-value indicates the rate of heat flow due to conduction, convection, and radiation through a window as a result of a temperature difference between the inside and outside. The higher U-value the more heat is transferred. SHGC indicates how much of the sun's energy striking the window is transmitted through the window as heat. As the SHGC increases, the solar gain potential through a given window increases.

Load due to conduction and convection can be calculated every hour from the following formula [97];

$$Q_{conv.,cond.} = U * A * \triangle T * \triangle t \tag{6.1}$$

where;

U : overall coefficient of heat transfer (kWh/m^{2}K).

A : window area (m^2).

$\triangle$T : total equivalent temperature difference, which takes into consideration the increase of wall temperature due to absorbtion of solar radiation ($^\circ$C).

$\triangle$t : length of the time step (hour).

Load due to solar transmission and radiation can be calculated every hour from the following formula [97];

$$Q_{tr.} = SC * SHGC * CLF * A * \triangle t \tag{6.2}$$

where;

SC : Shading Coefficient.

SHGC : Solar Heat Gain Coefficient (kW/m^2).

CLF : Cooling Load Factor.

Four window types have been investigated as well as windows' size by using TRNSYS software [7]. Four different types of windows are selected; single, double-Low, double-High and triple glazed. Windows' thermal characteristics are presented in Table (6.2).

Table 6.2: Thermal Characteristics of Windows (15% frame (U = 2.27 W/m^{2}K))

	Single Glazed	Double Glazed L	Double Glazed H	Triple Glazed
U$_g$	5.68	2.83	1.4	0.68
U$_{frame}$	2.27	2.27	2.27	2.27
SHCG	0.855	0.775	0.589	0.407
R$_f$-sol	0.075	0.126	0.266	0.231
T-vis	0.901	0.817	0.706	0.625
gas fill	-	Air	Argon	Krypton

where R$_f$-sol is solar reflectance of outer surface of glazing system and T-vis is visible transmittance of the window.

The Annual heating energy versus windows' area for different window types is presented in Figures (6.1, 6.2 and 6.3) for Amman, Aqaba and Berlin.
It is obvious from these Figures that the effect of decreasing windows' U-value is decreasing the annual heating energy in Amman, Aqaba and Berlin climate zones. Moreover, the highest annual heating energy is occurred at North façade for all locations due to low solar incident radiation at this façade. The lowest annual heating energy occurred at South façade in Amman, Aqaba and Berlin. This is due to high solar incident radiation at this façade as compared with other façades.
For single glazed windows, the annual heating energy is linearly increased as windows' area increased in all regions. That means this type of windows isn't sufficient energetically to be installed for heating purpose. This is due to high windows' U-value.
For double glazed-Low windows, the annual heating energy for all regions at North façade is always increased as windows' area increased. The heating load for South, East and West façades is decreased at the beginning then it is increased as windows' size increased in both Amman and Aqaba climate zones, as shown in Figures (6.1 and 6.2). In Berlin, the annual heating energy is linearly increased as windows' area increased, as plotted in Figure (6.3). The optimum windows' area in Amman is 40% for both South and East façades, 10% for North façade and 20% for West façade. The optimum size in Aqaba is 20% for both West and East façades, 10% for North façade and 30% for South façade. In Berlin, double glazed-Low doesn't show any sufficient decreasing in annual heating energy. This is due to very low ambient temperature in Winter.
For double glazed-High windows, the annual heating energy in all climates tends to decrease at the beginning then increase except at North façade which linearly increases as windows area increase. The optimum windows area in Amman, as shown in Figure (6.1), is 70% for both South and West façades where it is 10% and 80% for North and East façades, respectively. The thermal heat losses through windows become more than solar gain after these optimum percentages. This is happened when ambient temperature is lower than room temperature during Winter time that leads to increase the thermal heat losses. In Aqaba, the optimum windows area is 80% for South and West façades where it is 90% for East façade and 10% for North façade, as shown in Figure (6.2). For Berlin climate zone, Figure (6.3) shows that optimum windows area is 10% for East and North façades and it's 40% and 30% for South and West façades, respectively.
In case of using triple glazed windows, heating load tends to decrease as windows' area increase in all climate zones, till reaching the optimum windows' size, then it is increased except at North façade. It is shown from Figure (6.1) that the optimum windows' size in Amman is 10%, 90%, 90% and 90% for North, South, East and West

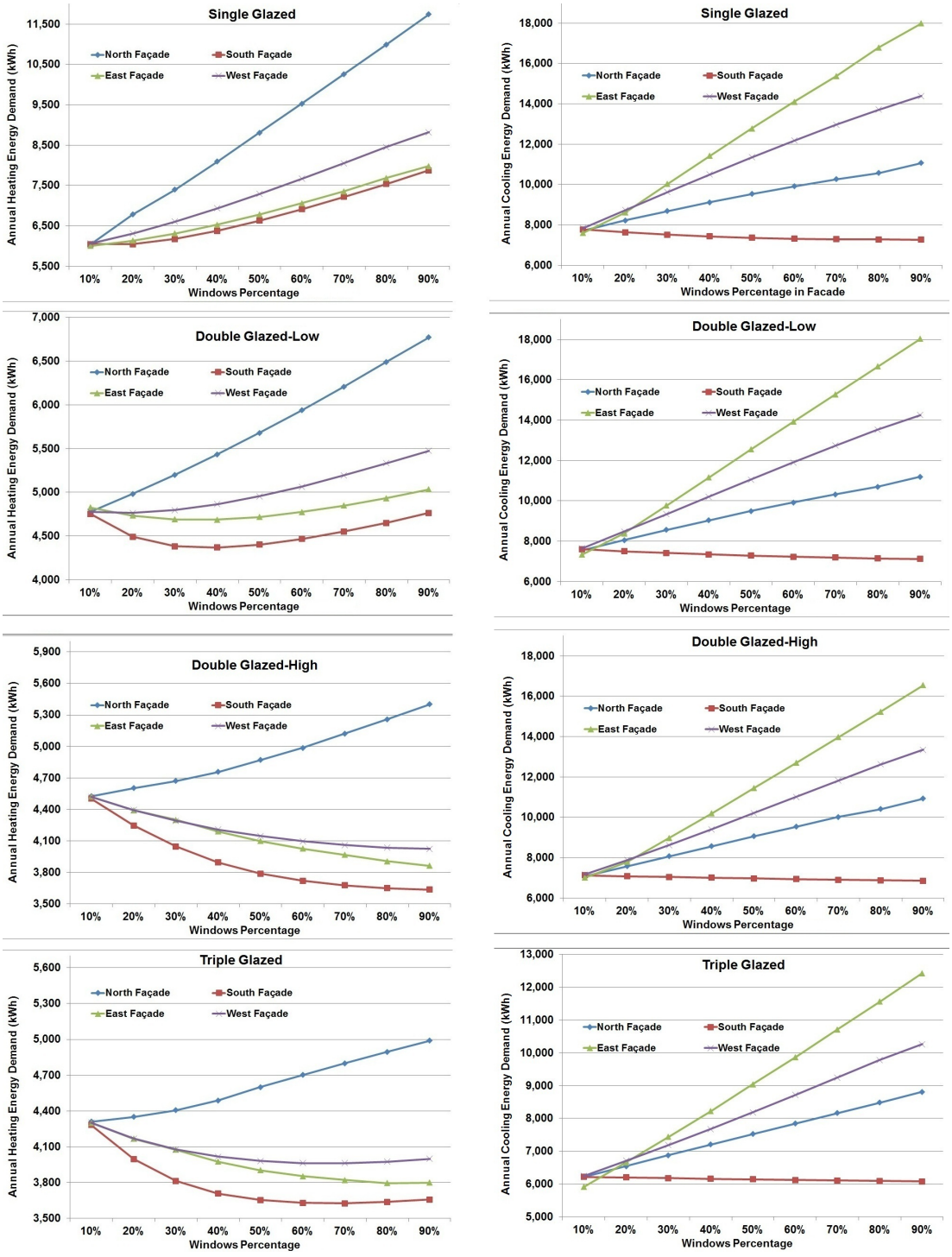

Figure 6.1: Effect of Windows' Type and Size on Heating and Cooling Load in Amman

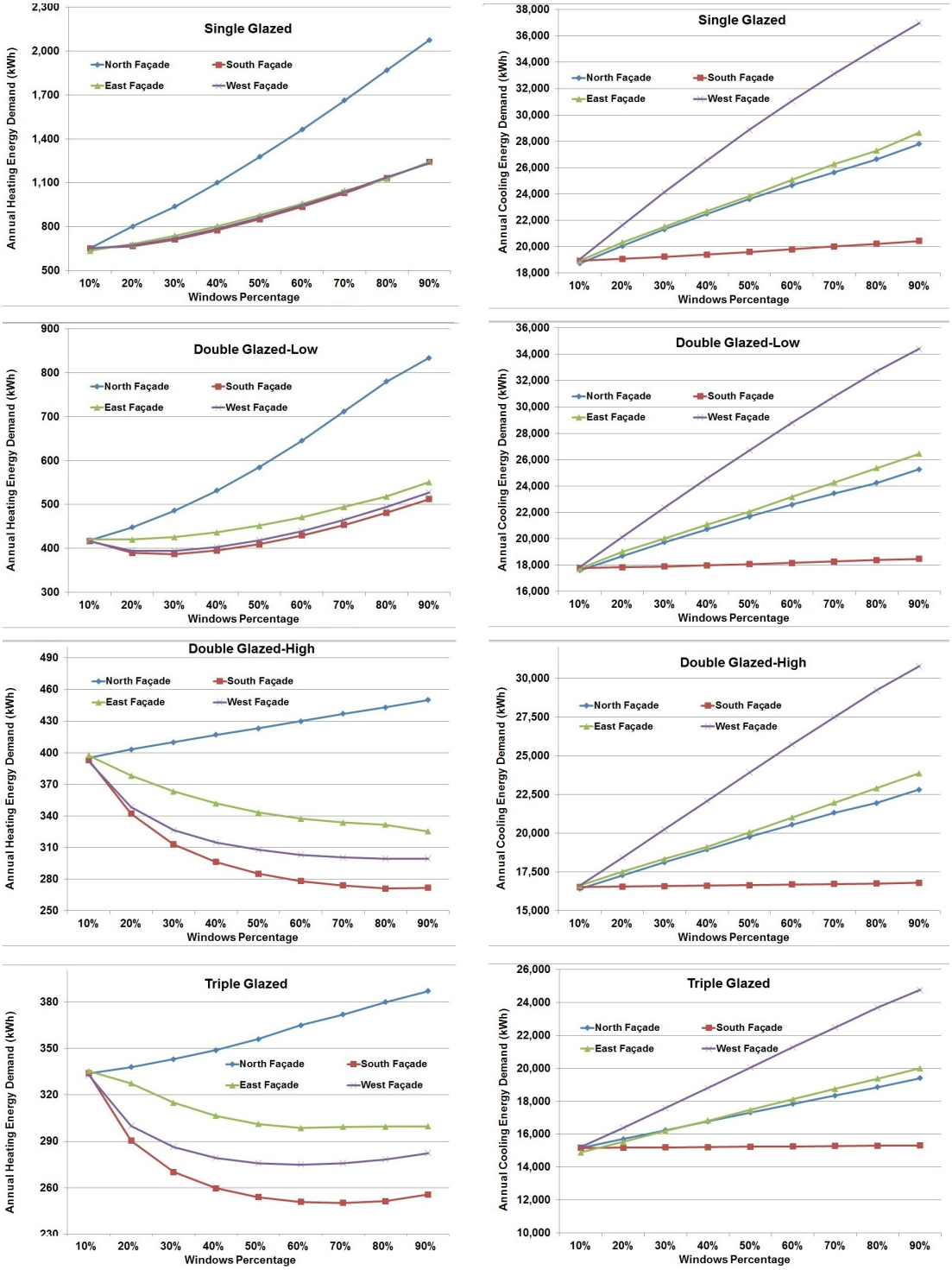

Figure 6.2: Effect of Windows' Type and Size on Heating and Cooling Load in Aqaba

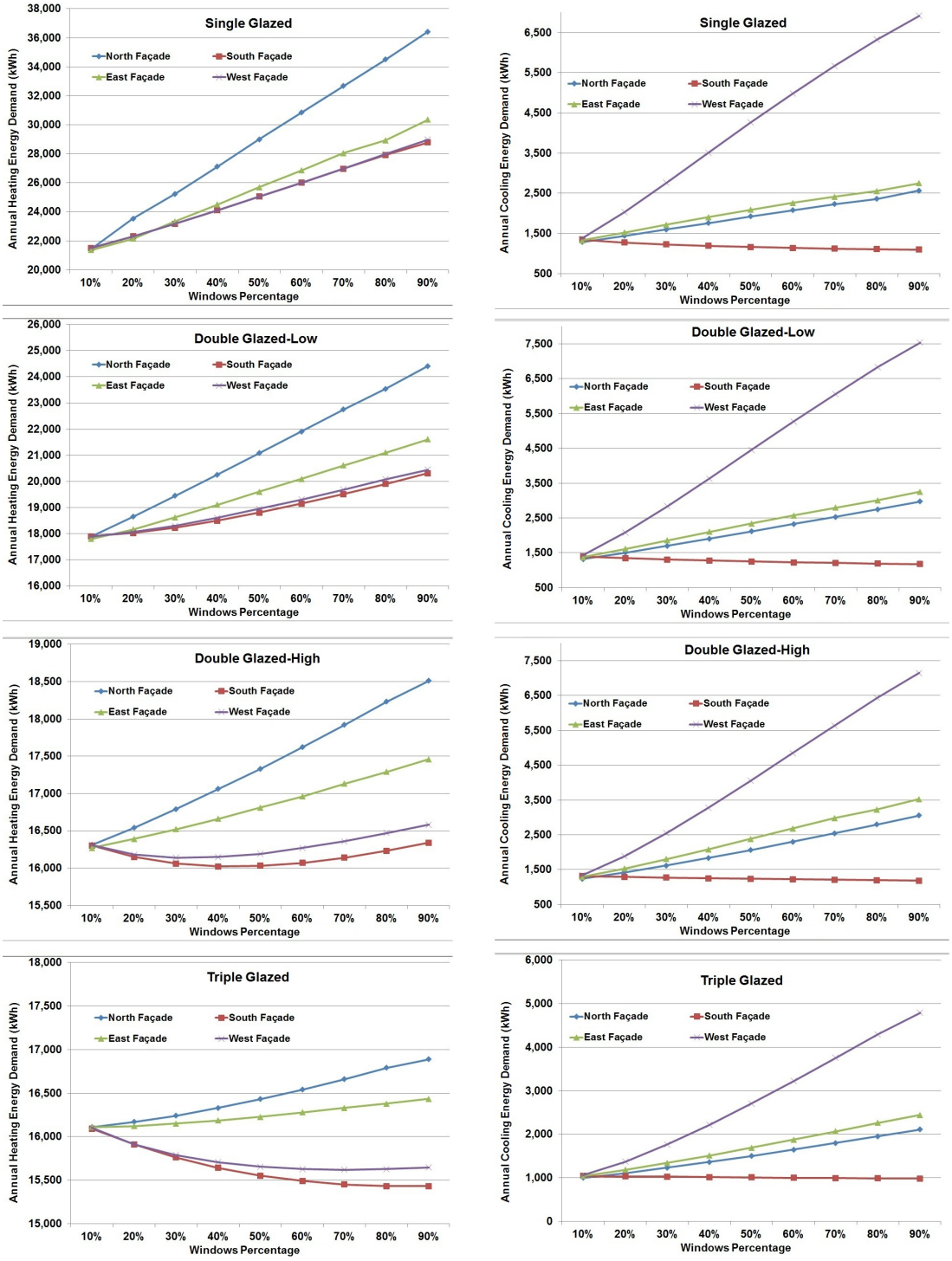

Figure 6.3: Effect of Windows' Type and Size on Heating and Cooling Load in Berlin

façades, respectively. The optimum windows' size in Aqaba is occurred at 70% for both South and West façades and at 10% and 60% for North and East façades, respectively as shown in Figure (6.2). In Berlin climate zone the optimum can be achieved, as shown in Figure (6.3), at 10% for both North and East façades and at 70% and 80% for West and South façades, respectively.

Once windows' area at South façade is increased the opportunity of saving energy is increased till optimum value is reached except for single glazed window in all climate zones and for double glazed-Low windows in Berlin, as shown in Figures (6.1 and 6.2). In these cases, the losses increase as windows' area increase due to high windows' U-value.

For East and West façades, good opportunity of energy saving can be achieved in triple and double glazed-High in all climate zones except double glazed-High in Berlin. On the other hand, the energy saving at West façade is slightly higher than East façade in Aqaba and Berlin. In Amman, East façade achieved higher energy, as shown in Figure (6.1. This is due to high temperature after mid-day than before mid-day which is the opposite in Amman.

The annual cooling energy versus windows' area for different windows' types is presented in Figures (6.1, 6.2 and 6.3) for Amman, Aqaba and Berlin. These results show that the annual cooling energy is slightly decreased as windows' U-value decreased for all locations. This is because of windows with low U-value conduct less energy from outside to inside building during hot Summer months. On the other hand, it is avoid the heat conduction from outside to inside the building when ambient temperature is less than room temperature during Summer night.

The annual cooling energy increases linearly as windows' area increase. This is due to the negative effect of solar radiation in Summer. That means the better solution to avoid high cooling energy is blocking the windows. On the other hand, windows' area decrease the heating energy in Winter and it should be existing to avoid artificial lighting and provide occupants with minimum level of comfort according to building codes and standards [100; 101]. Thus, in order to take best decision all above factors have to be taken into consideration as well as windows' cost.

Concerning Summer performance, the main argument against lower windows' U-value is the overheating and unwanted gains to the room. It is concluded from the simulation results that the peak energy demand is increased as windows U-value decreased. Thus, shading device has to be used at South façade to achieve Summer comfort.

Figure (6.2) and Figure (6.3) show that in Aqaba and Berlin, the cooling energy at West façade is more than at East façade. This is because of the ambient temperature and the solar radiation after mid-day is more than before mid-day.

Optimum windows' size at different windows' type are calculated by using LCC in

three climate zones. The objective function and constrain equations are discussed in Section (3.4.2). The results are presented in Table (6.3)
Table (6.3) shows that double glazed-Low windows are cost effective in both Amman and Aqaba. Windows' size of 10% at North façade, 30% at South façade, 20% at East façade and 10% at West façade achieve the minimum LCC in Amman. PbP of extra investment from annual saving is about 14 years. The optimum windows' size in Aqaba region are 10% at North façade, 10% at South façade, 10% at East façade and 10% at West façade. PbP is a little bit high which equal to 21 years.
In fact, double glazed-High and triple glazed windows are not existing in Jordanian market. The windows' price is estimated according to German market plus transportation costs. In future if these products are locally manufactured or exported in large amounts the initial cost will be reduced by 40% which will directly affect on its economic feasibility through the whole life of the building.
For Berlin climate zone, double glazed-High windows of 10% at North façade, 10% at South façade, 10% at East façade and 10% at West façade is the optimum case, as shown in Table (6.3). PbP is considered as reasonable value which is 11 years.
The lower PbP in Berlin as compared with Amman and Aqaba is due to lower interest and inflation rate in Berlin in addition to higher energy saving achieved and lower window's cost.

6.2.2 Thermal Insulation and Trombe Wall Optimization

Thermal insulation thickness in ceiling (t_c), thermal insulation thickness in wall (t_w) and Trombe wall area ratio (a) have been optimized by using LCC. The objective function and constraint equations are discussed in Section (3.7).
The outcomes show that Trombe wall system has a considerable benefit in Amman and Berlin climates while in Aqaba it doesn't have any economic effect due to low heating demand in this climate. The economic results are summarized and listed in Tables (6.4, 6.5 and 6.6).
The optimum size for thermal insulation and Trombe wall from thermal and economic point of view is (U_w = 0.123 W/m^{2}K, U_c = 0.143 W/m^{2}K, a = 36.59%) in Amman while it is (U_w = 0.11 W/m^{2}K, U_c = 0.18 W/m^{2}K, a = 45.73%) in Berlin. The optimum design has reduced LCC by 13.55% in Amman whereas in Berlin LCC has reduced by 22.30%. On the other hand, CO_2 emission will be reduced annually by 41% and 49.3% in Amman and Berlin, respectively.
In Aqaba, the optimum LCC occurs at (U_w = 0.10 W/m^{2}K, U_c = 0.18 W/m^{2}K, a = 0%) which has reduced LCC by 10.45%. The annual energy saving achieved is 25.31%. Annual CO_2 emissions will be reduced by 26.1%.

Table 6.3: Economic Analysis for Different Windows' Types in Amman, Aqaba and Berlin

	Energy Demand (kWh)	LCC (Euro)	Energy Saving (%)	PbP (Year)
Amman (N,S,E,W)				
Single Glazed (10%,10%,10%,10%)	13,290	81,475	-	-
Double Glazed-Low (10%,30%,20%,10%)	**12,567**	**77,412**	**5**	**14**
Double Glazed-High (10%,10%,10%,10%)	11,009	81,982	17	70
Triple Glazed (10%,10%,10%,10%)	10,488	86,614	21	109
Aqaba (N,S,E,W)				
Single Glazed (10%,10%,10%,10%)	19,215	85,072	-	-
Double Glazed-Low (10%,10%,10%,10%)	**17,886**	**81,842**	**7**	**21**
Double Glazed-High (10%,10%,10%,10%)	17,119	83,531	11	80
Triple Glazed (10%,10%,10%,10%)	15,327	89,476	20	128
Berlin (N,S,E,W)				
Single Glazed (10%,10%,10%,10%)	22,405	131,473	-	-
Double Glazed-Low (10%,10%,10%,10%)	19,052	119,121	15	3
Double Glazed-High (10%,10%,10%,10%)	**17,540**	**116,877**	**22**	**11**
Triple Glazed (10%,10%,10%,10%)	17,083	119,473	24	15

Table 6.4: Summary of Technical and Economic Analysis in Amman

	Heating energy kWh	Cooling energy kWh	Total energy kWh	Investment €	LCC €	Specific energy consumption kWh/m^2.a
Base case						
	4,781	8,784	13,565	10,246	78,698	88.08
Maximum load (kW)	5.55	6.11				
Windows and shading device optimum size						
	4,539	8,028	12,567	10,705	77,417	81.60
Maximum load (kW)	5.53	5.86				
U_w = 0.398 W/m^{2}K, U_c = 0.18 W/m^{2}K						
	3,506	7,286	10,792	12,507	72,500	70.08
Maximum load (kW)	4.65	5.01				
U_w = 0.213W/m^{2}K, U_c = 0.469 W/m^{2}K						
	3,762	8,185	11,947	12,073	75,288	77.58
Maximum load (kW)	4.99	5.75				
U_w = 0.133 W/m^{2}K, U_c = 0.149 W/m^{2}K						
	2,352	7,471	9,823	13,832	69,612	63.79
Maximum load (kW)	3.78	4.75				
U_w = 0.213 W/m^{2}K, U_c = 0.18 W/m^{2}K						
	2,758	7,473	10,231	12,824	70,317	66.44
Maximum load (kW)	4.11	4.91				
U_w = 0.133 W/m^{2}K, U_c = 0.149W/m^{2}K, a = 36.59%						
	1,596	7,471	9,067	15,092	68,442	58.87
Maximum load (kW)	3.78	4.75				
U_w = 0.123 W/m^{2}K, U_c = 0.143W/m^{2}K, a = 36.59% (OPTIMUM DESIGN)						
	1,556	7,465	9,021	15,345	68,037	58.58
Maximum load (kW)	4.00	4.72				
CO_2 reduction (Ton)	1.14	0.26	1.40			

Table 6.5: Summary of Technical and Economic Analysis in Aqaba

	Heating energy kWh	Cooling energy kWh	Total energy kWh	Investment €	LCC €	Specific energy consumption kWh/m^2.a
Base case						
	419	19,550	19,969	10,246	84,231	129.67
Maximum load (kW)	2.39	9.35				
Windows and shading device optimum size						
	406	17,480	17,886	10,537	81,842	116.14
Maximum load (kW)	2.39	9.35				
$U_w = 0.398$ W/m^{2}K, $U_c = 0.171$ W/m^{2}K						
	236	15,490	15,726	12,489	77,473	102.12
Maximum load (kW)	1.79	7.83				
$U_w = 0.246$ W/m^{2}K, $U_c = 0.469$ W/m^{2}K						
	300	17,110	17,410	10,770	80,054	113.05
Maximum load (kW)	2.11	8.79				
$U_w = 0.133$ W/m^{2}K, $U_c = 0.149$ W/m^{2}K						
	106	14,710	14,816	13,684	75,643	96.21
Maximum load (kW)	1.03	7.13				
$U_w = 0.246$ W/m^{2}K, $U_c = 0.171$ W/m^{2}K						
	158	15,150	15,308	12,883	76,418	99.40
Maximum load (kW)	1.42	7.5				
$U_w = 0.1$ W/m^{2}K, $U_c = 0.18$ W/m^{2}K, a = 0% (OPTIMUM DESIGN)						
	105	14,810	14,915	13,500	75,430	96.85
Maximum load (kW)	1.02	7.2				
CO_2 reduction (Ton)	0.11	0.93	1.04			

Table 6.6: Summary of Technical and Economic Analysis in Berlin

	Heating energy kWh	Cooling energy kWh	Total energy kWh	Investment €	LCC €	Specific energy consumption kWh/m^2.a
Base case						
	17,880	1,780	19,660	11,895	118,094	127.66
Maximum load (kW)	8.11	5.16				
Windows and shading device optimum size						
	16,310	1,230	17,540	19,101	116,877	113.90
Maximum load (kW)	7.53	4.62				
U_w = 0.398 W/m^{2}K, U_c = 0.132 W/m^{2}K						
	12,500	1,148	13,648	22,810	104,431	88.62
Maximum load (kW)	6.1	3.63				
U_w = 0.145 W/m^{2}K, U_c = 0.469 W/m^{2}K						
	13,200	1,424	14,624	20,078	1096,285	94.96
Maximum load (kW)	6.42	4.21				
U_w = 0.0.086 W/m^{2}K, U_c = 0.096 W/m^{2}K						
	8,326	1,483	9,809	26,785	93,820	63.69
Maximum load (kW)	4.59	3.42				
U_w = 0.145 W/m^{2}K, U_c = 0.132 W/m^{2}K						
	9,434	1,404	10,838	23,787	107,098	70.38
Maximum load (kW)	5.00	3.54				
U_w = 0.086 W/m^{2}K, U_c = 0.096 W/m^{2}K, a = 18.29%						
	8,019	1,483	9,502	27,595	93,542	61.70
Maximum load (kW)	4.59	3.42				
U_w = 0.11 W/m^{2}K, U_c = 0.18 W/m^{2}K, a = 45.73% (OPTIMUM DESIGN)						
	8,760	1,449	10,209	22,950	92,080	66.29
Maximum load (kW)	5.05	3.63				
CO_2 reduction (Ton)	3.23	0.06	3.29			

6.3 Energy Recovery System

The energetic, economic and environment effect of ERS have been investigated for typical residential building located in three climate zones; Amman, Aqaba and Berlin. Hour-by-hour energy performance of ERS has been studied and analyzed. Then, a complete economic equation of LCC has been built and optimized as a function of economic and thermal parameters according to each region.
The percentage of annual energy saving in three climate zones due to ERS is calculated at different heat exchanger areas, as shown in Figure (6.4). The outcomes show that ERS is feasible in the selected climate zones. From technical point of view ERS can cover up to 18%, 21% and 69% in Aqaba, Amman and Berlin climate zones, respectively. ERS in Berlin (cold climate) most effective due to high temperature difference between indoor and outdoor.

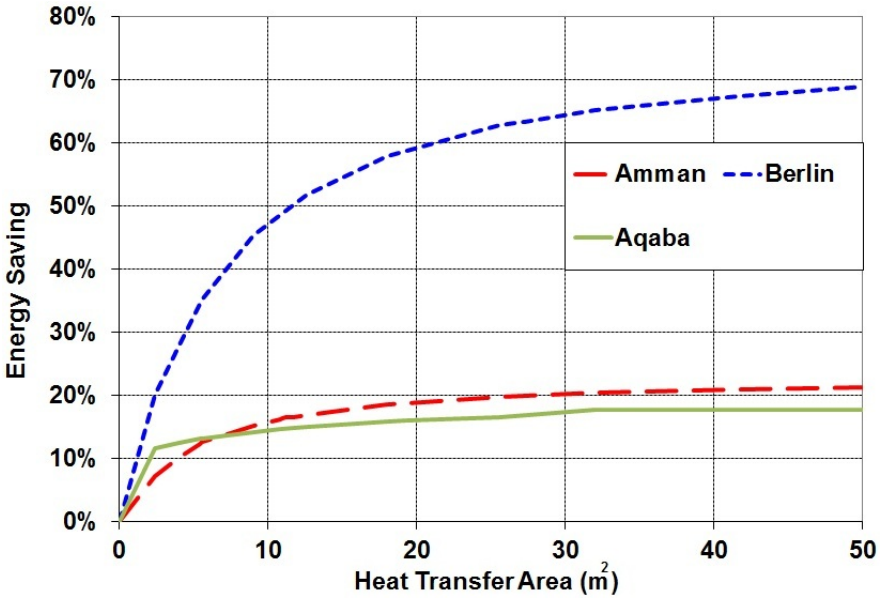

Figure 6.4: Energy Saving due to ERS in Different Climate Zones

Optimum heat transfer area is calculated by using LCC in three climate zones. The objective function and constrain equations are discussed in Section (4.3). ERS initial cost, annual auxiliary energy (heating and cooling) and LCC are presented in Figure (6.5).
The results show that minimum LCC over 30 years is occurred at heat transfer area of 11.2 m^2, 26.56 m^2 and 7.2 m^2 in Amman, Berlin and Aqaba, respectively. LCC of the building, after applying appropriate passive design techniques in addition to introducing ERS, is reduced from the basic case by 17%, 13.86% and 34.52% in Amman, Aqaba and Berlin, respectively. On the other hand, PbP from energy saving occurred is 7.4

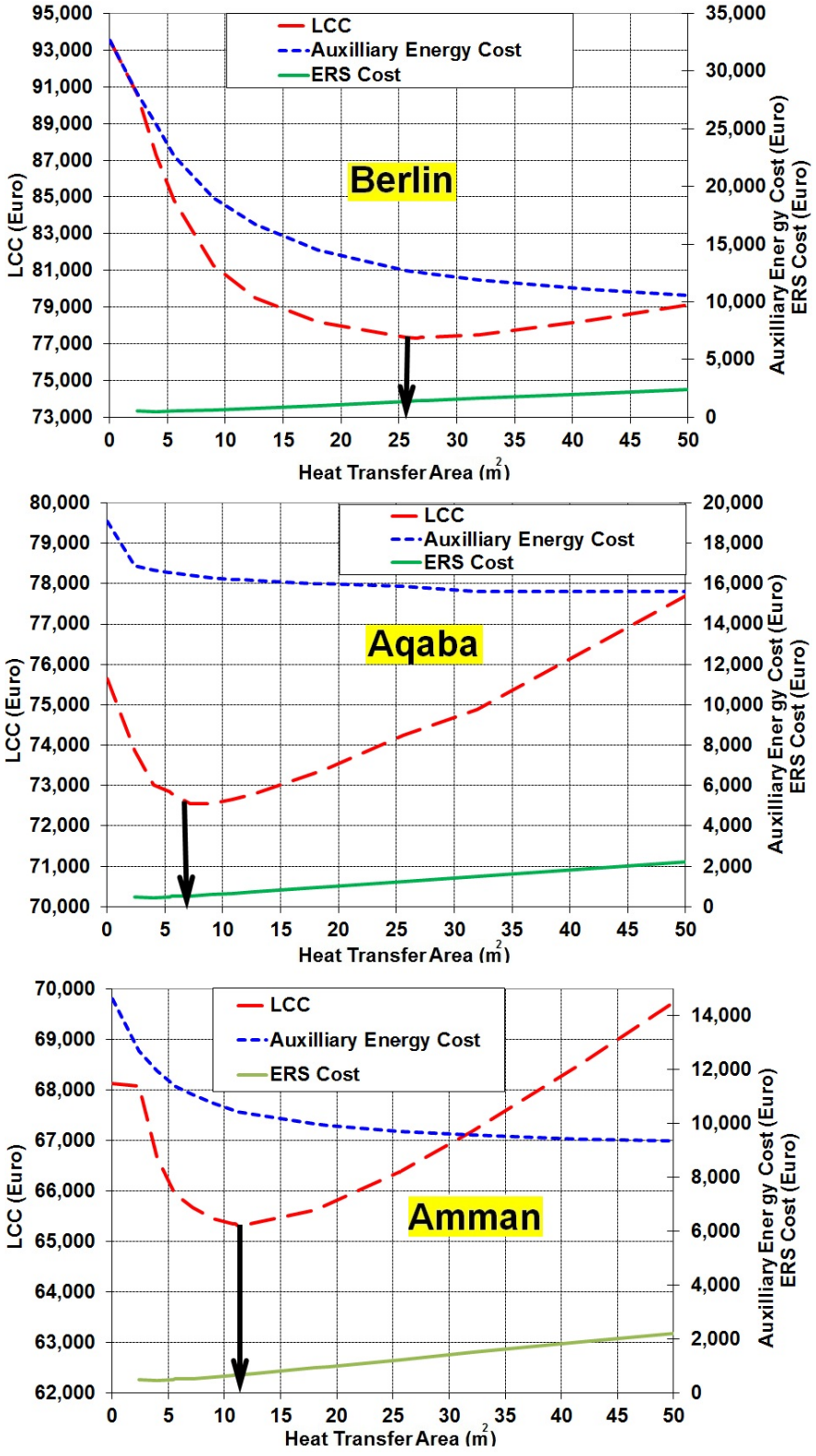

Figure 6.5: LCC in Different Climate Zones

years in Amman, 2.1 years in Berlin and 8.5 years in Aqaba.

6.4 Indirect Evaporative and Storage Unit

Recently thermal energy storage with PCM has become a topic with a lot of interest. Energy storage not only reduces the mismatch between supply and demand but also improves the performance and reliability of energy systems and plays an important role in conserving the energy [118]. IESU is an effective system of storing thermal energy and has the advantages of high-energy storage density and the isothermal nature of the storage process as discussed in Chapter (5). The performance study of IESU is based on theoretical model of the PCM employed to analyze the transient thermal behavior of the storage unit during the charge and discharge periods.
In Berlin climate zone, the optimum design of PCM melting temperature (T_m) is 18°C at any heat exchanger dimensions as shown in Figure (6.6).

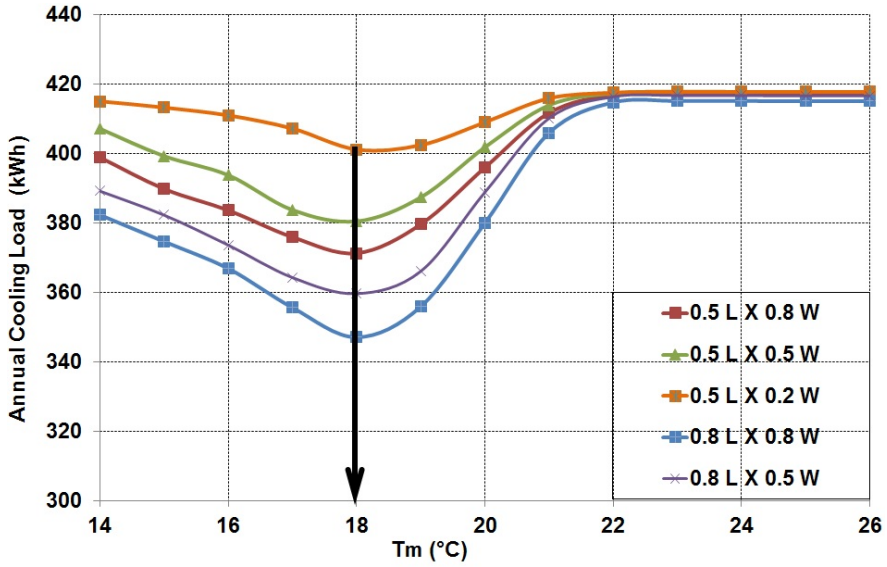

Figure 6.6: Effect of PCM Melting Temperature on Annual Cooling Load in Berlin

The optimum design of PCM melting temperature (T_m) in Aqaba is 20.5°C, as shown in Figure (6.7), but according to market $T_m = 20$°C is assumed at any heat exchanger dimensions . This melting temperature is the same as melting temperature in Amman as explained in Section (5.3.1).
Simulation has been done for more than 6,000 cases; each case has different IESU's size in order to find IESU's optimum size. In Amman climate zone, IESU of ($L_p = L_e = W_p = W_e = 0.8$ m, $t_p = t_e = 0.002$ m, $\dot{V} = 800$ l/s, $T_m = 20$°C) is needed to cover current cooling load, as discussed in Section (5.4). IESU costs about 5,671 €. In this

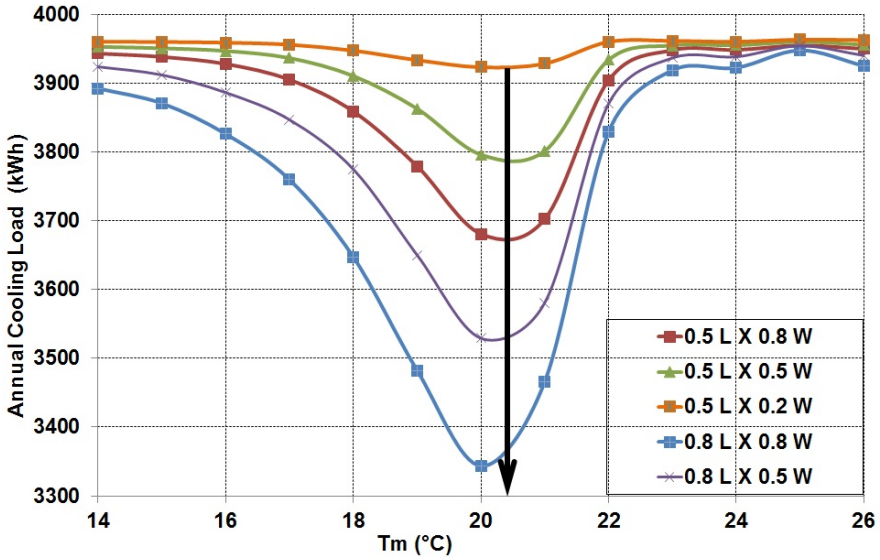

Figure 6.7: Effect of PCM Melting Temperature on Annual Cooling Load in Aqaba

size the annual running cost is more than the annual energy saving. That means this size isn't economically feasible.

Optimum size of IESU in Aqaba is the same in Amman from technical point of view. Thermal performance of technical optimum size in Aqaba is shown in Figure (6.8). It is clear from the output results that the energy saving is 85.43% from the annual cooling load.

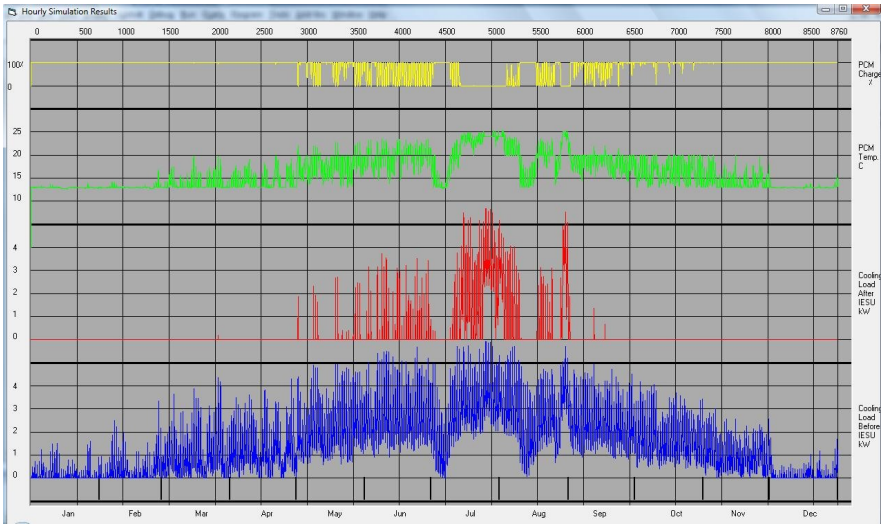

Figure 6.8: Thermal performance of technical optimum size in Aqaba

In Berlin, IESU of ($L_e = W_e = 0.8$, $L_p = W_p = 0.6$, $t_p = t_e = 0.002$ m, $\dot{V} = 800$ l/s, $T_m = 18°$C) is needed technically to cover the annual cooling load. The initial cost

needed is 4,542 €. This size isn't economically feasible because the annual running cost is more than the annual energy saving.

Optimum IESU's size is calculated by using LCC in three climate zones. The objective function and constrain equations are discussed in Section (5.4). In Amman climate the optimum IESU's size is (L_e = 0.6 m, W_e = 0.8 m, W_p = L_p = 0.4 m, t_p = 0.014 m, t_e = 0.006 m, $\dot{V}$ = 400 l/s, T_m = 20°C). This IESU is sufficient to save 80.03% of the annual cooling energy with additional cost of 1,195 €. PbP of this investment is 7.8 years. LCC is reduced by 2.66% as calculated in Section (5.4).

LCC at different IESU's size is plotted in Figure (6.9) for Berlin climate zone. IESU's size of (L_e = L_p = 0.4 m, W_p = 0.6, W_e = 0.8 m, t_p = t_e = 0.01 m, $\dot{V}$ = 400 l/s, T_m = 18°C) is economically optimum size. The annual cooling energy saving is 84.60% while the PbP of the initial cost (1,024 €) from the annual energy saving is 31.1 years. LCC is reduced by 11.21%. The Life Cycle Saving during the building life span is 8,674 €.

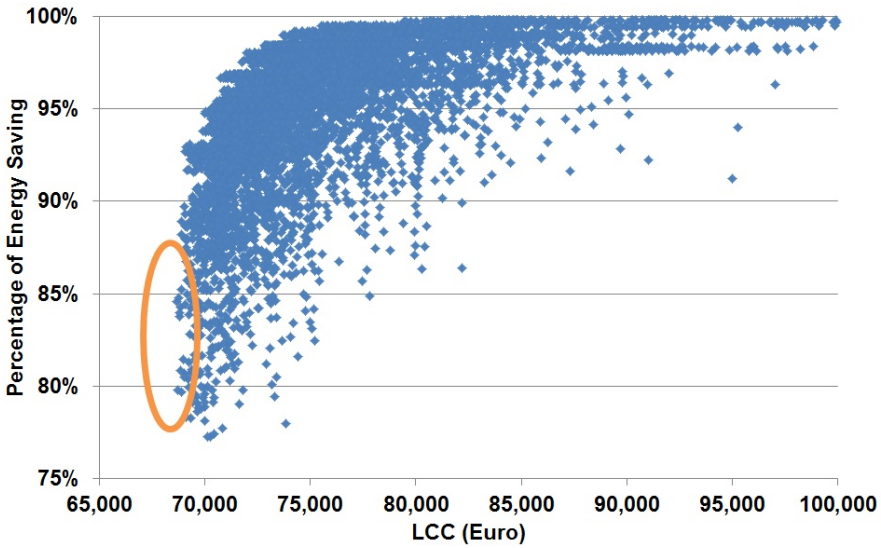

Figure 6.9: LCC at Different IESU's Sizes in Berlin

LCC and PbP at different IESU's size in Aqaba is calculated and plotted in Figures (6.10, 6.11). The optimum size of IESU is (L_e = L_p = 0.4 m, W_e 0.8 m, = W_p = 0.6 m, t_p = 0.018 m, t_e = 0.004 m, $\dot{V}$ = 400 l/s, T_m = 20°C). This optimum size is sufficient to save about 59.77% of the annual cooling load. The initial cost needed is 1,026 €. LCC is reduced by 1.58% and PbP of the initial cost from the saving occurred is 8.9 years.

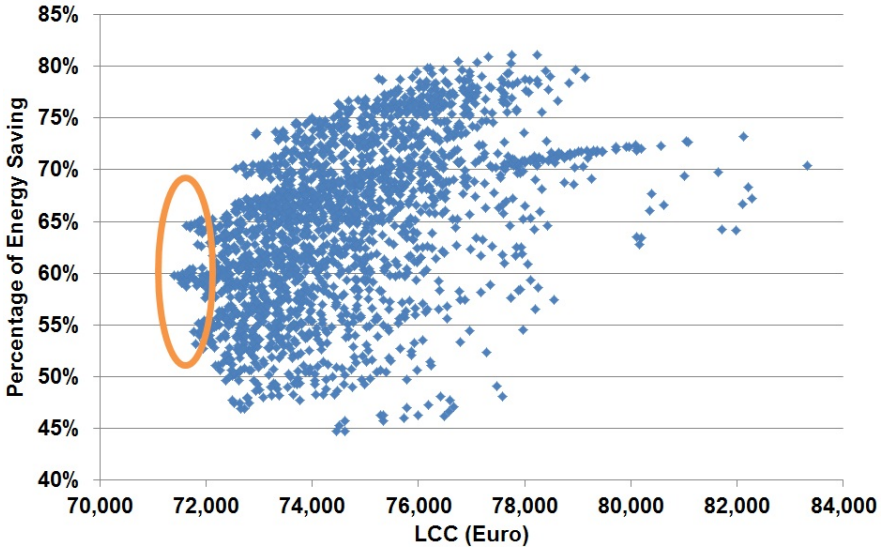

Figure 6.10: LCC at Different IESU's Sizes in Aqaba

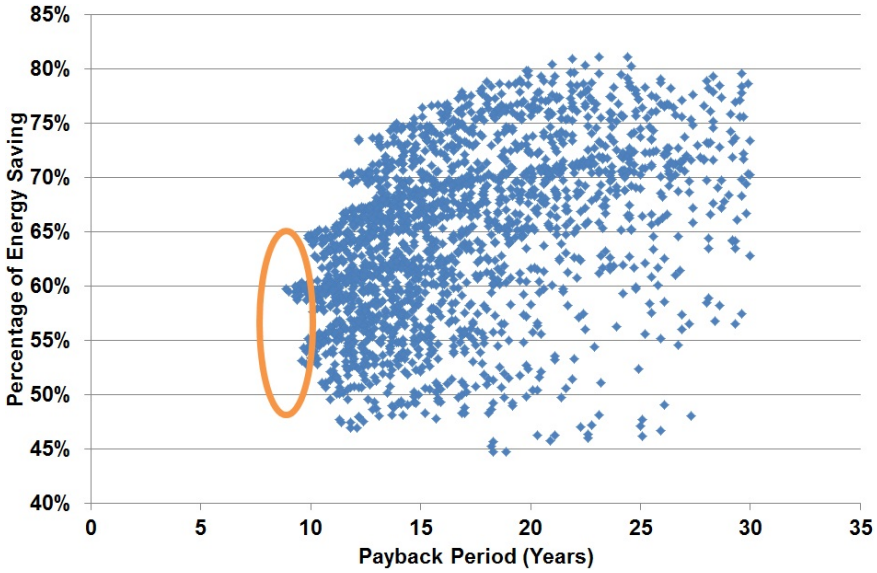

Figure 6.11: PbP at Different IESU's Sizes in Aqaba

Chapter 7

Conclusions and Recommendations

Introducing and promoting the concepts of architectural design (passive and climatic design) and energy systems for residential buildings have been discussed in this research for three climate zones. Moreover, a novel application of PCM for cooling purpose has been designed, simulated and optimized. The main aims are reducing the energy consumption as well as greenhouse gases to the environment without negatively affecting the thermal comfort.
The results show that CO_2 emissions can be reduced by 86.4%, 87.3%, 74.4%, if this research is applied in Berlin, Amman and Aqaba climate zones, respectively.

7.1 Conclusions

In this research guidelines in feasibility of passive solar systems, Energy Recovery System (ERS) and Indirect Evaporative and Storage Unit (IESU) in residential building were set. On the other hand, this work hasn't discussed before especially for Middle East region.
The main findings of this study are outlined as follows:

- Windows are like a knife has two sides; one is useful and the other is harmful.
- From economical point of view, double glazed-Low windows achieved minimum Life Cycle Cost (LCC) in both Amman and Aqaba climate zones whereas double glazed-High is the best choice for Berlin climate zone.
- Technically, triple glazed windows showed best performance than all other types but it isn't economically feasible in all climate zones.

- In future if double glazed-High and triple glazed windows are manufactured in Jordan or exported in large amount the initial cost will be reduced by 40% which will directly affect on its economic feasibility through the whole life of the building.

- The results showed that heating load is highly sensitive to windows size and type as compared with cooling load. Also, it is shown that with a well-optimized glazed window energy saving can be reached up to 21%, 20% and 24% for Amman, Aqaba and Berlin, respectively.

- Trombe wall system doesn't reduce the maximum load but it reduces the annual heating energy consumption.

- Literature showed that Trombe wall should be insulated for Summer cooling [119]. Thus, it is recommended to use roller shutters to prevent solar radiation from entering the building and insulation curtains between glass and masonry wall layer to avoid heat transfer to the building during Summer. Moreover, the foundation area should be insulated in the usual way with rigid insulation board to reduce heat loss from the Trombe wall to the foundation.

- In contrast, Legionnaires' disease is not a problem with IESU. Legionella growth is relative to the temperature of water. The optimum growth is occurring at about (37 - 41)°C [120]. In this research IEAC operates with water temperatures less than 24°C where the legionella bacteria are not active. Moreover, heat exchanger in Indirect Evaporative Air-Conditioning (IEAC) is designed with two discreet air passages. Water and air are circulated over the secondary air passage of the heat exchanger, while hot air passed through the primary air passage. The net effect is air that was cooled without contacting water or increasing in moisture content. Regularly maintaining, draining, cleaning and drying out of the indirect evaporative cooling system coupled with water treatment should be sufficient to reduce the possibility of Legionella originating.

- Indirect Evaporative and Storage Unit (IESU) is a new application of latent heat storage which can provide superior cooling while consuming less energy, reduced global warming and heal the environment than traditional air-conditioning.

- Optimum size of IESU in Amman is ($L_e = 0.6$ m, $W_e = 0.8$ m, $W_p = L_p = 0.4$ m, $t_p = 0.014$ m, $t_e = 0.006$ m, $\dot{V} = 400$ l/s, $T_m = 20$°C). This IESU's optimum size is sufficient to save 80.03% of the annual remaining cooling energy.

- Optimum size of IESU of ($L_e = L_p = 0.4$ m, $W_p = 0.6$, $W_e = 0.8$ m, $t_p = t_e = 0.01$ m, $\dot{V} = 400$ l/s, $T_m = 18$°C) in Berlin, is sufficient to reduce the annual remaining cooling energy by 84.60%.

- Optimum size of IESU in Aqaba is ($L_e = L_p = 0.4$ m, $W_e = 0.8$ m, $W_p = 0.6$ m, $t_p = 0.018$ m, $t_e = 0.004$ m, $\dot{V} = 400$ l/s, $T_m = 20°C$). This IESU's optimum size is sufficient to reduce the remain specific energy consumption by 59.77%.

- At present prices, IESU is mainly restricted to research or demonstration projects because its not competitive the traditional air-conditioning prices.

- In order to really identify the impacts of the amount of saving, the macro economic analysis should be considered. Once this research is applied in one million residential buildings in the selected climate zones, the annual estimated thermal energy saving will be about 23,421 GWh, 6,684 GWh and 633 GWh in Berlin, Amman and Aqaba, respectively. On the other hand, the annual electrical energy saving will be about 467 GWh in Berlin, 2,369 GWh in Amman and 4,688 GWh in Aqaba. The annual avoided CO_2 emissions are estimated to be about 5.7 MTon in Berlin. In Aqaba, around 2.96 MTon CO_2 emissions will be reduced annually. Moreover, about 2.98 MTon CO_2 emissions will be reduced annually in Amman.

- The payback period from the achieved saving is 18 years, 11 years and 8.6 years in Amman, Aqaba and Berlin, respectively.

7.2 Recommendations

Much work remains to be done in this field especially for Middle East region. However, the following research topics are considered of value:

- Thermal and economic investigation of adding vacuum insulation to a typical residential building in Mediterranean climate zone.

- Install three IESU's in three existing passive residential buildings located in Amman, Berlin and Aqaba. Then compare the simulation results with the experimental results.

- Construct three typical residential buildings in Berlin, Amman and Aqaba climate zones according to research findings. Thereafter, monitor the thermal performance of these buildings through over one year and compare the results with simulation results.

- Research and development is needed to reduce IESU cost.

Appendix

IESU software module has been developed by using Visual Basic 6. The main purpose of this software is simulating IESU performance every 10 minutes during the whole year. IESU's software is easy to use, contains six menus, 24 inputs and 59 outputs. These inputs and outputs are listed in Table (1).

Table 1: List of Inputs and Outputs

Symbol	**Unit**	**Description**
Input		
L_e	m	Length of heat exchanger Edge
W_e	m	Width of heat exchanger
t_e	m	Gap between PCM plates
$t_{w,e}$	m	Wall thickness of HX
$K_{w,e}$	W/m^2K	Thermal conductivity of HX wall
L_p	m	Length of heat exchanger Edge
W_p	m	Width of heat exchanger
t_p	m	Gap between PCM plates
$t_{w,p}$	m	Wall thickness of HX
$K_{w,p}$	W/m^2K	Thermal conductivity of HX wall
K_{pcm}	W/m.K	Thermal conductivity of PCM
λ	kJ/kg	Latent Heat of PCM
$C_{p,pcm}$	kJ/kg.K	Specific Heat of PCM
T_m	°C	Melting temperature of PCM
ρ_{pcm}	kg/m^3	Density of PCM
F	l/s	Flow rate
ρ_a	kg/m^3	Density of air
$C_{p,a}$	J/kg.K	Specific heat of air
μ_a	Ns/m^2	Dynamic viscosity of air

Continued on next page

Table 1 – continued from previous page

Symbol	Unit	Description
K_a	W/m.K	Thermal conductivity of air
P_{FP}	kW	Primary fan power
P_{FS}	kW	Secondary fan power
Water Consumption	m^3	Water Consumption
Water Cost	€/m^3	Water Cost Rate
Output		
Temperature multiplier	W/K	Temperature multiplier = α_p A
α_p	W/m.K	Fictive convective heat transfer coefficient
U_p	W/m.K	Overall heat transfer coefficient air to PCM
U_e	W/m.K	Overall heat transfer coefficient air to Air
NTU	-	Number of transfer units
ε	%	Effectiveness of Heat Exchanger
N_e	NO	Number of modules
A_e	m^2	Cross section area of gap for air for one module
P_e	m	Perimeter of heat exchanger module (for air gap)
D_{he}	m	Hydraulic diameter of duct
$A_{hxm,e}$	m^2	Heat transfer area per module
$A_{hx,e}$	m^2	Total heat transfer area
$R_{w,e}$	m^2.K/W	Thermal resistance for HX wall
ΔP_e	Pa	Pressure drop across heat exchanger
N_p	NO	Number of modules
V_p	m^3	Volume of PCM
A_p	m^2	Cross section area of gap for air for one module
P_p	m	Perimeter of heat exchanger module (for air gap)
D_{hp}	m	Hydraulic diameter of duct
$A_{hxm,p}$	m^2	Heat transfer area per module
$A_{hx,p}$	m^2	Total heat transfer area
$R_{w,p}$	m^2K/W	Thermal resistance for HX wall
ΔP_p	Pa	Pressure drop across heat exchanger
m_{pcm}	kg	Mass of PCM
$Q_{st,l,m}$	kWh	Max latent energy stored in PCM
$Q_{s,pcm}$	kWh/K	Specific Heat of PCM
R_{pcm}	m^2K/W	Thermal resistance for PCM
$F_{e,m}$	m^3/s	Flow rate per module-IEAC
$F_{p,m}$	m^3/s	Flow rate per module-IESU

Continued on next page

Table 1 – continued from previous page

Symbol	Unit	Description
ν_e	m/s	Air velocity-IEAC
ν_p	m/s	Air velocity-IESU
Re_e	-	Reynolds number-IEAC
Re_p	-	Reynolds number-IESU
Pr_e	-	Prandtl number-IEAC
Pr_p	-	Prandtl number-IESU
Nu_e	-	Mean Nusselt number-IEAC
Nu_p	-	Mean Nusselt number-IESC
$\mathrm{h}_{e,a}$	$\mathrm{W/m^2K}$	Mean heat transfer coefficient-IEAC
$\mathrm{h}_{p,a}$	$\mathrm{W/m^2K}$	Mean heat transfer coefficient-IESU
$\mathrm{R}_{e,a}$	$\mathrm{m^2K/W}$	Thermal resistance for air-IEAC
$\mathrm{R}_{p,a}$	$\mathrm{m^2K/W}$	Thermal resistance for air-IESU
$\mathrm{F}_{p,m}$	$\mathrm{m^3/s}$	Flow rate per module
ν_p	m/s	Air velocity
Re_p	-	Reynolds number
Pr_p	-	Prandtl number
Nu_p	-	Mean Nusselt number
$\mathrm{h}p, a$	$\mathrm{W/m^2K}$	Mean heat transfer coefficient
$\mathrm{R}p, a$	$\mathrm{W/m^2K}$	Thermal resistance for air
Electricity Cost	€/kWh	Electricity unit rate
F_{PC}	kWh	Fan power consumption
Total CEP Hrs	Hr	Total cooling hours by IEAC and PCM heat exchanger
Total CPO Hrs	Hr	Total cooling hours by PCM heat exchanger
Total CHR Hrs	Hr	Total charging hours
Total OFF Hrs	Hr	Total hours in OFF mode
IEAC Cost	€	IEAC initial cost
Fans Cost	€	Fans initial cost
PCM Cost	€	PCM initial cost
Control Cost	€	Control initial cost
IEAC HX Cost	€	IEAC heat exchanger initial cost
Actuators Cost	€	Actuators initial cost
PCM HX Cost	€	PCM heat exchanger initial cost
Structure Cost	€	Structure initial cost
Total Initial Cost	€	-
Total operating cost	€	Cost of electrical and water consumption

Continued on next page

Table 1 – continued from previous page

Symbol	Unit	Description
PbP	Years	Payback Period
Rem_{CL}	kWh	Remaining cooling load

The menus are; air,PCM, Heat Exchanger, Heat Transfer Parameters and IESU menus. Moreover, the user can chose one climate zone from Amman, Aqaba and Berlin. Snap shot of these menus are shown in Figures (1 - 5).

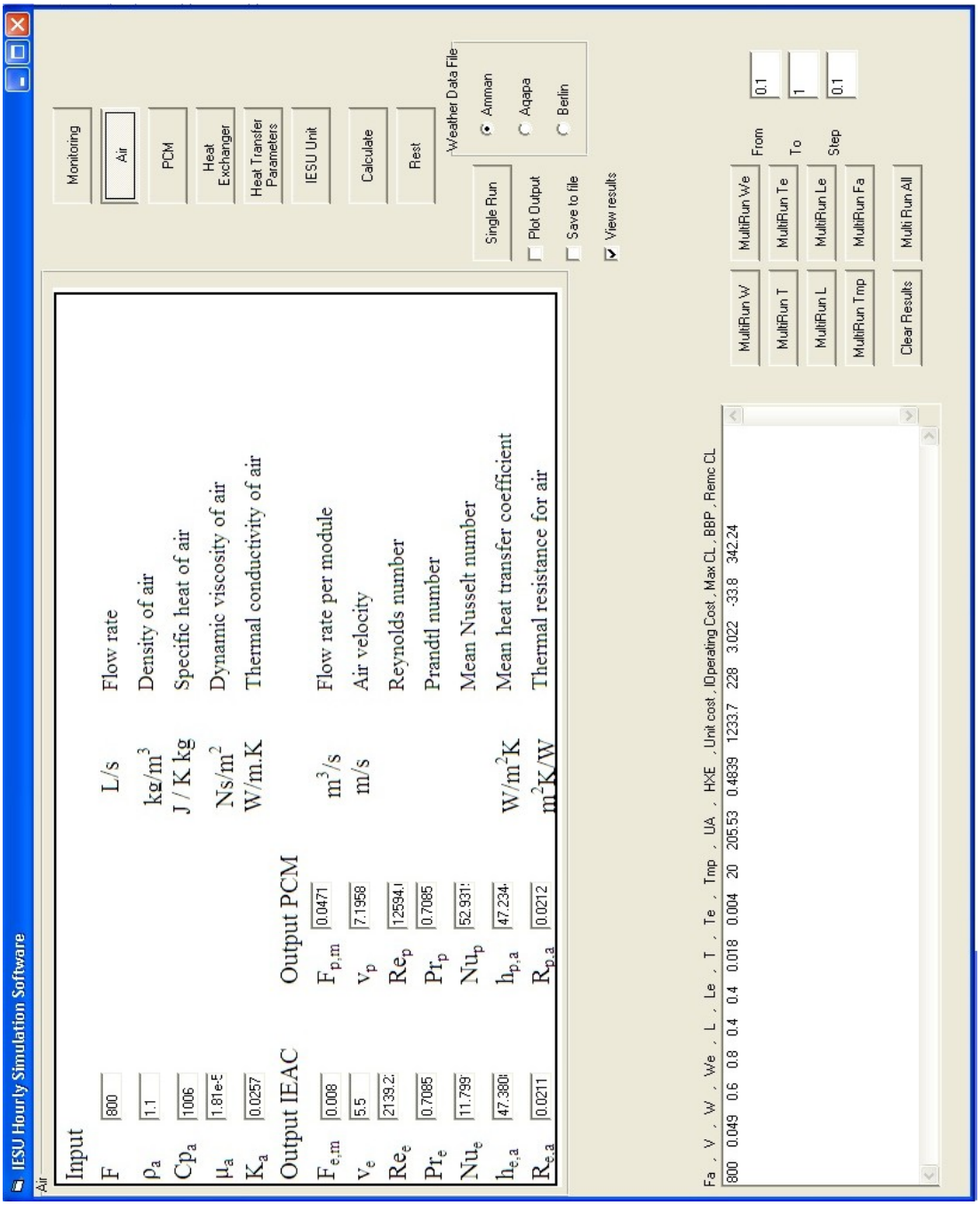

Figure 1: Air Menu

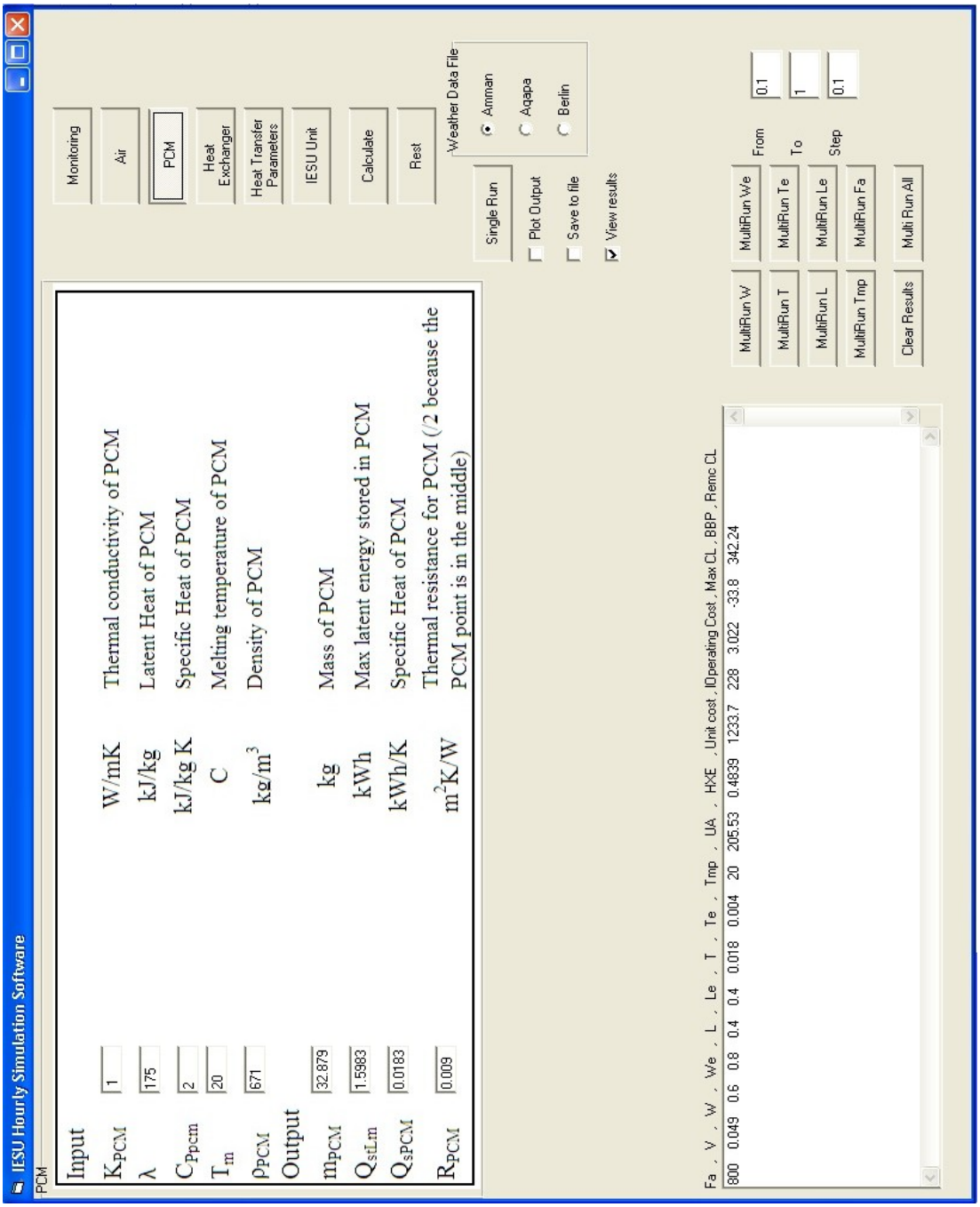

Figure 2: PCM Menu

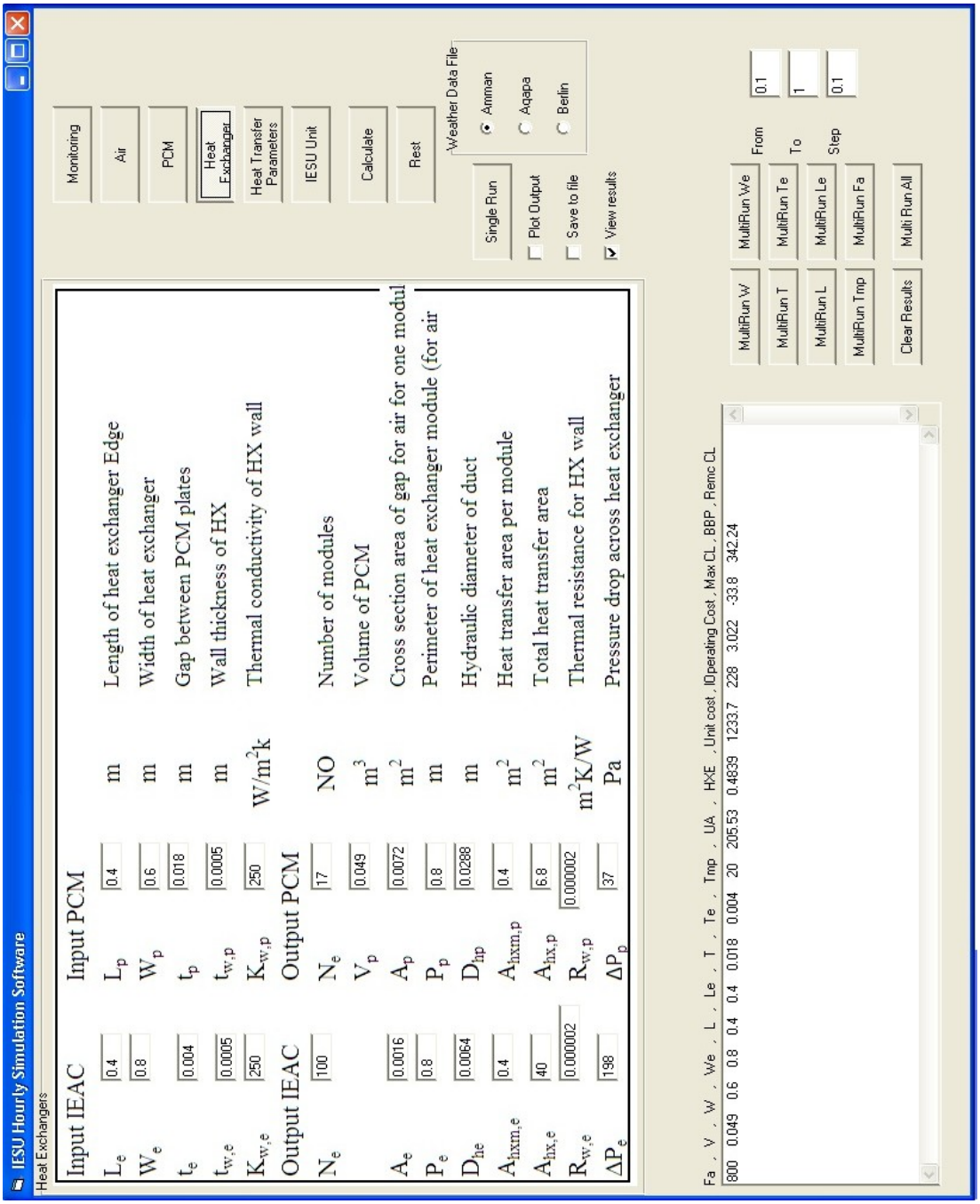

Figure 3: Heat Exchanger Menu

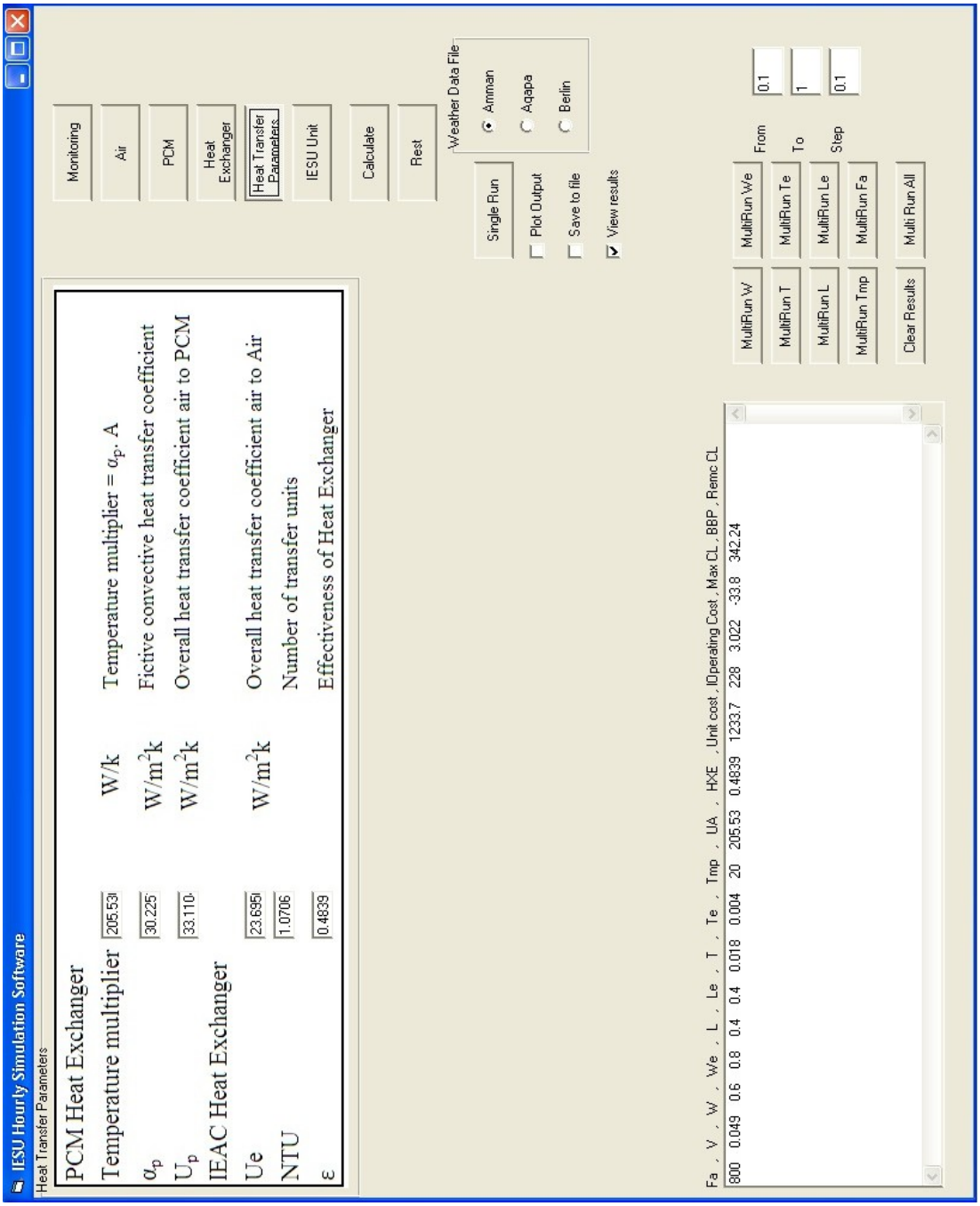

Figure 4: Heat Transfer Parameters Menu

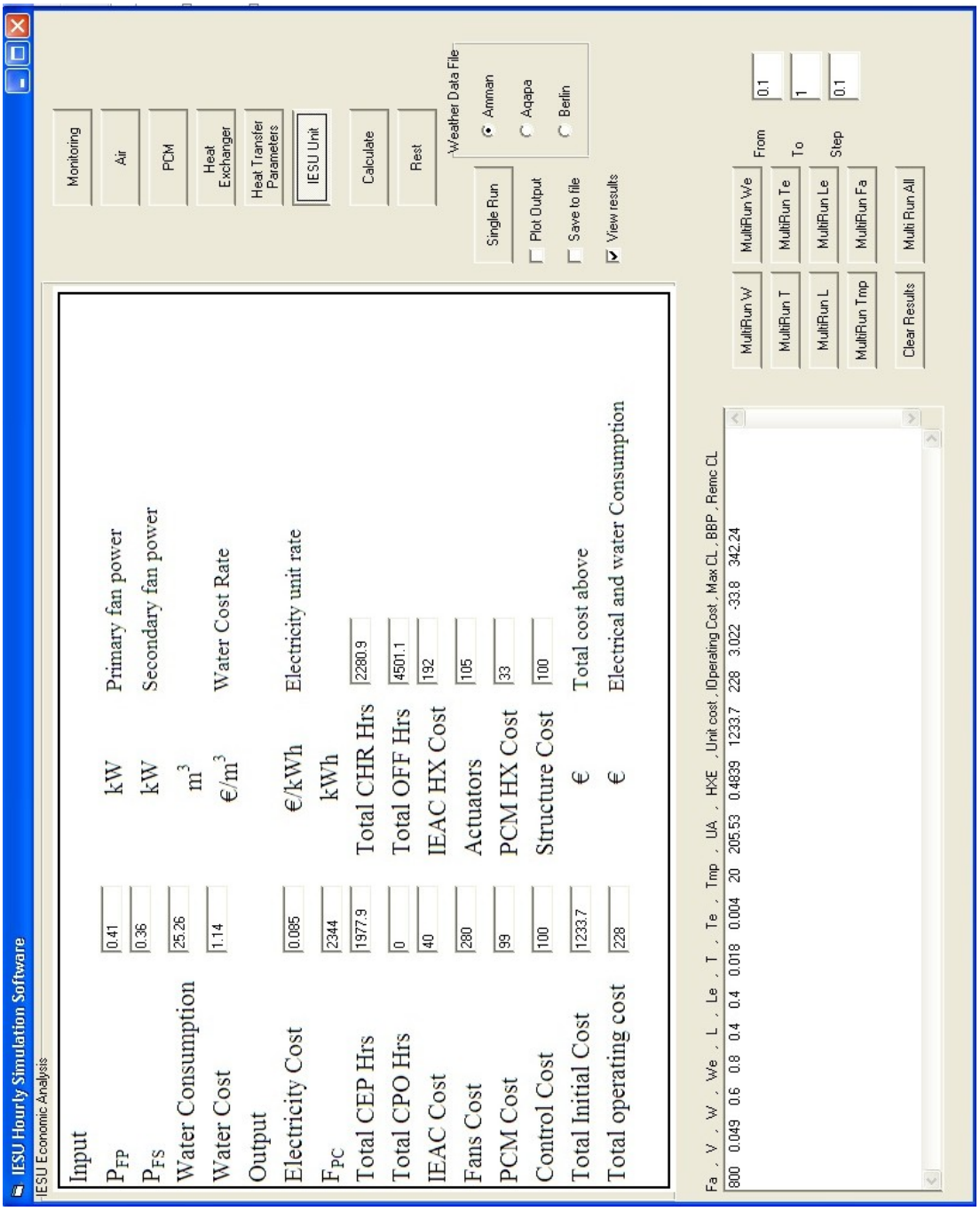

Figure 5: IESU Menu

The user can chose the output styles which are save data to file or plot output data or view output data directly in the software screen. An example for plotted output is shown in Figure (6).

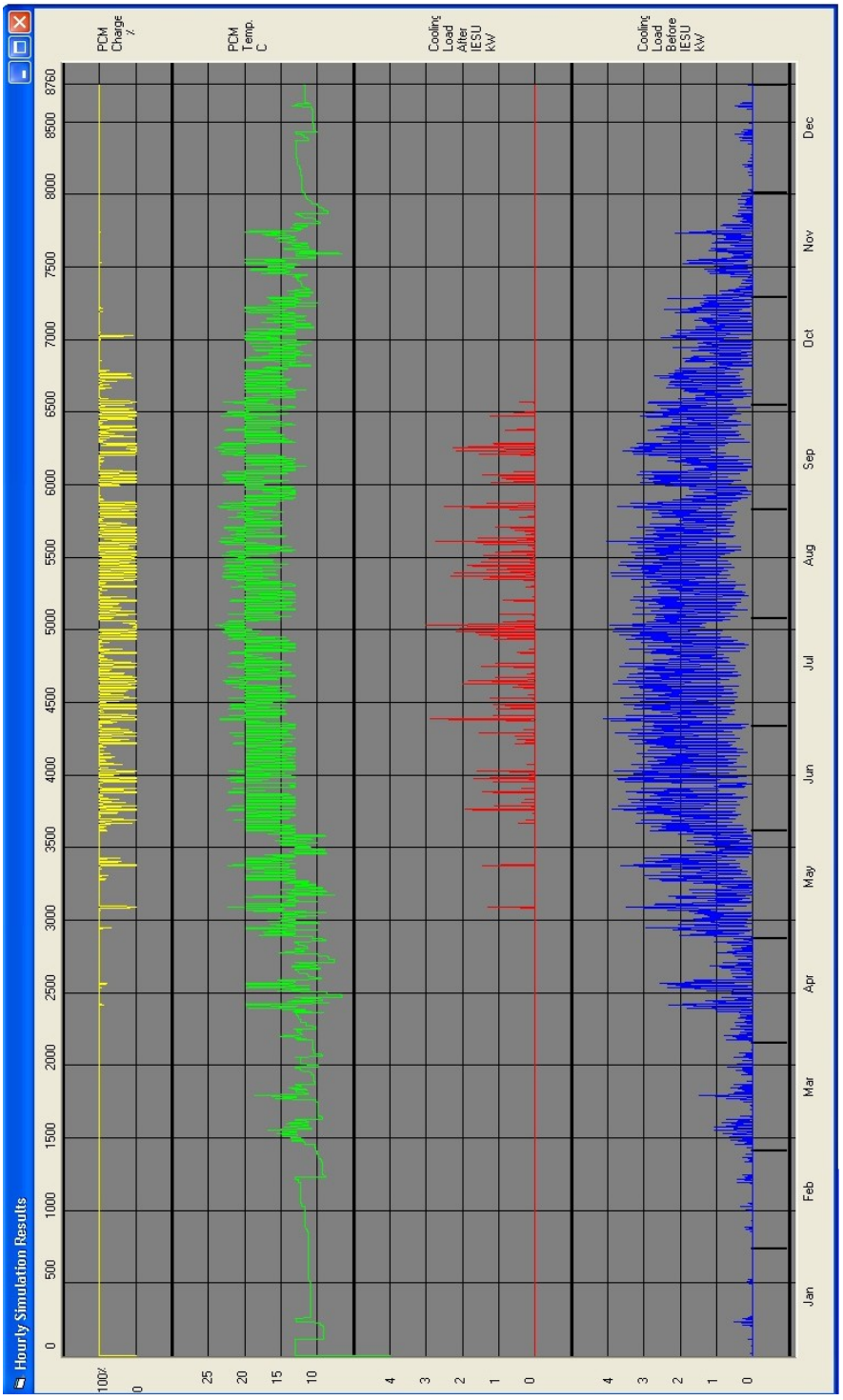

Figure 6: Output Results Example

Furthermore, The hourly output temperatures at different locations can be monitored, as shown in Figure (7). These temperatures are T_{pi}, T_{po}, T_{si}, T_{so}, T_s, T_{pcm}. Further-

more, in order to facilitate the optimization analysis the user can select 8 parameters and do multi-simulations for 8 parameters (L_e, W_e, t_e, L_p, W_p, t_p, $\dot{V}$, T_m).

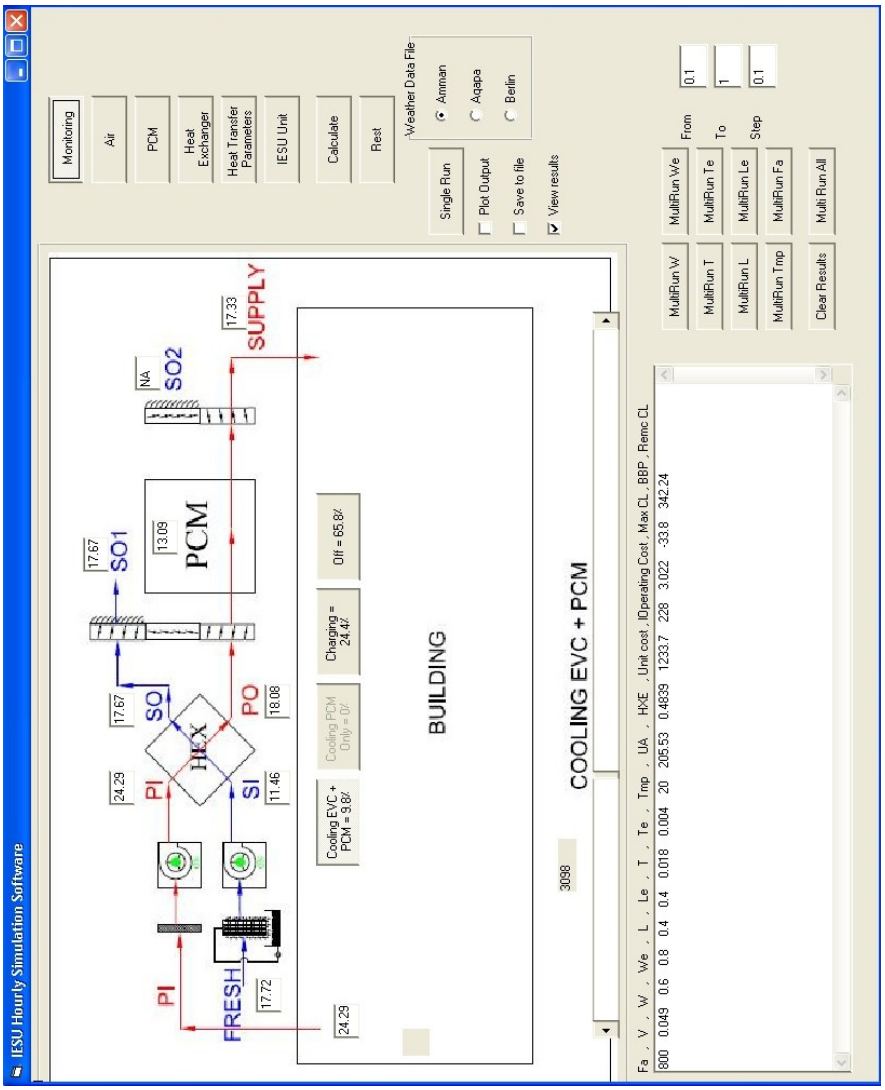

Figure 7: Monitoring Menu

References

[1] MEMR, "Facts and figures." Ministry of Energy and Mineral Resources, Amman - Jordan, 2010. ix, 2

[2] H. P. (ed.), *Thermal Energy Storage for Sustainable Energy Consumption: Fundamentals, Case Studies and Design*. Springer, 1th ed., 2007. ix, 9

[3] ASHRAE, *ASHRAE Handbook of Fundamentals*. American Society of Heating, Refrigeration and Air Conditioning Engineers, 2005. ix, 21, 22, 55, 56, 69

[4] Doppelintegral-GmbH, *INSEL Users Manual, MS Windows,*. Stuttgart, Germany., 8 ed., 2009. ix, 17, 23, 24, 57, 88, 89

[5] A.-S. El-Eish, "Thermal insulation code." Ministry of Public Work and Housing, Amman - Jordan, 2009. ix, xii, 19, 27, 28, 29, 30

[6] S. Jaber and S. Ajib, "Optimum design of trombe wall system in mediterranean region," *Solar Energy*, vol. 85, no. 9, pp. 1891 – 1898, 2011. ix, 42

[7] Solar-Energy-Laboratory, Universityof-Wisconsin-Madison, TRANSSOLAR-Energietechnik-GmbH, CSTB, and TESS, *TRNSYS User's Manual, a TRaNsient SYstem Simulation program*, 16 ed., 2006. x, 17, 31, 33, 37, 42, 43, 44, 57, 91

[8] S. Hasnain, "Review on sustainable thermal energy storage technologies, part i: heat storage materials and techniques," *Energy Conversion and Management*, vol. 39, no. 11, pp. 1127 – 1138, 1998. xii, 8

[9] PCM Energy P. Ltd, http://www.pcmenergy.com/. xii, 70

[10] IEA, "World energy outlook," tech. rep., International Energy Agency, Paris - France, 2004. 1

[11] R. York, "Demographic trends and energy consumption in european union nations, 1960-2025," *Social Science Research*, vol. 36, no. 3, pp. 855 – 872, 2007. 1

[12] B. Hunn, *Fundamentals of Building Energy Dynamics.* MIT Press, London - England, 1996. 1, 26

[13] A. Taher, N. Abdalla, S. Jaber, and W. Shahin, "Report on analysis of the political, socio-economic and climatic conditions in the mediterranean countries.," tech. rep., National Energy Research Center, Amman - Jordan, 2009. 2, 3, 22

[14] R. Luken and T. Grof, "The montreal protocols multilateral fund and sustainable development," *Ecological Economics*, vol. 56, pp. 241 – 255, 2006. 3

[15] DOS, "Jordan in figures." Department of Statistic, Amman - Jordan, 2004. 3

[16] CSBE. Center for the Study of the Built Environment, Amman - Jordan, .http://www.csbe.org/aree/press_release.htm. 3

[17] E. R. (Jr.), "Houses with no furnace but plenty of heat." New York Times, December 26, 2008. Retrieved December 27, 2008. 4

[18] "Timber frame takes the passivhaus tour," January 23, 2009. Retrieved June 5, 2009. 4

[19] T. Z. (Jr.), "Beyond fossil fuels: Can we build in a brighter shade of green?." New York Times, September 26, 2010. 4

[20] J. Schnieders, "Heat load calculations and passive house requirements in northwest european climates," *Proceedings of the 10th international passive house conference*, pp. 217 – 223, 2006. 4

[21] F. Ansari, A. Mokhtar, K. Abbas, and N. Adam, "A simple approach for building cooling load estimation," *American Journal of Environmental Sciences*, vol. 3, pp. 209 – 212, 2005. 4

[22] J. Bokel, "The effect of window position and window size of the energy demand for heating, cooling, and electrical lighting," in *Proceedings of the Building Simulation*, Beijing, China, 2007. 4

[23] A. Hasan, "Optimizing insulation thickness for buildings using life cycle cost," *Applied Energy*, vol. 63, no. 2, pp. 115 – 124, 1999. 4

[24] M. Bojic, F. Yik, and W. Leung, "Thermal insulation of cooled spaces in high rise residential buildings in hong kong," *Energy Conversion and Management*, vol. 43, no. 2, pp. 165 – 183, 2002. 4

[25] A. Ucar, "Thermoeconomic analysis method for optimization of insulation thickness for the four different climatic regions of turkey," *Energy*, vol. 35, no. 4, pp. 1854 – 1864, 2010. 4

[26] J. Yu, C. Yang, L. Tian, and D. Liao, "A study on optimum insulation thicknesses of external walls in hot summer and cold winter zone of china," *Applied Energy*, vol. 86, no. 11, pp. 2520 – 2529, 2009. 4

[27] J. Jie, Y. Hua, H. Wei, P. Gang, L. Jianping, and J. Bin, "Modeling of a novel trombe wall with pv cells," *Building and Environment*, vol. 42, no. 3, pp. 1544 – 1552, 2007. 4

[28] T. Oezbalta and S. Kartal, "Heat gain through trombe wall using solar energy in a cold region of turkey," *Scientific Research and Essays*, vol. 5, no. 18, pp. 2768 – 2778, 2010. 4

[29] W. Smolec and A. Thomas, "Some aspects of trombe wall heat transfer models," *Energy Conversion and Management*, vol. 32, no. 3, pp. 269 – 277, 1991. 4

[30] J. Shen, S. Lassue, L. Zalewski, and D. Huang, "Numerical study of classical and composite solar walls by trnsys," *Journal of Thermal Science*, vol. 16, pp. 46 – 55, 2007. 4

[31] A. Chel, J. Nayak, and G. Kaushik, "Energy conservation in honey storage building using trombe wall," *Energy and Buildings*, vol. 40, no. 9, pp. 1643 – 1650, 2008. 4

[32] A. Fernndez-Gonzlez, "Analysis of the thermal performance and comfort conditions produced by five different passive solar heating strategies in the united states midwest," *Solar Energy*, vol. 81, no. 5, pp. 581 – 593, 2007. 4, 5

[33] P. Torcellini and S. Pless, "Trombe walls in low-energy buildings: Practical experiences," tech. rep., NREL Report No. CP-550-36277, National Renewable Energy Laboratory, 2004. 5, 41

[34] E. Juodis, "Extracted ventilation air heat recovery efficiency as a function of a building's thermal properties," *Energy and Buildings*, vol. 38, no. 6, pp. 568 – 573, 2006. 5

[35] J. Liu, W. Li, J. Liu, and B. Wang, "Efficiency of energy recovery ventilator with various weathers and its energy saving performance in a residential apartment," *Energy and Buildings*, vol. 42, no. 1, pp. 43 – 49, 2010. 5

[36] M. Fehrm, W. Reiners, and M. Ungemach, "Exhaust air heat recovery in buildings," *International Journal of Refrigeration*, vol. 25, no. 4, pp. 439 – 449, 2002. 5

[37] Y. Zhou, J. Wu, and R. Wang, "Performance of energy recovery ventilator with various weathers and temperature set-points," *Energy and Buildings*, vol. 39, no. 12, pp. 1202 – 1210, 2007. 5

[38] L. Zhang and J. Niu, "Energy requirements for conditioning fresh air and the long-term savings with a membrane-based energy recovery ventilator in hong kong," *Energy*, vol. 26, no. 2, pp. 119 – 135, 2001. 5

[39] M. Rasouli, C. Simonson, and R. Besant, "Applicability and optimum control strategy of energy recovery ventilators in different climatic conditions," *Energy and Buildings*, vol. 42, no. 9, pp. 1376 – 1385, 2010. 5

[40] X. Zhao, Z. Duan, C. Zhan, and S. Riffat, "Dynamic performance of a novel dew point air conditioning for the uk buildings," *International Journal of Low-Carbon Technologies*, vol. 4, no. 1, pp. 27 – 35, 2009. 5

[41] R. Lazzarin, "Introduction of a simple diagram-based method for analyzing evaporative cooling," *Applied Thermal Engineering*, vol. 27, no. 11-12, pp. 2011 – 2025, 2007. 5, 64

[42] X. Zhao, J. Li, and S. Riffat, "Numerical study of a novel counter-flow heat and mass exchanger for dew point evaporative cooling," *Applied Thermal Engineering*, vol. 28, no. 14-15, pp. 1942 – 1951, 2008. 5, 64

[43] F. Khamamas, "Improving the environmental cooling for air-coolers by using the indirect-cooling method," *Journal of Engineering and Applied Science*, vol. 5 (2), pp. 66–73, 2010. 5, 64

[44] M. Steeman, A. Janssens, and M. Paepe, "Performance evaluation of indirect evaporative cooling using whole-building hygrothermal simulations," *Applied Thermal Engineering*, vol. 29, no. 14-15, pp. 2870 – 2875, 2009. 5, 64

[45] G. Maheshwari, F. Al-Ragom, and R. Suri, "Energy-saving potential of an indirect evaporative cooler," *Applied Energy*, vol. 69, no. 1, pp. 69 – 76, 2001. 5

[46] R. Lazzarin and M. Noro, "Energetic and economic savings of free cooling in different european climates," *International Journal of Low-Carbon Technologies*, vol. 4, pp. 213–223, 2009. 5

[47] W. Xin, Y. Zhang, W. Xiao, R. Zeng, Q. Zhang, and H. Di, "Review on thermal performance of phase change energy storage building envelope," *Chinese Science Bulletin*, vol. 54(6), pp. 920 – 928, 2009. 5

[48] W. Saman, F. Bruno, and E. Halawa, "Thermal performance of pcm thermal storage unit for a roof integrated solar heating system," *Solar Energy*, vol. 78, no. 2, pp. 341 – 349, 2005. 5

[49] M. Farid and W. Kong, "Underfloor heating with latent heat storage," *Proceedings of the Institution of Mechanical Engineers, Part A: Journal of Power and Energy*, vol. 215, pp. 601 – 609, 2001. 5

[50] K. Lin, Y. Zhang, X. Xu, H. Di, R. Yang, and P. Qin, "Modeling and simulation of under-floor electric heating system with shape-stabilized pcm plates," *Building and Environment*, vol. 39, no. 12, pp. 1427 – 1434, 2004. 5

[51] S. Haghshenaskashani and H. Pasdarshahri, "Simulation of thermal storage phase change material in buildings," *World Academy of Science, Engineering and Technology*, vol. 58, pp. 111 – 115, 2009. 5

[52] B. Zalba, J. M. Marn, L. F. Cabeza, and H. Mehling, "Free-cooling of buildings with phase change materials," *International Journal of Refrigeration*, vol. 27, no. 8, pp. 839 – 849, 2004. 5

[53] G. Hed and R. Bellander, "Mathematical modelling of pcm air heat exchanger," *Energy and Buildings*, vol. 38, no. 2, pp. 82 – 89, 2006. 5, 70

[54] B. Cerne and S. Medved, "The dynamic thermal characteristics of lightweight building elements with a forced ventilated cavity and radiation barriers," *Energy and Buildings*, vol. 37, no. 9, pp. 972 – 981, 2005. 5

[55] A. Lazaro, P. Dolado, J. Marn, and B. Zalba, "Pcm-air heat exchangers for free-cooling applications in buildings: Experimental results of two real-scale prototypes," *Energy Conversion and Management*, vol. 50, no. 3, pp. 439 – 443, 2009. 5

[56] U. Stritih and P. Novak, "Thermal storage of solar energy in the wall for building ventilation," in *IEA, ECES IA Annex 17, Advanced Thermal Energy Storage Techniques Feasibility Studies and Demonstration Projects 2nd Workshop*, Ljubljana, Slovenia, 2002. 5

[57] G. Zhou, Y. Zhang, X. Wang, K. Lin, and W. Xiao, "An assessment of mixed type pcm-gypsum and shape-stabilized pcm plates in a building for passive solar heating," *Solar Energy*, vol. 81, no. 11, pp. 1351 – 1360, 2007. 5

[58] A. Chan, "Energy and environmental performance of building faades integrated with phase change material in subtropical hong kong," *Energy and Buildings*, vol. In Press, Accepted Manuscript, pp. –, 2011. 5

[59] V. Butala and U. Stritih, "Cold storage with phase change material for building ventilation," *International Journal of Ventilation*, vol. 5, no. 2, pp. 189 – 198, 2006. 6

[60] U. Stritih and V. Butala, "Energy saving in building with pcm cold storage," *International Journal of Ventilation*, vol. 31 (15), pp. 1532 – 1544, 2007. 6

[61] B. Zalba, J. Marin, L. Cabeza, and H. Mehling, "Free cooling of buildings with phase change materials," *International Journal of Ventilation*, vol. 27 (28), pp. 839 – 849, 2004. 6

[62] V. Butala and U. Stritih, "Experimental investigation of pcm cold storage," *Energy and Buildings*, vol. 41, no. 3, pp. 354 – 359, 2009. 6

[63] C. Arkar, B. Vidrih, and S. Medved, "Efficiency of free cooling using latent heat storage integrated into the ventilation system of a low energy building," *International Journal of Refrigeration*, vol. 30, no. 1, pp. 134 – 143, 2007. 6

[64] C. Arkar and S. Medved, "Free cooling of a building using pcm heat storage integrated into the ventilation system," *Solar Energy*, vol. 81, no. 9, pp. 1078 – 1087, 2007. 6

[65] S. Takeda, K. Nagano, T. Mochida, and K. Shimakura, "Development of a ventilation system utilizing thermal energy storage for granules containing phase change material," *Solar Energy*, vol. 77, no. 3, pp. 329 – 338, 2004. 6

[66] S. Medved and C. Arkar, "Correlation between the local climate and the free-cooling potential of latent heat storage," *Energy and Buildings*, vol. 40, no. 4, pp. 429 – 437, 2008. 6

[67] S. MOZHEVELOV, G. ZISKIND, and R. LETAN, "Temperature moderation in a real-size room by pcm-based units," *Journal of solar energy engineering*, vol. 128, no. 2, pp. 178 – 188, 2006. 6

[68] G. Zhou, Y. Yang, X. Wang, and S. Zhou, "Numerical analysis of effect of shape-stabilized phase change material plates in a building combined with night ventilation," *Applied Energy*, vol. 86, no. 1, pp. 52 – 59, 2009. 6

[69] K. Yanbing, J. Yi, and Z. Yinping, "Modeling and experimental study on an innovative passive cooling system–nvp system," *Energy and Buildings*, vol. 35, no. 4, pp. 417 – 425, 2003. 6

[70] J. Turnpenny, D. Etheridge, and D. Reay, "Novel ventilation cooling system for reducing air conditioning in buildings.: Part i: testing and theoretical modelling," *Applied Thermal Engineering*, vol. 20, no. 11, pp. 1019 – 1037, 2000. 6

[71] J. Turnpenny, D. Etheridge, and D. Reay, "Novel ventilation system for reducing air conditioning in buildings. part ii: testing of prototype," *Applied Thermal Engineering*, vol. 21, no. 12, pp. 1203 – 1217, 2001. 6

[72] C. Arkar and S. Medved, "Enhanced solar assisted building ventilation system using sphere encapsulated pcm thermal heat storage," in *IEA, ECES IA Annex 17, Advanced Thermal Energy Storage Techniques Feasibility Studies and Demonstration Projects 2nd Workshop*, Ljubljana, Slovenia, 2002. 6

[73] N. Zhu, S. Wang, Z. Ma, and Y. Sun, "Energy performance and optimal control of air-conditioned buildings with envelopes enhanced by phase change materials," *Energy Conversion and Management*, vol. 52, no. 10, pp. 3197 – 3205, 2011. 6

[74] D. Etheridge, K. Murphy, and D. Reay, "A pcm/heat pipe cooling system for reducing air conditioning in buildings: Review of options and report on field tests," *Building Services Engineering Research & Technology*, vol. 27, no. 1, pp. 27 – 39, 2006. 6

[75] Q. Qi, S. Deng, and Y. Jiang, "A simulation study on a solar heat pump heating system with seasonal latent heat storage," *Solar Energy*, vol. 82, no. 8, pp. 669 – 675, 2008. 6

[76] H. Lund, "The kyoto mechanisms and technological innovation," *Energy*, vol. 31, no. 13, pp. 2325 – 2332, 2006. 6

[77] Y. Dutil, D. Rousse, N. BenSalah, S. Lassue, and L. Zalewski, "A review on phase-change materials: Mathematical modeling and simulations," *Renewable and Sustainable Energy Reviews*, vol. 15, no. 1, pp. 112 – 130, 2011. 6

[78] H. Mehling and L. Cabeza, *Heat and Cold Storage with PCM: An up to date introduction into basics and applications*. Springer, 1th ed., 2008. 7

[79] M. Farid, A. Khudhair, S. Razack, and S. Al-Hallaj, "A review on phase change energy storage: materials and applications," *Energy Conversion and Management*, vol. 45, no. 9-10, pp. 1597 – 1615, 2004. 8, 9

[80] J. Duffie and W. Beckman, *Solar Engineering of Thermal Processes.* John Wiley and Sons, Inc., 2006. 11, 13, 26, 41, 42, 43, 44

[81] P. Atrill and E. McLaney, *Management Accounting for Decision Makers.* Pearson Education Limited, 6th ed., 2009. 12

[82] D. Wilde, *Globally Optimal Design.* John Wiley and Sons, Inc., New York, 1978. 13

[83] J. Arora, *Introduction to Optimum Design.* Academic Press, 2nd ed., May 2004. 14

[84] R. Pike, *Optimization for Engineering Systems.* Van Nostrand Reinhold Company, 2001. 14

[85] J. Abadie and S. Vajda, *Nonlinear programming.* North-Holland Pub. Co.; Wiley, Amsterdam, New York, 1967. 14

[86] P. Gill, W. Murray, and M. Wright., *Practical Optimization.* Academic Press, New York, 1981. 14

[87] A. Colville, "A comparative study of nonlinear programming codes," *IBM Scientific Center Report No. 320-2949. IBM, New York*, 1968. 14

[88] G. Reklaitis, A. Ravindran, and K. Ragsdell, *Engineering Optimization: Methods and Applications.* John Wiley and Sons, Inc., New York, 1983. 14

[89] J. Rawlings, S. Pantula, and D. Dickey, *Applied Regression Analysis: A Research Tool.* Springer, 2nd ed., 1998. 16

[90] EIA. Energy Information Administration, http://www.eia.doe.gov. 18

[91] DOS, "Population and housing census." Department of Statistic, Amman - Jordan, 2004. 19

[92] ASHRAE, "Thermal environmental conditions for human occupancy." American Society of Heating, Refrigerating and Air conditioning Engineers. ANSI/ASHRAE Standard 55-1992. 22

[93] ASHRAE, "Addendum to thermal environmental conditions for human occupancy." American Society of Heating, Refrigerating and Air conditioning Engineers. ANSI/ASHRAE Standard 55a-1995. 22

[94] NERC. National Center for Research and Development, http://www.nerc.gov.jo. 25

[95] Ministry of Energy and Mineral Resources, www.memr.gov.jo. 25, 90

[96] Miyahuna. Jordan Water Company, http://www.miyahuna.com.jo. 25

[97] M. Alsaad and M. Hammad, *Heating and Air Conditioning*. University of Jordan, 3rd ed., 1995. 27, 91

[98] S. Jaber and S. Batayneh, "Solar energy code." Ministry of Public Work and Housing, Amman - Jordan, 2010. 31

[99] S. Jaber and S. Ajib, "Optimum, technical and energy efficiency design of residential building in mediterranean region," *Energy and Buildings*, vol. 43, no. 8, pp. 1829 – 1834, 2011. 33

[100] T. Awad-Allah, H. Adas, E. Jarrar, and Y. Obeidat, "Energy efficient building code." Ministry of Public Work and Housing, Amman - Jordan, 2009. 33, 96

[101] IBC, "International building code," 2009. International Code Council. 33, 96

[102] E. Morse, "Warming and ventilating apartments by sun's rays, u. s. patent 246,626," 1881. 41

[103] P. Ellis, *Development and validation of the unvented Trombe wall model in energyplus*. PhD thesis, University of Illinois at Urbana-Champaign, Illinois - United States, 2003. 41

[104] M. Utzinger, "Analysis of building components related to direct solar heating of buildings," Master's thesis, University of Wisconsin-Madison, 1979. 43

[105] ASHRAE, "Ventilation and acceptable air quality in low-rise residential buildings standard, american society of heating, refrigerating and air conditioning engineers." American Society of Heating, Refrigerating and Air conditioning Engineers. 62.2-2004. 54

[106] ASHRAE, "Ventilation of health care facilities, american society of heating, refrigerating and air conditioning engineers." American Society of Heating, Refrigerating and Air conditioning Engineers. 170-2004. 54

[107] M. Fauchoux, "The effect of energy recovery on indoor climate, air quality and energy consumption using computer simulations," Master's thesis, University of Saskatchewan, Saskatchewan - Canada, 2006. 54

[108] M. Orme, "Estimates of the energy impact of ventilation and associated financial expenditures," *Energy and Buildings*, vol. 33, no. 3, pp. 199 – 205, 2001. 54

[109] F. Rey and E. Velasco, "Experimental study of indoor air quality, energy saving and analysis of ventilation norms in climatised areas," *Energy and Buildings*, vol. 33, no. 1, pp. 57 – 67, 2000. 54

[110] ASHRAE, *ASHRAE Handbook of HVAC Systems and Equipment.* American Society of Heating, Refrigerating and Air conditioning Engineers, 2008. 61, 64, 65, 68

[111] S. Jaber and S. Ajib, "Evaporative cooling as an efficient system in mediterranean region," *Applied Thermal Engineering*, vol. 31, no. 14-15, pp. 2590 – 2596, 2011. 65

[112] J. P. Holman, *Heat Transfer.* McGraw-Hill College, 9th ed., 2001. 73

[113] ASHRAE, *ASHRAE Handbook - HVAC Applications.* American Society of Heating, Refrigerating and Air conditioning Engineers, 2007. 75

[114] Klingenburg Energy Recovery, http://www.klingenburg.de. 84

[115] TECSON. http://www.tecson.de. 90

[116] VERIVOX. http://www.verivox.de. 90

[117] S. Jaber and S. Ajib, "Thermal and economic windows design for different climate zones," *Energy and Buildings*, vol. 43, no. 11, pp. 3208 – 3215, 2011. 90

[118] H. Garg, S. Mullick, and A. Bhargava, *Solar thermal energy storage.* D. Reidel Publishing Company, 1985. 104

[119] G. Gan, "A parametric study of trombe walls for passive cooling of buildings," *Energy and Buildings*, vol. 27, no. 1, pp. 37 – 43, 1998. 109

[120] P. Puckorius, "Why evaporative coolers have not cause legionnaires disease," *American Society of Heating, Refrigerating and Air conditioning Engineers*, 1995. 109

Curriculum Vitae

Samar Juma'h Jaber

E-mail: samar.jaber@tu-ilmenau.de / s0jaber@gmail.com

Personal Information

Nationality: Jordanian **Martial status**: Married **Gender**: Female

Education

High School: Universal school (Amman-Jordan).

Passed The Jordanian General Secondary Education Certificate Examination (Scientific Stream) in 2000.

Colleges:

- University of Jordan, Faculty of engineering & Technology (Amman- Jordan), Graduated in 2008 with **M.Sc. degree in Mechanical Engineering.**

  Thesis Title " Thermal Design of Renewable Energy Building, Towards Low Energy Houses in Jordan"
- Mu'tah University, Faculty of engineering & Technology (Amman- Jordan), Graduated in 2004 with **B.Sc. degree in Mechanical Engineering,** & have accomplished 166 credited hours.

Professional experience

(October, 2009 – Present) PhD Student at
Institut für Thermo-und Fluiddynamik – Teschnische Universität Ilmenau – Germany.

(May, 2009 – October, 2009) Energy Efficiency & Solar Energy Freelancer

- Consult designing of several solar water heating projects, Amman, Jordan.
- Prepare statistical studies of "Solar Water Heater Manufacturers/Suppliers Problems and Needs". This study is part of "Promotion of innovation and technology for SME in Near East" Projects which conducted by Regional – German Development Cooperation (GTZ), Damascus, Syria.

(July 3rd, 2005– May 20th, 2009) Consultant at Rational Use of Energy and Solar Thermal Division at National Energy Research Center (NERC), Amman, Jordan.

- Thermal and economic feasibility studies for different solar projects.
- Climatic Design in Buildings.
- Energy conservation in Refrigeration systems.
- Prepare statistical studies for several European projects for Middle East & North Africa regions (MENA).
- Detailed Energy Audit Studies for large Industries such as Arab Fertilizers and Chemicals Industries (KEMARA), American Jordanian Com. for Apparel (JORDACHE), Canning Industries Co. Ltd., … etc
- Detailed Energy Audit Studies for large Commercial such as Four Seasons Hotel, Ministry of Planning and International Cooperation (MOPIC), Movenpick Aqaba & Dead Sea, King Abdullah II Design and Development Bureau (KADDB) … etc.
- Join a Value Engineering team to conduct Value Engineering Study to Ayla Oasis and German Jordanian University
- Monitor the solar cooling system at Aqaba Residence Energy Efficiency (AREE).
- Industrial water Management.
- Lecturer for many training courses.

(June 3rd, 2004 – June 24th, 2005) Supplies Engineer in Engineering Supplies Officer "Al Bashaer Trading Company", Amman, Jordan.

-Obtaining offers for public tenders of engineering supplies through commercial correspondences as well as performing the awarded tenders, opening Letters of Credit (LC)….etc.

Training Courses

As a participant:

- Technical Writing, Jordan Engineers Association, March 30 – April 2, 2009.
- Infrared Camera (BCAM Basics), Center for Renewable Energy Sources (CRES)–Greece, March 9-13, 2009
- Microsoft Project Management, Royal Scientific Society (RSS), January 11-15, 2009.
- Report Writing, Team International Engineering and Management Consultants, December 21-24, 2008.
- Strategic Planning, Team International Engineering and Management Consultants, December 1-4, 2008.
- 45th UNEP/UNESCO/BMU International Short Course on Energy Efficiency and Renewable Energy Sources, University of Dresden – Germany, October 21 – November 13, 2008.
- Training session on solar collectors testing, Fraunhofer ISE (Institut Solare Energiesysteme) – Germany, July 28 – August, 1, 2008.
- Value Engineering Training Workshop,SAVE International Approval Number 200603800, July 20-24, 2008.
- Climatic Design of Building and Urban Areas, Lund University – Sweden, April 15 – May 31, 2007.
- Employees' performance Development, Royal Scientific Society (RSS), April 1-3, 2007.
- Efficient Operation & design of steam boilers and systems, National Energy Research Center (NERC), November 21-24, 2005.
- Heating Ventilation Air Conditioning and Refrigeration (HVAC and R), Jordan Engineers Association, August 3-24, 2005.
- Energy Conservation in pumps and Fans and pumping system design, National Energy Research Center (NERC), August, 21-23, 2005.
- Energy Conservation in Electrical Systems, National Energy Research Center (NERC), June 19-21, 2005.

As a lecturer:

- Solar Water Heating Systems (SWHS): Optimum Design & Economic Evaluation, National Energy Research Center (NERC), February 23-25, 2009.
- Energy Conservation in Commercial Building, National Energy Research Center (NERC), June 29 – July 3, 2008.
- Solar Water Heating Systems (SWHS): Optimum Design & Economic Evaluation, National Energy Research Center (NERC), May 7-9, 2008.
- Energy Engineers Program, National Energy Research Center (NERC), June 28 – July 5, 2007.
- Energy Auditing, National Energy Research Center (NERC), March 18-22, 2007.
- Efficient Operation & design of steam boilers and systems, National Energy Research Center (NERC), November 27-30, 2006.
- Energy Conservation in Commercial Buildings, National Energy Research Center (NERC), August 6-10, 2006.
- Energy Audit in industry, National Energy Research Center (NERC), April 16-20, 2006.

Professional Activities Seminars, Conferences and Publications

- Publishing "Evaporative Cooling as an Efficient System in Mediterranean Region" in Applied Thermal Engineering Journal, 31(14-15):2590-2596, 2011.
- Publishing "Optimum, Technical and Energetic Residential Building Design in Mediterranean region" in Energy and Buildings Journal, 43(8):1829-1834, 2011.
- Publishing "Optimum Design of Trombe Wall System in Mediterranean Region" in Solar Energy Journal, 85(9):1891-1898, 2011.
- Publishing "Thermal and Economic Windows Design for Different Climate Zones" in Energy and Buildings Journal, In Press, 2011.
- "Novel Cooling Unit Using PCM for Residential Application", submitted to International Journal of Refrigeration.
- "Optimum Design of Heat Recovery System in Mediterranean Region in Mediterranean region", submitted to Sustainable Cites and Society Journal.
- Publishing "Thermal and Economical Investigation of Evaporative Air-Conditioning in Europe and Middle East" in 4th International Conference Solar Air-Conditioning, Larnaka-Cyprus, October 12 – 14, 2011.
- Publishing "Feasibility Study of Trombe Wall System in Middle East" in Solar World Congress 2011, Kassel-

Germany, August 28 – September 2, 2011.

- Publishing "Evaporative Cooling as an Efficient System in Mediterranean Region in Global Conference on Renewable Energy Efficiency for Dessert Regions (GCREEDER), Amman – Jordan, April 26– 28, 2011.
- Publishing "Technical and Economical comparison of windows in Europe and Middle East" in Global Conference on Renewable Energy Efficiency for Dessert Regions (GCREEDER), Amman – Jordan, April 26– 28, 2011.
- Publishing " Thermal and economical design of low energy house in Jordan " in International Engineering of Conference on Hot Arid Regions (IECHAR), Al-Ahsa – Kingdom of Saudi Arabia, March 1 – 2, 2010.
- Authoring the Solar Thermal Code, 2010.
- Member of scientific committee of Queen Alia Competition for Social Responsibility, University Competition "JOGREEN", 2010.
- Member of scientific committee of Queen Alia Competition for Social Responsibility "Energy Responsibility", 2009.
- Publishing "Thermal and economical analysis of renewable energy buildings, towards low energy house in Jordan" in Global Conference on Renewables and Energy Efficiency for Desert Regions (GCREEDER 2009), Amman – Jordan, March 31 – April 2, 2009.
- "Promotion of innovation and technology for SME in Near East" Workshop, Cairo – Egypt, March 23-24, 2009.
- Work on Combined solar power and desalination plants: technicoeconomic potential in Mediterranean Partner countries project "CSD", EU Funded project, 2008 – 2010. Work on Promotion of a New Generation of Solar Thermal Systems in the MPC project "SOLATERM", EU Funded project, 2006 – 2008.
- Judge in First Lego League Jordan 2007, Dead Sea – Jordan.
- Participated in The First German –Jordanian Winter Academy 2006, Jordan, February 4-11, 2006).
- Participated in the First German-Jordanian Conference for Renewable Energy and Energy Efficiency (2006).

Computer Skills

- Good knowledge in Visual Basic.
- Drawing using AutoCAD 2D & 3D.
- Visio 2003.
- TRNSYS Simulation Software.
- INSEL Simulation Software.
- Solar System Designing (F-Chart Software's).
- DEROB-LTH and F-Load.
- Very good using Microsoft Office and LATEX.
- Very Good skills in web browsing.

Languages

Arabic (Mother Tongue)**:** Excellent (Reading, Writing and speaking)

English: Very good (Reading, Writing and speaking).

German: Intermediate (Reading, Writing and speaking).

Erklärung gemäß Anlage 1 der Promotionsordnung

Ich versichere, dass ich die vorliegende Arbeit ohne unzulässige Hilfe Dritter und ohne Benutzung anderer als der angegebenen Hilfsmittel angefertigt habe. Die aus anderen Quellen direkt oder indirekt übernommenen Daten und Konzepte sind unter Angabe der Quelle gekennzeichnet.

Bei der Auswahl und Auswertung folgenden Materials haben mir die nachstehend aufgeführten Personen in der jeweils beschriebenen Weise entgeltlich/unentgeltlich geholfen:
1. .....
2. .....
3. .....

Weitere Personen waren an der inhaltlich-materiellen Erstellung der vorliegenden Arbeit nicht beteiligt. Insbesondere habe ich hierfür nicht die entgeltliche Hilfe von Vermittlungs- bzw. Beratungsdiensten (Promotionsberater oder anderer Personen) in Anspruch genommen.
Niemand hat von mir unmittelbar oder mittelbar geldwerte Leistungen für Arbeiten erhalten, die im Zusammenhang mit dem Inhalte der vorgelegten Dissertation stehen.
Die Arbeit wurde bisher weder im In- noch im Ausland in gleicher oder ähnlicher Form einer Prüfungsbehörde vorgelegt.
Ich bin darauf hingewiesen worden, dass die Unrichtigkeit der vorstehenden Erklärung als Täuschungsversuch angesehen wird und den erfolglosen Abbruch des Promotionsverfahrens zu Folge hat.

(Ort, Datum) (Unterschrift)